A Non-Uniform User Distribution and its Performance Analysis on K-tier Heterogeneous Cellular Networks Using Stochastic Geometry

by

Chao Li

Thesis submitted in partial fulfillment
of the requirements for the
Doctorate in Philosophy degree in
Electrical and Computer Engineering

School of Electrical Engineering and Computer Science
Faculty of Engineering
University of Ottawa

Abstract

In the cellular networks, to support the increasing data rate requirements, many base stations (BSs) with low transmit power and small coverage area are deployed in addition to classical macro cell BSs. Low power nodes, such as micro, pico, and femto nodes (indoor and outdoor), which complement the conventional macro networks, are placed primarily to increase capacity in hotspots (such as shopping malls and conference centers) and to enhance coverage of macro cells near the cell boundary. Combining macro and small cells results in heterogeneous networks (HetNets).

An accurate node (BS or user equipment (UE)) model is important in the research, design, evaluation, and deployment of 5G HetNets. The distance between transmitter (TX), receiver (RX), and interferer determines the received signal power and interference signal power. Therefore, the spatial placement of BSs and UEs greatly impacts the performance of cellular networks. However, the investigation on the spatial distribution of UE is limited, though there is ample research on the topic of the spatial distribution of BS. In HetNets, UEs tend to cluster around BSs or social attractors (SAs). The spatial distribution of these UEs is non-uniform. Therefore, the analysis of the impact of non-uniformity of UE distribution on HetNets is essential for designing efficient HetNets. This thesis presents a non-uniform user distribution model based on the existing K-tier BS distribution. Our proposed non-uniform user distribution model is such that a Poisson cluster process with the cluster centers located at SAs in which SAs have a base station offset with their BSs. There are two parameters (cluster radius and base station offset) the combination of which can cover many possible non-uniformity. The heterogeneity analysis of the proposed non-uniform user distribution model is also given.

The downlink performance analysis of the designed non-uniform user model is investigated. The numerical results show that our theoretical results closely match the simulation results. Moreover, the effect of BS parameters of small cells such as BS density, BS cell extension bias factor, and BS transmit power is included. At the same time, the uplink coverage probability by the theoretical derivation is also analyzed based on some simplifying assumptions as a result of the added complexity of the uplink analysis due to the UEs' mobile position and the uplink power control. However, the numerical results show a small gap between the theoretical results and the simulation results, suggesting that our simplifying assumptions are acceptable if the system requirement is not very strict. In addition to the effect of BS density, BS cell extension bias factor, and BS transmit power, the effect of fractional power control factor in the uplink is also introduced. The comparison between the downlink and the uplink is discussed and summarized at the end.

The main goal of this thesis is to develop a comprehensive framework of the non-uniform user distribution in order to produce a tractable analysis of HetNets in the downlink and the uplink using the tools of stochastic geometry.

Acknowledgements

Firstly, I would like to express my sincere gratitude to my supervisors Prof. Abbas Yongacoglu and Prof. Claude D′Amours for their continuous support during the last five years technically and financially. I am also thankful for their patience, wide knowledge and constructive comments on my research. Without their precious support it would not be possible to conduct this research. Their guidance helped me so much in research and writing of my thesis. I am so lucky and proud to be their student.

Besides my supervisors, I would like to thank Prof. Halim Yanikomeroglu and Prof. Maher Arar for their insightful comments.

Special thanks go to my colleagues, Elham Kalantari, Suzan Ureten, Jun Shi, Jing Wang, Kerem Karatas, Safwan Alfattan, Nesrine Cherif and all my friends who helped me during the study here. Finally, I would like to thank my family, my husband Chenjin, my sons Jerry and Henry, my parents and my sisters, for their strong support, love and caring which encourages me to continue to achieve my goal.

Table of Contents

List of Tables **xi**

List of Figures **xii**

List of Abbreviations **xix**

List of Symbols **xxi**

1 Introduction **1**

1.1 Problem Definition 4

1.2 Motivation 5

1.3 Contributions 5

1.4 Thesis Organization 8

1.5 Publications 9

2 Background and Literature Reivew **10**

2.1 Classical Poisson Distribution 11

2.2 Temporal Point Process 12

2.3 Spatial Point Process 12

2.3.1 Poisson Point Process (PPP) 13

2.3.1.1 Homogeneous PPP 13

2.3.1.2 Heterogeneous PPP 16

2.3.1.3 Practical Scenarios and Examples 17

2.3.2 Transforming a Spatial Point Process 17
2.3.2.1 Displacement 17
2.3.2.2 Thinning 19
2.3.2.3 Superposition 19
2.3.2.4 Practical Scenarios and Examples 20
2.3.3 Hard Core Point Process (HCPP) 22
2.3.3.1 Hard Core Point Process Introduction 22
2.3.3.2 Practical Scenarios and Examples 25
2.3.4 Poisson Cluster Process (PCP) 25
2.3.4.1 Poisson Cluster Process Introduction 25
2.3.4.2 Practical Scenarios and Examples 27
2.4 Literature Review of Non-Uniform UE Distribution 28

3 System Model **32**
3.1 Introduction 32
3.2 BS Distribution 32
3.2.1 Related Work on BS Distribution in the Literature . . 32
3.2.2 BS Distribution Model Used In the Thesis 33
3.3 User Distribution 34
3.3.1 Non-Uniform User Distribution in a Single Tier BS System 35
3.3.1.1 Set Initial BS Density 35
3.3.1.1.1 UE Distribution Pattern 35
3.3.1.1.2 Coverage Map and Cell Boundaries . 36
3.3.1.1.3 Performance 37
3.3.1.2 Increasing Macro BS Density 38
3.3.1.2.1 UE Distribution Pattern 38
3.3.1.2.2 Coverage Map and Cell Boundaries . 39
3.3.1.2.3 Performance 39

3.3.2 Non-Uniform User Distribution in a 2-tier BS System . 40
3.3.2.1 Replacing Macro BSs with Pico BSs 40
3.3.2.1.1 UE Distribution Pattern 40
3.3.2.1.2 Coverage Map and Cell Boundaries . 40
3.3.2.1.3 Performance 41
3.3.2.2 Increasing Pico BS Density 43
3.3.2.2.1 UE Distribution Pattern 43
3.3.2.2.2 Coverage Map and Cell Boundaries . 43
3.3.2.2.3 Performance 44
3.3.3 Non-uniform User Distribution in a 3-tier BS System . 45
3.3.3.1 Replacing Pico BSs with Femto BSs 45
3.3.3.1.1 UE Distribution Pattern 45
3.3.3.1.2 Coverage Map and Cell Boundaries . 45
3.3.3.1.3 Performance 46
3.3.4 Summary of User Distribution 47
3.4 User Connectivity 47
3.4.1 Connectivity Rule 47
3.4.2 Connectivity Model 49
3.5 Conclusions 50

4 User Model and Heterogeneity Analysis 51
4.1 Introduction 51
4.2 Non-Uniform User Distribution 52
4.2.1 Definition 52
4.2.2 Parameters 53
4.2.3 Attraction Level and Dependency Level 55
4.2.3.1 Attraction Level 55
4.2.3.2 Dependency Level 56

4.2.4 UE Realization 56
4.3 Heterogeneity Analysis of Non-Uniform User Distribution . . 61
4.3.1 Definition of CoV (Coefficient of Variation) 61
4.3.1.1 One Dimension (1D) or Time Domain 61
4.3.1.2 Two Dimensions (2D) or Space Domain . . . 62
4.3.2 CoV Measurement 64
4.3.3 CoV Simulation Results 66
4.4 Conclusions 67

5 Downlink Performance Analysis 69
5.1 Introduction 69
5.2 Model Performance Analysis 72
5.2.1 Distance Characterization 73
5.2.1.1 PDF and CCDF of Random Variable V . . . 73
5.2.1.2 PDF and CCDF of Random Variable L . . . 74
5.2.2 Interference Characterization 77
5.2.3 Downlink Coverage Probability for Case1 (associated with the BS to which the UE belongs) 78
5.2.4 Downlink Coverage Probability for Case2 (associated with a BS in all tiers except the BS to which UE belongs) 79
5.2.5 Overall Downlink Coverage Probability 80
5.3 Simulation Results 81
5.3.1 Matching between Simulation and Theoretical Analysis 83
5.3.2 Effect of Base Station Offset 84
5.3.3 Effect of System Parameters 84
5.3.3.1 Effect of BS Density Ratio between Small Cells and Macro Cells 85
5.3.3.2 Effect of Cell Extension of Small Cells 88
5.3.3.3 Effect of BS Transmit Power of Small Cells . 91
5.4 Conclusions 93

6 Uplink Performance Analysis **94**

6.1 Introduction 94

6.2 Simplifying Assumptions 99

6.3 Uplink Power Control 101

6.4 Model Performance Analysis 102

6.4.1 Distance Characterization 104

6.4.2 Interference Characterization 104

6.4.3 Uplink Coverage Probability 105

6.4.4 Overall Uplink Coverage Probability 107

6.5 Simulation Results 107

6.5.1 Matching between Simulation and Theoretical Analysis 108

6.5.2 Effect of Base Station Offset 110

6.5.3 Effect of System Parameters 111

6.5.3.1 Effect of BS Density Ratio between Small Cells and Macro Cells 111

6.5.3.2 Effect of Cell Extension of Small Cells 114

6.5.3.3 Effect of BS Transmit Power of Small Cells . 116

6.5.3.4 Effect of Fractional Power Control Factor . . 117

6.6 Conclusions 118

7 Comparison between Downlink and Uplink **120**

7.1 Introduction 120

7.2 Non-uniform UE Model 120

7.3 Coverage Probability Performance Analysis 121

7.3.1 Coverage Probability Definition 122

7.3.1.1 Downlink 122

7.3.1.2 Uplink 123

7.3.1.3 Difference 123

7.3.2 Assumptions . . . 123
7.3.2.1 Downlink . . . 124
7.3.2.2 Uplink . . . 124
7.3.2.3 Difference . . . 124
7.3.3 Coverage Probability Derivation . . . 124
7.3.3.1 Downlink . . . 124
7.3.3.2 Uplink . . . 125
7.3.3.3 Difference . . . 126
7.3.4 Simulation Results . . . 126
7.3.4.1 Downlink . . . 127
7.3.4.2 Uplink . . . 127
7.3.4.3 Difference . . . 127
7.4 Effect of System Parameters . . . 129
7.4.1 Effect of BS Density Ratio between Small Cells and Macro Cells . . . 129
7.4.2 Effect of Cell Extension of Small Cells . . . 130
7.4.3 Effect of Transmit Power of Small Cells . . . 131
7.5 Conclusions . . . 132

8 Conclusions and Future Work **134**
8.1 Conclusions . . . 134
8.2 Future Work . . . 136

Appendix **138**

A Downlink Coverage Performance Analysis **139**
A.1 Proof of Corollary 5-1 . . . 139
A.2 Proof of Lemma 5-2 . . . 144
A.3 Proof of Lemma 5-3 . . . 145
A.4 Proof of Lemma 5-4 . . . 146

B Uplink Coverage Performance Analysis **147**

B.1 Proof of Lemma 6-4 147

C Simulation Setting **148**

C.1 Downlink Coverage Probability 148

C.2 Uplink Coverage Probability 150

C.3 Heterogeneity Analysis based on CoV 151

References **153**

List of Tables

1.1 Typical parameters of different tiers of cells 3

5.1 PDF and CCDF of the random variable L 76

5.2 Parameters about BSs of a 2-tier system 82

5.3 Parameters of effect of BS density ratio between small cells and macro cells 85

5.4 Parameters of effect of BS cell extension bias factor of small cells 88

5.5 Parameters of effect of BS transmit power of small cells . . . 91

List of Figures

1.1 Network architecture for 5G HetNets 2

2.1 Probability of Poisson distribution 11
2.2 Realization of homogeneous PPP and heterogeneous PPP . . 16
2.3 Example of the Voronoi region of homogeneous PPP and heterogeneous PPP 17
2.4 Realization 1 of displacement (points are displaced by shifting) 18
2.5 Realization 2 of displacement (points are displaced by contraction) 18
2.6 Realization of thinning (black points are thinned with the probability of 70%) 19
2.7 Realization of superposition (superposition of two point patterns with the same density) 20
2.8 Example of displacement points and their Voronoi region . . . 20
2.9 Example of thinning points and their Voronoi region 21
2.10 Example of generating non-uniform users using thinning . . . 21
2.11 Example of superposition points and their Voronoi region . . 22
2.12 Rule to select HCPP points 23
2.13 Realization of hard core point process 24
2.14 Example of hard core point process and their Voronoi region . 25
2.15 PDF distribution example in PCP 26
2.16 Realization of PCP 27
2.17 Example of PCP and their Voronoi region 28

3.1 A realization of a 3-tier BS distribution 34
3.2 UE distribution pattern with uniform UEs and non-uniform UEs. Red triangles are macro BSs. Blue curves are cell boundaries. Black points are uniform UEs in (a) while magenta points are non-uniform UEs in (b). 36
3.3 Coverage map (a) and cell boundaries (b) in a single tier BS system (3 BSs) where the transmit power of BS1, BS2 and BS3 is the same. 37
3.4 Coverage map (a) and cell boundaries (b) in a single tier BS system (3 BSs) where the transmit power of BS2 and BS3 is the same and the transmit power of BS1 is 4 times of the transmit power of BS2 and BS3. 37
3.5 Performance of DL and UL in a signal tier (3 macro BSs, the non-uniform UE cluster centers are randomly distributed.). . 38
3.6 UE distribution pattern with non-uniform UEs where three additional macro BSs are deployed in the UE cluster centers. . . 38
3.7 Coverage map (a) and cell boundaries (b) in a single tier BS system (6 BSs where 3 macro BSs are put randomly and another 3 macro BSs are put in the user cluster centers) 39
3.8 Performance of DL and UL in a signal tier (red curve is for 3 macro BSs in a single tier where 3 macro BSs are independent with UE cluster distribution, black curve is for 6 macro BSs in a single tier where 3 macro BSs are independent with UE cluster distribution and another 3 macro BSs are deployed in UE cluster centers.) 39
3.9 UE distribution pattern with non-uniform UEs in which pico BSs are deployed in the UE cluster centers. 40
3.10 Coverage map (a) and cell boundaries (b) in a 2-tier BS system (6 BSs where 3 macro BSs (red triangles) are put randomly and 3 pico BSs (black triangles) are put in the user cluster centers) 41

3.11 Performance of DL and UL (blue curve is for 3 macro BSs in a single tier where 3 macro BSs are independent with UE cluster distribution, red curve is for 6 macro BSs in a single tier where 3 macro BSs are independent with UE cluster distribution and another 3 macro BSs are deployed in UE cluster centers, black curve is for 3 macro BSs and 3 pico BSs in a 2-tier system.) . 41

3.12 Coverage probability of cluster users (magenta points) when $P_1 = 2P_2$, $P_1 = 10P_2$, and $P_1 = 20P_2$ in a 2-tier BS system. . 42

3.13 Coverage probability of cluster users (magenta points) with different path loss exponents in a 2-tier BS system when $P_1 = 10P_2$. 42

3.14 UE distribution pattern with non-uniform UEs in which new 6 pico BSs are deployed in these additional 6 UE cluster centers in green. 43

3.15 Coverage map (a) and cell boundaries (b) in a 2-tier BS system (9 BSs where 3 macro BSs (red triangles) are put randomly, 3 pico BSs (black triangles) are put in the user cluster centers in magenta and 6 pico BS (black triangles) are put in the user clusters in green.) 44

3.16 Performance of DL and UL in a 2-tier BS system (red curve is for 3 macro BSs and 3 pico BSs in a 2-tier system and black curve is for 3 macro BSs and 9 pico BSs in a 2-tier system.) . 44

3.17 UE distribution pattern with non-uniform UEs in which new 6 femto BSs are deployed in these additional 6 UE cluster centers in green. Red triangles are macro BSs. Black triangle are pico BSs. Blue triangles are femto BSs. 45

3.18 Coverage map (a) and cell boundaries (b) in a 3-tier BS system (12 BSs where 3 macro BSs (red triangles) are put randomly, 3 pico BSs (black triangles) are put in the user cluster centers in magenta and 6 femto BSs (blue triangles) are put in the user clusters in green.) 46

3.19 Performance of DL and UL in a 2-tier and a 3-tier (red curve is for 3 macro BSs and 9 pico BSs in a 2-tier system and black curve is for 3 macro BSs, 3 pico BS and 6 femto BSs in a 3-tier system.) 46

3.20 Cell coverage boundaries diagram for a 2-tier cellular network based on user connectivity rule of maximum received power. (a) $P_1 = 1000P_2$, $\lambda_1 = 4\lambda_2$. (b) $P_1 = 100P_2$, $\lambda_1 = 4\lambda_2$. (c) $P_1 = 1000P_2$, $\lambda_1 = 8\lambda_2$. (d) $P_1 = 100P_2$, $\lambda_1 = 8\lambda_2$. 48

3.21 Cell extension example. (a) and (b) have the exactly same BS locations. (a) is $\{C_1, C_2\}$=$\{1, 1\}$ without cell extension and (b) is $\{C_1, C_2\}$=$\{1, 6.3\}$ with cell extension. The area is 1 km by 1 km. 49

4.1 Non-uniform user distribution example (D_2 is 55 m with orange line and it is Matern cluster process with radius $R = 40$ m). . 53

4.2 Range of attraction level and dependency level. 55

4.3 A user distribution realization of the non-uniform model (attraction level = 0.75 for (a), attraction level = 0.6 for (b) and attraction level = 0 for (c), dependency level = 1, blue curves are assumed to be cell boundaries). 56

4.4 A user distribution realization of the non-uniform model with a dependency level is 0.6 (attraction level is 0.8 for (a), attraction level is 0.7 for (b), attraction level is 0.5 for (c), blue curves are assumed to be cell boundaries). 57

4.5 Non-uniform user distribution Scenario 1 (a-f). The area is 1 km by 1 km. Green triangles are macro BSs and black triangles are small BSs. 58

4.6 Non-uniform user distribution Scenario 1 (g-l). The area is 1 km by 1 km. Green triangles are macro BSs and black triangles are small BSs. 59

4.7 Non-uniform user distribution Scenario 2. There are non-uniform cluster users (magenta points) distributed for small cells. Magenta circles are UE cluster boundaries distributed for small cells. Black diamonds are UE cluster centers. There are also almost uniform users (black points) distributed for macro cells in (b). Black circles are UE cluster boundaries for macro cells. The blue curves are the cell boundaries. The area is 1 km by 1 km. Green triangles are macro BSs and black triangles are small BSs. 60

4.8 Two ways to capture the traffic property in 1D 62
4.9 Pattern of 1D from left to right with sub-Poisson ($0 < C_E < 1$), Poisson ($C_E = 1$) and super-Poisson ($C_E > 1$) 63
4.10 Pattern of 2D from left to right with sub-Poisson ($0 < C_E < 1$), Poisson ($C_E = 1$) and super-Poisson ($C_E > 1$) 64
4.11 Example of Voronoi and Delaunay tessellations (Delaunay cell edges with blue lines and Voronoi cell edges with black lines, and the pattern points with red diamonds). 65
4.12 Measured normalized CoV for Delaunay cell edge length, Delaunay cell area, and Voronoi cell area (without base station offset between SAs and BSs.) 66
4.13 Measured CoV based on the attraction level and the dependency level 67
4.14 Measured coverage probability based on the attraction level and the dependency level 67

5.1 Example of spatial distances between UE, BS, and SA and the related notation in a 2-tier downlink system 70
5.2 Calculation example of PDF and CCDF of Random Variable L in the mth tier 74
5.3 PDF and CCDF example of L ($R = 100, D = 50$) 75
5.4 Downlink coverage probability of our designed non-uniform user distribution model, in which non-uniform users are distributed in small cells 83
5.5 Effect of base station offset D_2 on the downlink coverage probability 84
5.6 Downlink coverage probability as a function of BS density ratio $\frac{\lambda_2}{\lambda_1}$ between small cells and macro cells 86
5.7 Downlink coverage probability as a function of BS cell extension bias factor C_2 in small cells 89
5.8 Downlink coverage probability as a function of BS transmit power P_2 in small cells 91

6.1 System model example with the same cell extension association for both downlink and uplink 95
6.2 System model example with SINR in the downlink 96
6.3 System model example with SINR in the uplink 96
6.4 Example of spatial distances between UE, BS, and SA and the related notation in a 2-tier uplink system 97
6.5 Assumption of an active UE 100
6.6 Uplink Coverage probability of our designed non-uniform UE distribution model, in which non-uniform UEs are distributed in small cells (fractional power control factor $\epsilon = 0.5$) 109
6.7 Effect of the base station offset D_2 on the uplink coverage probability 110
6.8 Uplink coverage probability as a function of BS density ratio $\frac{\lambda_2}{\lambda_1}$ between small cells and macro cells 112
6.9 Uplink coverage probability as a function of BS cell extension bias factor C_2 in small cells 115
6.10 Uplink coverage probability as a function of BS transmit power P_2 in small cells 116
6.11 Uplink coverage probability as a function of fractional power control ϵ 118

7.1 Example of coverage probability definition 122
7.2 Comparison of the coverage probability of the downlink and the uplink in a single tier system (compared with the reference literature) 128
7.3 Comparison of the coverage probability of the downlink and the uplink in a 2-tier system 129

A.1 PDF and CCDF when $D_m \geq R_m$ and $l \leq D_m - R_m$ 139
A.2 PDF and CCDF when $D_m \geq R_m$ and $D_m - R_m < l \leq \sqrt{{D_m}^2 + R_m^2}$ 140
A.3 PDF and CCDF when $D_m \geq R_m$ and $\sqrt{{D_m}^2 + R_m^2} < l < D_m + R_m$ 140

A.4 PDF and CCDF when $D_m \geq R_m$ and $D_m + R_m \leq l$ 141
A.5 PDF and CCDF when $D_m < R_m$ and $l \leq R_m - D_m$ 141
A.6 PDF and CCDF when $D_m < R_m$ and $R_m - D_m < l \leq \sqrt{R_m^2 - {D_m}^2}$ 142
A.7 PDF and CCDF when $D_m < R_m$ and $\sqrt{R_m^2 - {D_m}^2} < l \leq \sqrt{R_m^2 + {D_m}^2}$ 142
A.8 PDF and CCDF when $D_m < R_m$ and $\sqrt{R_m^2 + {D_m}^2} < l < R_m + D_m$ 143
A.9 PDF and CCDF when $D_m < R_m$ and $R_m + D_m \leq l$ 143
A.10 PDF and CCDF when $D_m = 0$ and $l \geq R_m$ 144
A.11 PDF and CCDF when $D_m = 0$ and $l < R_m$ 144

C.1 An Example of BS Pattern (Red triangles are BSs in the first tier with $\lambda_1 = 3 * 10^{-6}$. Black triangles are BSs in the second tier with $\lambda_2 = 3 * 10^{-6}$. Cyan triangles are BSs in the third tier with $\lambda_3 = 6 * 10^{-6}$. The area is a square of 1 km by 1 km. Blue curves are cell boundaries.) 149

List of Abbreviation

2D	Two Dimension
3GPP	Third Generation Partnership Project
5G	Fifth Generation
AWGN	Additive White Gaussian Noise
BLER	Block Error Rate
BRP	Bias Received Power
BS	Base Station
BSO	Base Station Offset
CDF	Cumulative Distribution Function
CCDF	Complementary Cumulative Distribution Function
CDMA	Code Division Multiple Access
CoV	Coefficient of Variation
CRE	Cell Range Extension
DL	Downlink
DSPP	Doubly Stochastic Poisson Process
EE	Energy Efficiency
GSM	Global System for Mobile Communication
HCN	Heterogneous Cellular Network
HCPP	Hard Core Point Process
HetNets	Heterogeneous Networks
IAT	Inter Arrival Time
LOS	Line of Sight

LT	Laplace Transform
LTE	Long Term Evolution
NLOS	Non Line of Sight
MIMO	Multi Input Multi Output
MMWave	Millimeter Wave
OFDM	Orthogonal Frequency Division Multiplexing
PCP	Poisson Cluster Process
PDF	Probability Density Function
PGFL	Probability Generating Functional
PHP	Poisson Hole Process
PP	Point Process
PPP	Poisson Point Process
RX	Receiver
SA	Social Attractor
SE	Spectral Efficiency
SG	Stochastic Geometry
SINR	Signal to Interference Plus Noise Ratio
SNR	Signal to Noise Ratio
SPPP	Spatial Poisson Point Process
TX	Transmitter
UE	User Equipment
UL	Uplink
UAV	Unmanned Aerial Vehicle
UMTS	Universal Mobile Telecommunications System
WCDMA	Wideband Code Division Multiple Access

List of Symbols

α_i	path loss exponent in the ith tier
B_{ji}	coordinates of the ith BS in the jth tier
B_0	coordinates of the associated BS
BS_i^j	jth BS in the ith tier
C_i	cell extension bias factor in the ith tier
CoV	ratio of the standard deviation of the measurement to the mean of the measurement
C_I	Normalized Cov in 1D time domain
C_E	Normalized Cov in 2D space domain
D_i	base station offset in the ith tier
E	rate parameter of exponential cluster process
${}_2F_1$	Gauss hypergeometric function
$\bar{F}(g)$	CCDF of g
$f_u(r)$	probability density function (PDF) of UEs
$f(g)$	PDF of g
G_i	channel random power gain in the ith tier
I_k	Inter arrival time
I_{rj}	total received interference from the jth tier
K	total number of tiers
k	index of tier
κ	subset of cell tiers
L_0	path loss at a reference distance 1 m

L	distance between the UE and the BS that the UE belongs to
N_m	average number of users in each cluster
P_i	BS transmit power in the ith tier
$\mathbb{P}_{dl,c}$	the overall downlink coverage probability of the designed non-uniform distribution model
$\mathbb{P}_{ul,c}$	the overall uplink coverage probability of the designed non-uniform distribution model
R	cluster radius of linear or Matern cluster process
r_{ji}	distance of the user at the origin to the ith BS in the jth tier (i.e. B_{ji})
$\mathbb{S}$	subset of small cell tiers
S	total number of small cell tiers distributed with non-uniform user
SA_i^j	jth SA in the ith tier
T_i	SINR coverage target of the ith tier
V	the distance between a UE and the closest BS
x_i	coordinates of a random point in a subset
$\beta(x, y)$	density function at the coordinates of (x,y)
λ	point density
σ^2	power of the additive white Gaussian noise (AWGN)
ϕ	spatial Poisson point process
σ	variance of Thomas cluster process
ϵ	fractional power control factor

Chapter 1

Introduction

The remarkable increase of mobile users as well as applications for video streaming, social media, and data cloud services have created the need for higher data rates and increased system capacity. For example, data traffic increased 11-fold between 2013 and 2018 [1]. A 1000-fold increase of traffic demand as well as an increase of connected devices to 100 billion is predicted between 2020 and 2030 [2]. The exponentially increased traffic demand raises severe challenges to future cellular networks.

The 5G and future networks will be heterogeneous and include both macro and small cells, such as micro, pico, and femto cells. Heterogeneous Networks (HetNets) are defined as networks that are made up of different types of cells [3–9]. In 3GPP standard body, HetNets are proposed as a key candidate for solving the traffic demand challenge and for accommodating the increased number of mobile users. Some technically challenging issues of HetNets have been widely discussed (e.g., see [10–13]). Even higher densification of base stations (BSs) would be built into HetNets of 5G. Therefore, HetNets in 5G would provide significant improvement in both spectral efficiency (SE) and energy efficiency (EE). Network densification is adding more cell sites in order to increase network capacity. Densification is not a new paradigm in the cellular networks of 5G; it has existed since 1G [2]. In 1G voice only networks, a BS can cover a cell radius of about 10 miles and the densification is splitting the cell coverage into two or more smaller cells so as to combat path loss and accommodate more users. In 2G networks with low 64kbps speed data service, a macro BS can cover a cell radius a hundred meters to a few kilometers and the densification is such that small cells are deployed in order to offload the traffic data from macro cells. In 3G and 4G networks with high speed data services (up to 2Mbps for 3G and up to 1Gbps for 4G), small cells [14, 15] are covered by low-power radio access nodes that help provide cellular services to both indoor and outdoor areas from an open outdoor environment to

indoor buildings and homes. Small cells are set up to enhance range and capacity in areas that contain densely distributed users in urban areas and bring the dual benefit of high capacity and improved mobile traffic. In 5G networks with data services of extremely high speeds (above 1Gbps), such as in the fiber-like experience, the density of small cells will accelerate even faster in contrast to 4G in order to provide extremely high data rates and capacity.

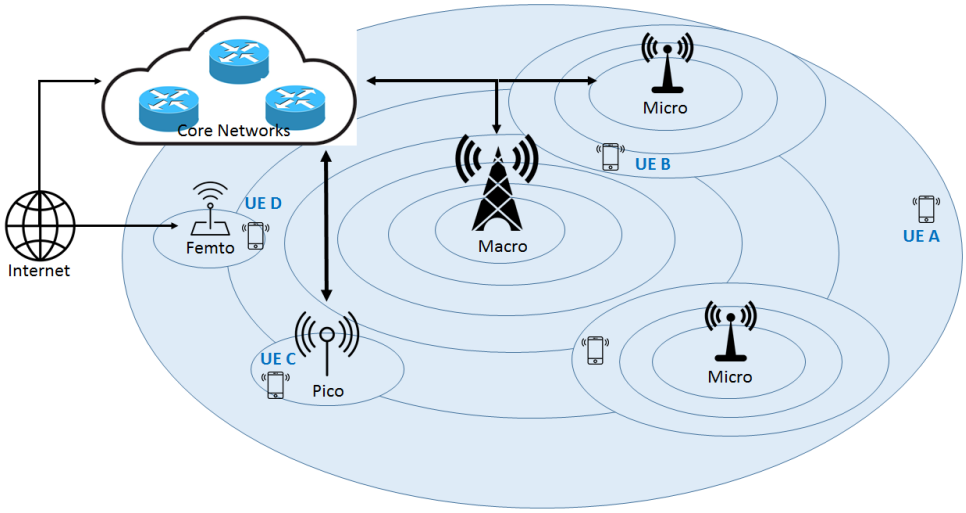

Figure 1.1: Network architecture for 5G HetNets

HetNets are multi-tier cellular networks where macro cells and small cells (micro cells, pico cells, and femto cells) coexist. Figure 1.1 presents the network architecture of 5G HetNets. For example, the user equipment named UE A is in the coverage of the macro cell. UE A will communicate with other users through the macro cell's BS and core networks. Similarly, users named UE B, UE C, and UE D are in the coverage of the micro cell, pico cell, and femto cell respectively. Macro cells supported by high transmit power BSs cover a wide area (particularly in rural areas or along highways) while small cells are deployed in hot spots in order to improve the capacity, enhance coverage of macro cells near cell boundaries, and increase the frequency reuse factor. A micro cell is used in a densely populated urban area. Pico cells are used in areas smaller than micro cells, such as a large office, a mall, or train station. Femto cells are used at homes or small offices. Femto cells can be installed by any consumer while macro cells, micro cells, and pico cells can be deployed only by operators. User-deployed femto cell can have open access, which allows any user to access the femto cell, or closed access where only certain users are permitted to access the femto cell. In Table 1.1, the parameters of different cell tiers are provided. For example, the transmit power of macro BS is around 46 dBm, the transmit powers of

micro BS and pico BS are around 16 dB lower than that of macro BS. Transmit power of a femto BS is around 26 dB lower than that of macro BS. A conventional macro cell network or a small cell network makes up a network tier. The conventional macro cell network is called a single-tier network. We call a network consisting of macro cells and any type of small cells as a 2-tier network. And then the networks consisting of multiple type of cells as multi-tier networks. Multi-tier networks support expansion in conventional cellular network with a flexible and economic architecture design [16].

Differences between macro cell, micro cell, pico cell, and femto cell are shown in the following table (referred from [17] and link: *//www.rfwireless-world.com/Tutorials/femtocell-vs-picocell-vs-microcell.html*).

Table 1.1: Typical parameters of different tiers of cells

	macro cell	**micro cell**	**pico cell**	**femto cell**
Transmit power	46 dBm	30 dBm	30 dBm	20 dBm
Coverage radius	1 km to 20 km	500 m to 2 km	50 m to 500 m	4 m to 10 m
Deployment location	outdoor	outdoor	outdoor as well as indoor	indoor
Installation	by operator	by operator	by operator	by user

All of the network tiers reuse the available spectrum to improve the spatial spectrum efficiency and network capacity. However, in doing so, cross-tier and co-tier interference is created. The spatial distribution of BS and user equipment (UE) has a big impact on the performance of cellular networks because the received signal power and interference signal power depend on the distance between transmitter (TX), receiver (RX), and interferer. Emerging network paradigms, such as femto cells, which are overlaid upon conventional cellular networks, improve the system capacity and throughput. In these new paradigms, BSs and UEs appear to be randomly located. Therefore, it is important to create accurate spatial models to evaluate the impact of the cross-tier and co-tier interference on the overall performance of the network that occur in HetNets. An accurate node (BS or UE) model is a key factor in the research and design of 5G heterogeneous cellular networks.

1.1 Problem Definition

In single-tier networks, the distribution of BSs is assumed to be a regular grid model, in which BSs are deployed on a two-dimensional grid (e.g., a square lattice or a hexagonal lattice). Researchers analyze single-tier networks by either Monte Carlo simulations [18] or simplifying assumptions that inter-cell interference only comes from two neighboring cells [19]. Nowadays, the distribution of BS is becoming more heterogeneous due to the introduction of small cell tiers such that Poisson point process (PPP) distribution of BSs is assumed where the distance between BSs is totally random. However, operators do not randomly place their macro cell BSs over a given area. To tackle the distribution model of macro BSs, hard core point process (HCPP) rather than PPP distribution is considered as a candidate, in which there is a defined minimum distance between any two macro BSs. Therefore, for macro BSs distribution model, there are two main approaches according to the above discussion. The first approach is a PPP distribution while the second approach is a HCPP. For the other tiers of the networks, such as small cell tiers, there are also two main approaches. The first approach is also a PPP, in which different tiers of BSs have different parameters (e.g., transmit power, density, and signal to interferenc plus noise ratio (SINR) coverage threshold) while the second approach is a Poisson cluster process (PCP) to specify the cluster property of small BSs. Although the second approaches of both macro BSs and small BSs are more practical, we still choose the first PPP approaches of both macro BSs and small BSs as the basic assumptions in this thesis. The reasons are as follows. First, it is possible to achieve a tractable closed-form performance analysis for BSs using the PPP distribution. Second, the first PPP approaches of both macro BSs and small BSs are very popular assumptions in the literature. We may take the BS distribution assumption as PPP and focus our research on non-uniform UE distribution. Finally, we can take our research as the baseline or lower bound of practical BS cases (for instance, HCPP, or PCP distribution) and extend our research to more complicated and practical BS distribution in future work. Hence, in this thesis we make the assumptions of BS distribution as the first PPP approaches for both macro BSs and small BSs. This is called the K-tier model, which is a popular multi-tier BS distribution model of HetNets in the literature. In K-tier networks, each tier of BSs, such as macro BSs and small BSs, are distributed according to a homogeneous spatial Poisson point process (SPPP) [20–22]. SPPPs are independent between tiers. BS locations in the kth tier are generated by SPPP with density λ_k, transmit power P_k, Signal to interference plus noise ratio (SINR) coverage threshold T_k, and path loss exponent α_k.

In the literature, the locations of BSs are modeled as K-tier PPP in the spatial domain

and the locations of UEs are usually modeled by another independent PPP or are called uniform distribution[1]. But in practice, UEs often concentrate or cluster near some social attractors (SAs), such as bus stops, shopping malls, or convention centers rather than distributed randomly. Moreover, there is a spatial dependency between BSs and SAs locations and a simple PPP does not represent the UE distribution. Hence, the model or the framework with non-uniform UE distribution[2] in heterogeneous networks must be a realistic scenario, which can be represented by spatial dependency between UEs, SAs, and BSs.

1.2 Motivation

5G supports the proliferation of devices that need a mobile connection. The devices can be phones, computers, home appliances, cars, wearables, and other devices that are connected to the multi-tier networks. As a result, the complex networks and the volume of devices make 5G difficult to analyze. Accurate performance analysis is important for enabling system developers to design networks that meet quality of service requirements. The performance analysis of the networks is normally obtained through time-consuming system simulation based on simple assumptions of the location of BSs and UEs. Analysis provides the design baseline, system insight, and parameter dependencies for network operators and carriers. However, the mathematical performance analysis of networks are challenging. Presently, stochastic geometry is adopted as a new approach to model the multi-tier cellular network. It provides the tools and techniques for computing the distribution of SINR, especially with the node distribution of PPP, which causes the possibility of the mathematical analysis of coverage probability in the downlink and the uplink.

1.3 Contributions

On the design and research of HetNets, there are two aspects that we should tackle. The first aspect is to build system models that cover the heterogeneity and irregularity in BS distribution and UE distribution. The system models should be realistic and simple enough to be used. The second aspect is to carry out the performance analysis like coverage probability as a function of SINR such that we better understand the system design foundation

[1]In this thesis, the uniform UE distribution means that the average UE density is the same.
[2]In this thesis, the non-uniform UE distribution means that the average UE density is different.

and system infrastructure of HetNets. The main goal of this thesis is to develop a comprehensive framework of the non-uniform UE distribution such that it has tractable analysis in HetNets. The main contributions are summarized as follows.

- **New non-uniform UE model based on K-tier BS HetNets**
  - **New non-uniform UE model.** We develop a flexible and practical non-uniform UE model, where UEs are distributed around cluster centers called social attractors (e.g., SAs, such as bus stops, shopping malls, conference centers). Here UEs are symmetrically, independently, and identically distributed around SAs, which is Possion cluster process (PCP) to capture the correlation between UEs and SAs. SAs have base station offset (BSO) with their BSs to capture the correlation between SAs and BSs.
    - **Parameters in new non-uniform UE model.** There are two parameters of our non-uniform UE model. One parameter is the cluster radius, which determines the correlation (represented as attraction level) between UEs and SAs and the other parameter is the base station offset, which determines the correlation (represented as dependency level) between SAs and BSs. The designers can adjust two parameters to obtain their preferred and specific heterogeneity. This non-uniform UE model is tunable such that it can cover the wide possibilities from homogeneous to heterogeneous.
    - **Definition of attraction level and dependency level.** We define the attraction level and the dependency level, which are determined from the parameters of the cluster radius and the base offset. The attraction level and the dependency level are one possible way to express these two parameters. Because we confine the value range from 0 to 1, the attraction level and dependency level better represent the degree of correlation. In the simulations and visualized figures of this thesis, we use the attraction level and dependency level to stand for the characteristic of non-uniform user model. The concept of the attraction level is not new and it has been utilized in the research [23, 24]. High attraction level stands for the case of high heterogeneity around SAs (low cluster radius), while low attraction level stands for the case of approaching uniform distribution with low heterogeneity. However, the dependency level is novel in this thesis in that it indicates the placement relationship between SAs and BSs. Because of physical constraints, BSs can not be deployed exactly in the cluster centers

(e.g., SAs). This thesis considers the joint relationship between BSs, UEs, and SAs.

- **Heterogeneity analysis of non-uniform UE distribution.** The relationship between UE heterogeneity and designed user model's characteristics, such as the attraction level and dependency level are presented based on the normalized coefficient of variation (CoV), which is the standard deviation of measured Voronoi cell area are divided by the mean of measured Voronoi cell area.

- **Performance analysis**
  This thesis carries on the research of both downlink and uplink performance analysis for non-uniform UE distribution.

  - **Downlink.**

    * **Downlink coverage probability.** In this thesis, the performance analysis of the downlink coverage probability based on our non-uniform UE model is derived step by step.
    * **Derivation challenges.** Because the coverage probability is the complementary cumulative distribution function of SINR, the challenging part of the performance analysis is the characterization of the total interference. And the derivation of the probability density function (PDF) and complementary cumulative distribution function (CCDF) of the distance between a UE and its associated BS is also crucial.
    * **Simulations.** The simulation results demonstrate the accuracy of the performance analysis. In practice, we can do away with the time consuming system simulations and use the equations given in this thesis to provide the downlink coverage performance.
    * **System Insight.** Based on the derived performance analysis, the effect of system parameters is shown. The performance is quite different in contrast to the well researched case on the uniform UE distribution. This justifies the reason to seek for a system insight, such as the effect of system parameters on the non-uniform UE distribution. For example, for uniform UE distribution on K-tier HetNets, the increase of the density of small BS will not decrease the downlink coverage probability (e.g., more BSs can be deployed without decreasing the downlink coverage probability while the capacity increases with the increase of the density of small BSs). But for

non-uniform UE distribution, the above conclusion does not hold. Therefore, the system insight from the derived performance equations is helpful to understand the networks, especially since it will show that the system insight does not align with our expectation and is different from the system insight on the widely researched uniform UE distribution in the literature.

- **Uplink**
  - **Uplink coverage probability.** The performance analysis of the uplink coverage probability for the non-uniform UE model is also derived.
  - **Derivation challenges.** The uplink performance analysis is more challenging than the downlink case due to the characterization of the uplink interference and the uplink power control. We make some assumptions so that it is possible to obtain the performance analysis of the uplink coverage probability since the characterization of the uplink interference is not available and the uplink power control causes UE transmit power to fluctuate.
  - **Simulations.** The simulation results have limited mismatch (less than 1 dB) with the analytical equations due to the assumptions made. It still can be regarded as a reference if the system requirement is not very strict.
  - **System insight.** The effect of system parameters in the uplink is also obtained.

1.4 Thesis Organization

The organization is as follows.

Chapter 2 provides the background on stochastic geometry, which focuses on point processes. Then, a literature review about non-uniform UE distribution is provided.

Chapter 3 presents the system model, which includes BS distribution, user distribution, and UE connectivity. We also introduce the coverage map, cell boundaries and performance of non-uniform users in single tier or multi-tier BS systems to demonstrate the benefits of deploying small cells.

Chapter 4 defines a spatial distribution of non-uniform UE model. In the model, the UEs are distributed in a cluster with the center being SA, which has base station offset to its BS. The corresponding UE patterns or distribution examples are demonstrated in this chapter. Finally, the heterogeneity analysis of non-uniform UE distribution is illustrated.

Chapter 5 explains the downlink coverage probability analysis. The analytical performance expression of the coverage probability is achieved through mathematical derivation. The simulation results included demonstrate the accuracy of the analytical expression. The effect of system parameters based on the above theoretical analysis is given.

Chapter 6 shows the uplink coverage probability analysis. The analytical performance equations of the uplink coverage probability are given. The effect of system parameters are also investigated.

Chapter 7 summarizes the comparison between the downlink and the uplink analysis.

Chapter 8 concludes the thesis and explores possibilities for future work.

1.5 Publications

- Chao Li, Abbas Yongacoglu, and Claude D′Amours, Downlink Coverage Probability with Spatial Non-uniform User Distribution Around Social Attractors, IEEE 24th International Conference on Telecommunication (ICT), Cyprus, May, 2017
- Chao Li, Abbas Yongacoglu, and Claude D′Amours, Coverage Probability of the Downlink in Heterogeneous Cellular Networks on Nakagami-m Fading Channel,IEEE 15th International Conference on Communication Systems (ICCS), China, Dec, 2016
- Chao Li, Abbas Yongacoglu, and Claude D′Amours, Heterogeneous Cellular Network User Distribution Model, IEEE 8th Latin-American Conference on Communications (LATINCOM), Colombia, Nov, 2016
- Chao Li, Abbas Yongacoglu, and Claude D′Amours, Coverage Probability of the Downlink in Heterogeneous Cellular Networks Considering the Effect of User Clustering Around Spatially Depended Social Attractors, IEEE Computer-Aided Modeling Analysis and Design of Communication Links and Networks (CAMAD), Canada, Oct, 2016
- Chao Li, Abbas Yongacoglu, and Claude D′Amours, Mixed Spatial Traffic Modeling of Heterogeneous Cellular Networks, IEEE International Conference on ubiquitous Wireless Broadband (ICUWB), Canada, Sep, 2015
- Chao Li, Abbas Yongacoglu, and Claude D′Amours, Spatial traffic modeling with adjustable heterogeneity based on signal to interference ratio, 2nd International Conference on Telecommunication Systems and Networks in Istanbul (MIC-Telecom), Turkey, Dec, 2014

Chapter 2

Background on Stochastic Geometry and Literature Review of Non-Uniform User Models

Stochastic geometry is the study of random spatial realizations [25, 26]. It is a powerful mathematical tool to model single-tier and multi-tier cellular networks for wireless networks with random topologies. Before the stochastic geometry became popular, the mathematical performance analysis depended on overly-simplified assumptions. For example, the Wyner model in [27] assumes only one or two interferers, while in [18] the authors consider the total interference as a random variable and the interferers in [28] are assumed to be the same distance from the transmitter (TX). Using stochastic geometry, the spatial randomness is reflected and tractable analysis[1] is also achieved. By averaging over many random spatial realizations, stochastic geometry gives a method of defining the characteristics of networks, whose nodes are placed according to some probability distribution.

In wireless networks, such as cellular networks, the geometry (the locations of BSs and UEs) plays a key role because of the random interference. The assumption of simple traditional single-tier BSs is the hexagonal grid [29–31], which leads to either time-consuming analysis or inaccurate results. In practice, the position of BSs follows a random pattern as opposed to the grid pattern. Multi-tier cellular networks where each tier is deployed independently have even more spatial randomness. The received interference signal power can limit the system performance. The received signal power and interference signal power are random variables due to the random placement of BSs, the random placement of UEs, and

[1] Tractable analysis means that the analysis could be handled or managed through mathematical derivations. The analysis could be expressed with closed-form mathematical equations.

the random fading power gain that is present in the channel. Dealing with the above random items, the techniques based on stochastic geometry provide the performance analysis, such as connectivity, capacity, coverage probability, and other performance metrics. [32–40] also give more details about stochastic geometry. Normally, the location of the nodes is modeled as a point process. A point process is one of the important aspects in stochastic geometry. A point process is a kind of random process for which one pattern makes up of a set of isolated points and is a countable random collection of points that reside in some measure space. A point process (PP) can capture the network properties. A temporal point process is a collection of mathematical points with random intervals defined in one dimension, such as the time of arrival points. A spatial point process is a collection of mathematical points randomly located in a space, which is a multiple dimensional domain. A spatial point process is frequently used in geographical models, such as positions of towns, cities, BSs, or UEs.

2.1 Classical Poisson Distribution

The Poisson distribution is the basis of most point processes.

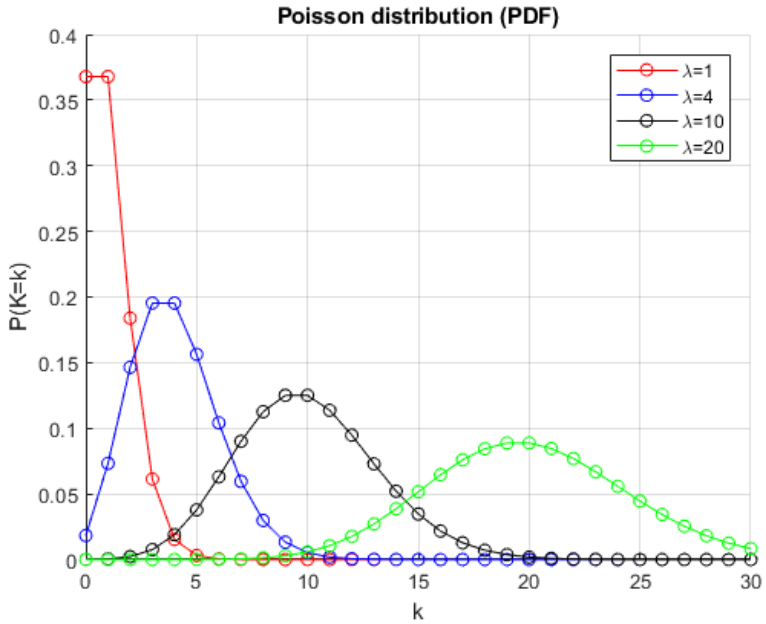

Figure 2.1: Probability of Poisson distribution

Definition 2-1. A Poisson distribution is defined as follows.

Let K be the number of events in a given time period. If the mean number of events in a given time period is λ, the probability of observing k events in a given time period is:

$$P(K = k) = e^{-\lambda}\frac{\lambda^k}{k!}. \tag{2.1}$$

The random variable K is said to follow a Poisson distribution with a mean parameter λ, denoted $K \sim Poi(\lambda)$. Figure 2.1 gives examples of Poisson distributions with different values of λ.

2.2 Temporal Point Process

A temporal point process is a stochastic, or random process composed of isolated events that occur in continuous time [41].

Definition 2-2. A temporal point process is a random process whose realizations consist of the times τ_j, $\tau_j \in \mathbb{R}$, $j = 0, \pm1, \pm2$ of isolated events scattered in time [42].

Normally, there are three types of representations of temporal point process:

- Step function: the total number of events since the time τ_j.
- Dirac delta function: dirac delta function is presented at τ_j where the event occurs.
- Event intervals: the time interval from the current event τ_j to the previous event τ_{j-1}.

2.3 Spatial Point Process

According to the network topology assumed, a matching spatial point process is chosen to represent the network nodes, such as BSs and UEs. In the following subsections, the most popular spatial point processes in cellular networks are listed. The practical scenarios and examples based on BS distribution are also given.

2.3.1 Poisson Point Process (PPP)

Poisson point process plays a fundamental role in the theory of PPs. Since they carry the property of complete spatial randomness, the mathematical model is highly tractable. But it is not realistic to assume a complete random model. However, it can be regarded as a reference or a baseline.

Definition 2-3. A point process is a PPP if and only if [32]

- The number of points $N(B_1)$,...,$N(B_k)$,...,$N(B_K)$ in disjoint subsets B_1,...,B_k,...,B_K is a Poisson random variable.
- The number of points $N(B_1)$,...,$N(B_k)$,...,$N(B_K)$ in disjoint subsets B_1,...,B_k,...,B_K are independent.

2.3.1.1 Homogeneous PPP

Definition 2-4. A PPP is a homogeneous PPP (i.e. uniform) if the density λ is the same in all subsets. The mean number of points in disjoint subsets B_1,...,B_k,...,B_K is $A(B_1)\lambda$,...,$A(B_k)\lambda$,...,$A(B_K)\lambda$. $A(B_k)$ is the area in subset B_k.

The probability when the number of points in the subset B_k is n is

$$P(n, B_k) = \frac{(A(B_k)\lambda)^n \exp(-A(B_k)\lambda)}{n!}. \tag{2.2}$$

The complete independent property of homogeneous PPP leads to some useful properties, such as the superposition and thinning properties. The superposition of n homogeneous PPPs with the densities λ_1 to λ_n is a homogeneous PPP with the density $\lambda_T = \sum_{j=1}^{n} \lambda_i$. Furthermore, randomly thinning a homogeneous PPP with the density λ, where each point is independently removed with some probability p, forms another homogeneous PPP with the density $\lambda_T = (1-p)\lambda$.

The homogeneous PPP of a cellular network proves to be more tractable than a hexagonal model [43,44] because the Campbell's theorem and Probability Generating Functional (PGFL) based on PPP simplify the calculation and result in the closed-form equations. Traditionally, the positions of BSs are well represented in a hexagonal model. However, the

problem with the hexagonal model is that the performance analysis is intractable[1]. The resulting SINR with hexagonal model is still a random variable in the case of shadowing and fading and it is difficult to match the distribution of the related SINR random variable. Homogeneous PPPs were introduced due to their well-defined tractability.

The tractability of homogeneous PPP comes from the two properties explained in [45]. These two properties can transform the unlimited sum or the unlimited product over PPP into tractable mathematical integral expression. Let ϕ be a homogeneous PPP set with mean measure λ and let $f(x)$ be a function in $\mathbb{R}^2$.

Property 2-1. Sums over PPP (Campbell's Theorem):

$$\mathbb{E}[\sum_{x_i \in \phi} f(x_i)] = \lambda \int_{\mathbb{R}^2} f(x) dx, \tag{2.3}$$

- $f(x_i)$ can be any function.
- The expectation of the function summed over a PPP ϕ can be obtained through Campbell's theorem.
- The expectation is equal to an integral involving the mean measure λ of the point process.

An example in wireless network communication is when a BS sends a signal to a UE, all other BSs can be regarded as interferers. If the locations of the interfering BSs form a PPP, the expectation of the sum of the interference can be calculated by an integral using Campbell's theorem, which is the stochastic geometry model of wireless networks.

Example 2-1. Calculate the expectation of total interference power at the origin from the BSs with homogeneous PPP if path loss exponent is α and constant transmit power of BSs is P. Assume the distance $\|x_i\|$ between the interference and origin is $d_{min} < \|x_i\| < d_{max}$.

[1]Intractable analysis means that the analysis could be not handled or managed through mathematical derivations. The analysis could not be expressed with the closed-form mathematical equations.

The total interference is

$$I_r = \sum_{x_i \in \phi} f(x_i) = \sum_{x_i \in \phi} P\|x_i\|^{-\alpha}. \tag{2.4}$$

According to Campbell's theorem, the expectation of the total interference is

$$\begin{aligned} \mathbb{E}[I_r] &= \mathbb{E}[\sum_{x_i \in \phi} P\|x_i\|^{-\alpha}], \\ &= \lambda \int_{\mathbb{R}^2} P\|x\|^{-\alpha} dx, \\ &= \lambda \int_{d_{min}}^{d_{max}} \int_0^{2\pi} P r^{-\alpha} d\theta r dr, \\ &= 2\pi\lambda \int_{d_{min}}^{d_{max}} P r^{-\alpha+1} dr, \\ &= \frac{2\pi\lambda P}{2-\alpha} ({d_{max}}^{2-\alpha} - {d_{min}}^{2-\alpha}). \end{aligned} \tag{2.5}$$

Property 2-2. If ϕ is a Poisson point process with mean measure λ, products over PPP ϕ for any function $f(x_i)$(Probability Generating Functional (PGFL)) is:

$$\mathbb{E}[\prod_{x_i \in \phi} f(x_i)] = \exp(-\lambda \int_{\mathbb{R}^2} (1 - f(x)) dx). \tag{2.6}$$

Example 2-2. Calculate the Laplace transform of the total interference at the origin.

$$\begin{aligned} \mathbb{E}[e^{-sI_r}] &= \mathbb{E}[e^{-s\sum_{x_i \in \phi} P\|x_i\|^{-\alpha}}], \\ &= \mathbb{E}[\prod_{x_i \in \phi} e^{-sP\|x_i\|^{-\alpha}}], \\ &= \exp(-\lambda \int_{\mathbb{R}^2} (1 - e^{-sP\|x\|^{-\alpha}}) dx), \\ &= \exp(-2\pi\lambda \int_{d_{min}}^{d_{max}} (1 - e^{-sPr^{-\alpha}}) r dr). \end{aligned} \tag{2.7}$$

The Laplace transform of the total interference is the key step in the closed-form tractable analysis of a homogeneous PPP. For example, the coverage probability analysis depends on SINR, which is the ratio between the received signal to the total interference

plus noise. If the Laplace transform of the total interference is characterized by an integral as in Equation 2.6, it is easy to determine the coverage probability.

2.3.1.2 Heterogeneous PPP

Definition 2-5. A PPP is a heterogeneous PPP or inhomogeneous PPP if the density is not equal among each subset. Assume that the density function is $\beta(x, y)$, $x, y \in \mathbb{R}^2$. The density measure $\lambda(B_k)$ over B_k is $\int_{B_k} \beta(x, y)dxdy$. The mean number of points in subsets B_1,...,B_k,...,B_K is $A(B_1)\lambda(B_1)$,...,$A(B_k)\lambda(B_k)$,...,$A(B_K)\lambda(B_K)$.

The probability when the number of points in the subset B_k is n is

$$P(n, B_k) = \frac{(A(B_k)\lambda(B_k))^n \exp(-A(B_k)\lambda(B_k))}{n!}. \tag{2.8}$$

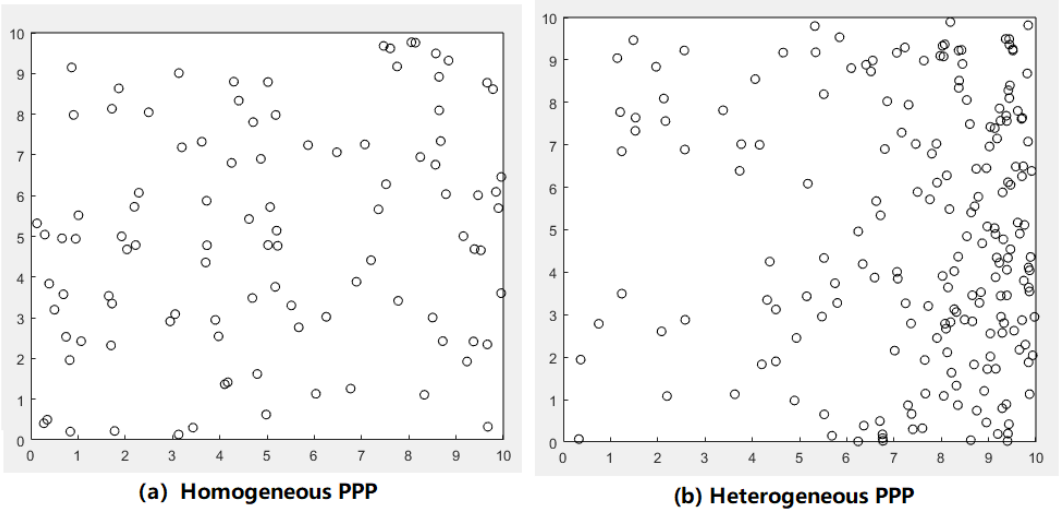

Figure 2.2: Realization of homogeneous PPP and heterogeneous PPP

Figure 2.2 (a) shows a realization of a homogeneous PPP while Figure 2.2 (b) shows a realization of a heterogeneous PPP. A realization of a spatial point process is considered as spatial point pattern with countable collection of points. The square is 10 m by 10 m and split into 100 grid squares of 1 m by 1 m. In this realization, the density λ is 1 user per square meter for homogeneous PPP and the density function β is $\frac{\exp(1+0.3x)}{10}$ users per square meter (x is the horizontal coordinate) for heterogeneous PPP.

2.3.1.3 Practical Scenarios and Examples

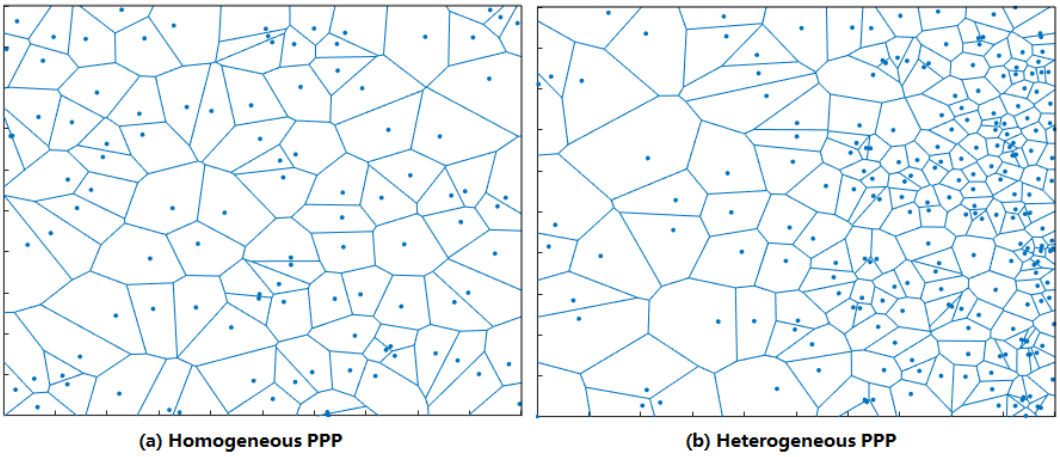

Figure 2.3: Example of the Voronoi region of homogeneous PPP and heterogeneous PPP

PPP, especially homogeneous PPP, is a very popular distribution for modeling the nodes, such as BSs and UEs. Figure 2.3 gives an example of points with PPP distribution and their Voronoi cells. If we assume the points as BSs, curves are cell boundaries with the closest BS association rule. In Figure 2.3 (a), the mean density is the same across the whole area such that it is possible to get the tractable performance analysis using the Campbell's theorem and PGFL. In Figure 2.3 (b), the mean density is not the same across the whole area. The density is higher when approaching the right side. It models the scenario that more UEs need to be served on the right side if points are assumed as BSs. However, it is challenging for heterogeneous PPP to get a tractable analysis.

2.3.2 Transforming a Spatial Point Process

For different conditions we may want to modify a uniform PPP to obtain a new PP. This new point process is obtained by transforming an existing point process. It includes displacement, thinning, and superposition [46].

2.3.2.1 Displacement

Displacement is the mapping of points in a point process to the same or another space by a defined mapping rule.

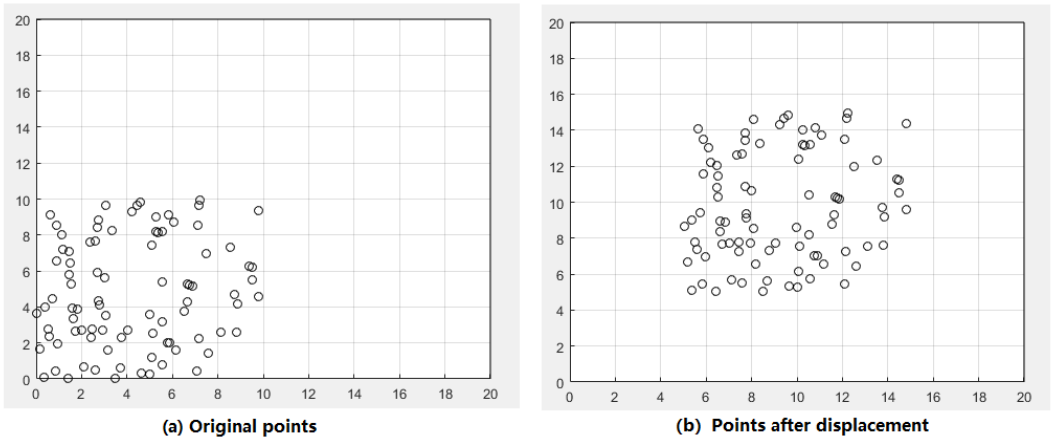

Figure 2.4: Realization 1 of displacement (points are displaced by shifting)

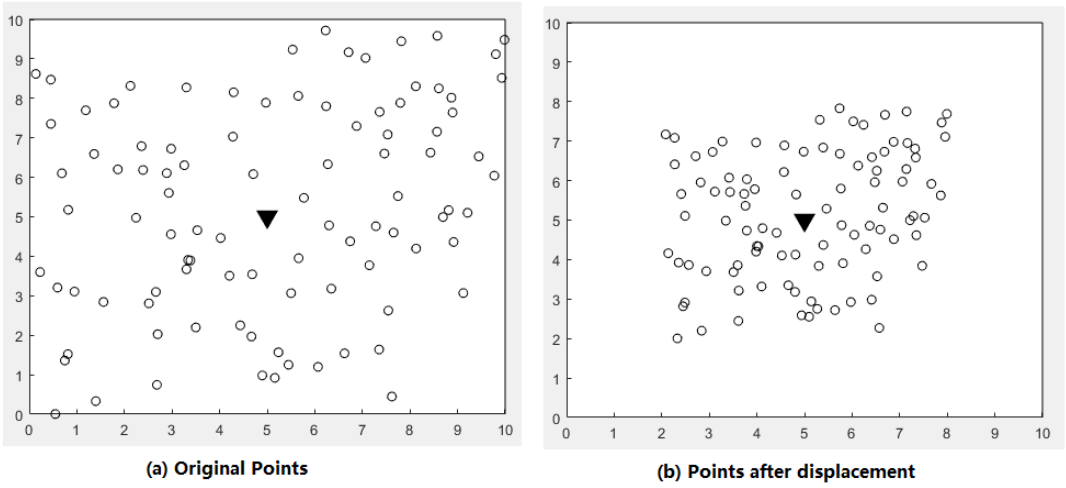

Figure 2.5: Realization 2 of displacement (points are displaced by contraction)

Figure 2.4 and Figure 2.5 show the realizations of displacing a point process to another point process in two dimensions. The mapping rule of Figure 2.4 is from (x, y) to $(x + 10, y + 10)$. The mapping rule of Figure 2.5 is from (x, y) to $(0.6x + 2, 0.6y + 2)$. (x, y) are the original point coordinates.

Independent displacement consists of independently mapping each point of the original PPP to a random placement. The result of independent displacement of PPP is still a PPP .

The displacement of PPP has two advantage. The first advantage is that the displacement of PPP would result in the expected user distribution, such as more users around the

cell center. The second advantage is that the performance analysis is potentially tractable if it is displaced from a tractable homogeneous PPP.

2.3.2.2 Thinning

Thinning of a point process is to remove some points according to defined thinning rule. There is independent thinning and dependent thinning. If the original point process is homogeneous PPP, the remaining independent points also belong to a homogeneous PPP.

Figure 2.6 sketches a realization of thinning. Thinning rule in this example is that each point is retained with the probability of 30%. In Figure 2.6, (a) shows original points in black. (b) includes the same points as in (a) except that retained points are labeled in red during thinning. (c) includes retained points in red.

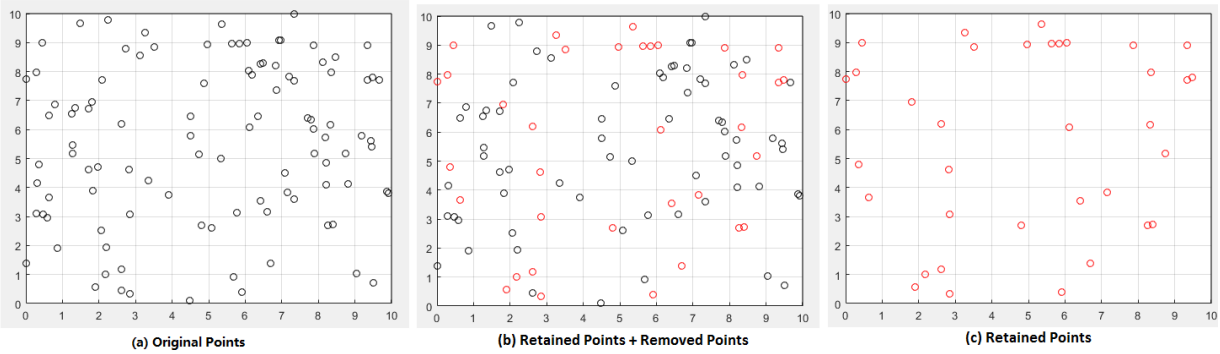

Figure 2.6: Realization of thinning (black points are thinned with the probability of 70%)

2.3.2.3 Superposition

Superposition is the operation of the sum of two or more point processes. The superposition of two independent PPP with a density λ_1 and λ_2 is still a PPP with a density $\lambda_1 + \lambda_2$.

Figure 2.7 shows a realization of superposition of two PPP. (a) is PPP with a density $\lambda = 1$ in black . (b) is PPP with a density $\lambda = 1$ in red . (c) is the resulting superposition of (a) and (b). (c) is still a PPP with a density $\lambda = 2$.

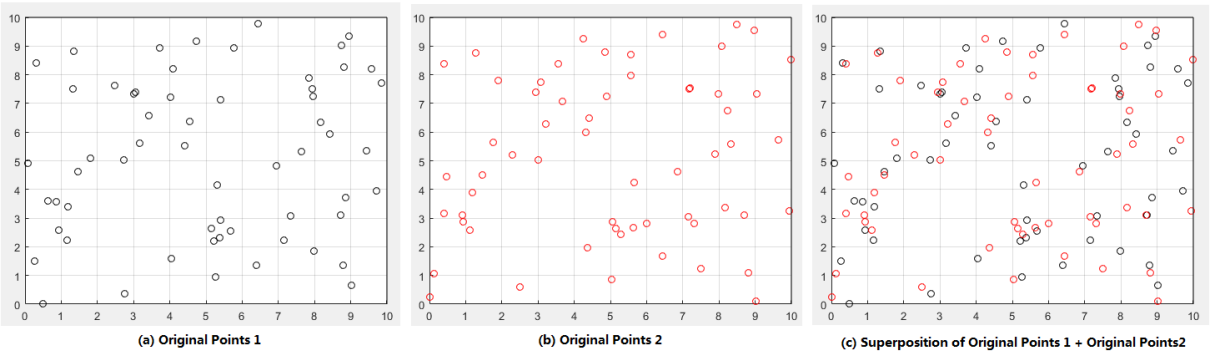

Figure 2.7: Realization of superposition (superposition of two point patterns with the same density)

2.3.2.4 Practical Scenarios and Examples

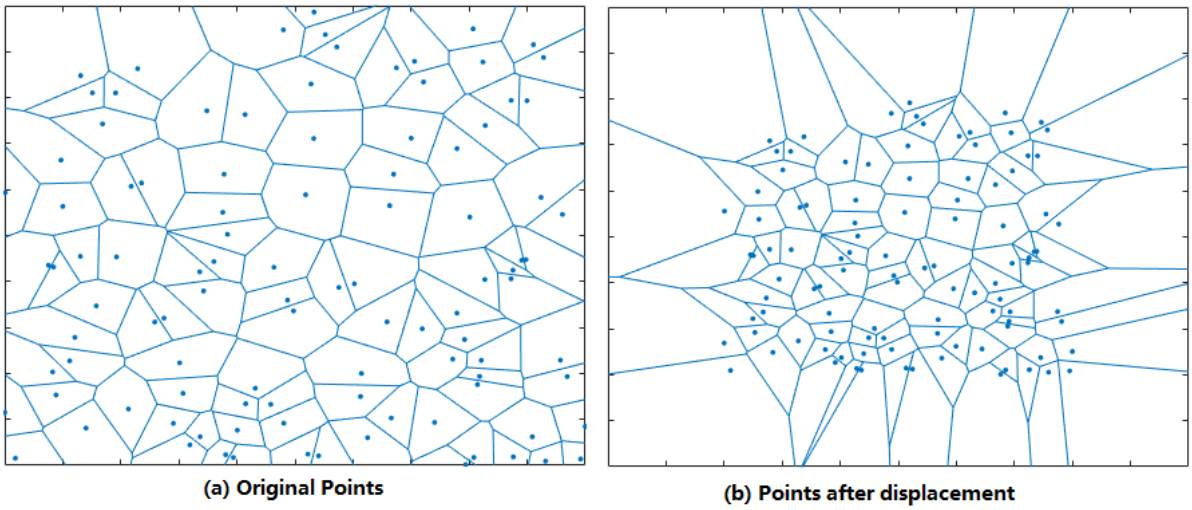

Figure 2.8: Example of displacement points and their Voronoi region

Figure 2.8 gives an example of point distribution of displacement and the Voronoi region of points. The original point process is a homogeneous PPP. Any mapping or displacement rule can be applied to obtain the resulting distribution. In this example, the resulting distribution of displacement is shifting the points position toward to the area center according to a parameter. The cell boundaries of original PPP BS distribution and displaced BS distribution are all shown in this figure if we assume the points are BSs with closest BSs association rule. The cell coverage area are the Voronoi region. This example represents the scenario where more users are distributed at the center area and fewer users are distributed at the edge if points are assumed as BSs. Hence, more BSs should be distributed

at the center area so that the cell radius of BSs at the center becomes smaller such that it serves and supports more users. Resulting displacement is obtained from homogeneous PPP so that it is possible to get the closed-form performance analysis.

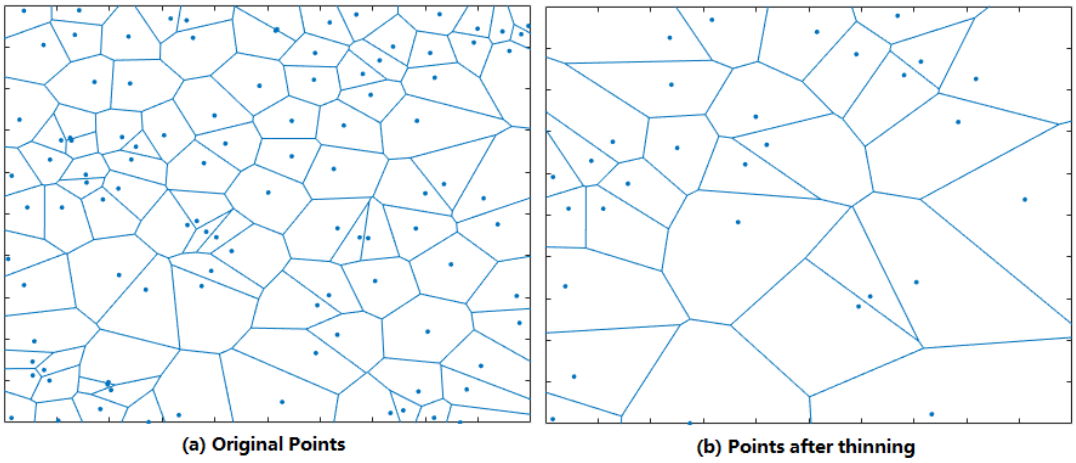

Figure 2.9: Example of thinning points and their Voronoi region

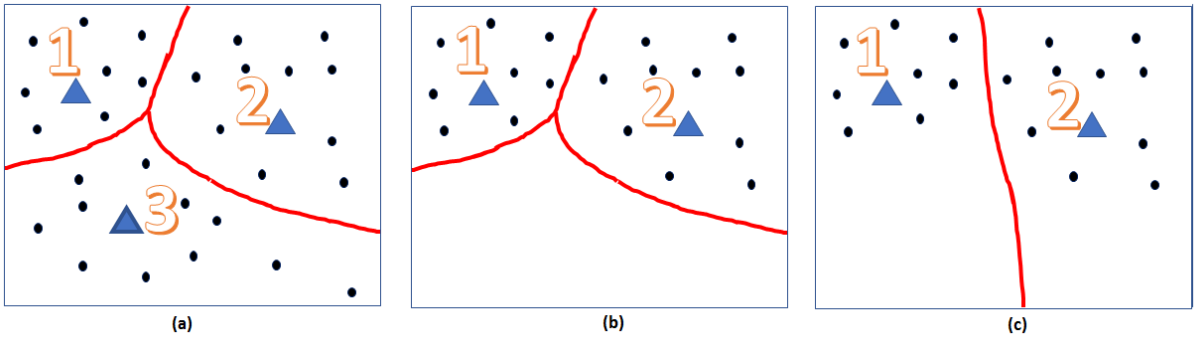

Figure 2.10: Example of generating non-uniform users using thinning

Figure 2.9 indicates an example of point distribution of thinning and the Voronoi region of points. The original point process is also a homogeneous PPP. Thinning process retains each point independently with a given probability. The retained or kept BSs will have larger cell coverage areas if we assume the retained points are BSs. The retained points distribution is still homogeneous PPP. Figure 2.10 gives an example how to generate non-uniform user distribution using thinning process. Blue triangles are BSs, black points are users and red curves are cell boundaries. The users are distributed uniformly and independently in the original point process (a). The third BS is thinned and the users associated with the third BS is also thinned shown in (b). There are only two BSs left

after thinning process. New cell boundaries are shown in (c) where the user distribution is non-uniform. This has been widely discussed in [47].

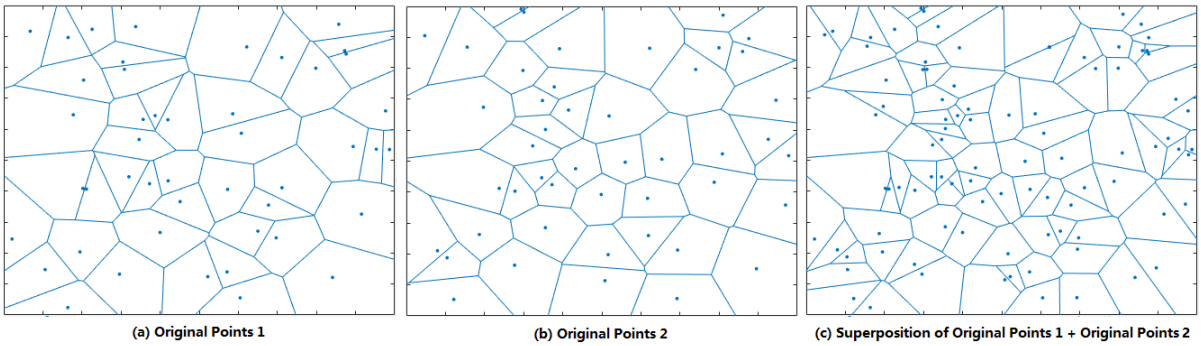

Figure 2.11: Example of superposition points and their Voronoi region

Figure 2.11 presents an example of point distribution of superposition and their Voronoi region. Both original points 1 and original points 2 are a homogeneous PPP. The superposition of original points 1 and original points 2 is still a homogeneous PPP. The Voronoi region is shown with closest BSs association if we assume points as BSs. In the literature, this superposition of multi-homogeneous PPPs with different BS density in each tier is called K-tier networks [20]. If the cell association rule is such that a UE connects to the BS with maximum SINR, the cell coverage area in each tier will be different due to different BS transmit powers in each tier (e.g., the cell coverage area of BSs with low transmit power will be relatively small.)

2.3.3 Hard Core Point Process (HCPP)

2.3.3.1 Hard Core Point Process Introduction

The hard core point process (HCPP) is a repulsive point process, in which the distance between any two points is more than the prescribed hard core threshold [26]. HCPP belongs to the thinning point process introduced in subsection 2.3.2.2. Because HCPP is a practical and important node model, for instance any two BS nodes or two UE nodes cannot be closer than a certain distance in real deployment, here we introduce HCPP as a separate subsection.

Definition 2-6. A PP $\phi = \{x_i, i = 1, 2, 3, ...\} \subset R$ is hard core point process if and only if $\|x_i - x_j\| \geq d$, $\forall x_i, x_j \in \phi$, $i \neq j$.

The rule used to select which points are retained and which points are removed is as shown in Figure 2.12.

UE_x; (the horizontal coordinate of UE is given)
UE_y; (the vertical coordinate of UE is given)
$Number_{UE}$; (Number of UE is given)
$UE_{x_{retained}} = [\,]$; (the horizontal coordinate of retained UE)
$UE_{y_{retained}} = [\,]$; (the vertical coordinate of retained UE)
$Number_{UE_{retained}} = 0$; (Number of retained UE)
Distance $= 0$; (distance between points)
Radius $= 1$; (the prescribed minimum distance between hard core points)
Indication $= 0$; (Indication if the point is removed. 0 − retained and 1 − removed.)
for i $= 1 : (Number_{UE} - 1)$
    for j $= (i + 1) : Number_{UE}$
        Distance $= \sqrt{(UE_x(i) - UE_x(j))^2 + (UE_y(i) - UE_y(j))^2}$
        if Distance $<$ Radius
            Indication $= 1$;
        else
        end
    end
    if indication $== 1$
    else
        $Number_{UE_{retained}} = Number_{UE_{retained}} + 1$;
        $UE_{x_{retained}}(Number_{UE_{retained}}) = UE_x(i)$;
        $UE_{y_{retained}}(Number_{UE_{retained}}) = UE_y(i)$;
    end
end

Figure 2.12: Rule to select HCPP points

To put it simply, HCPP has a prescribed minimum distance between the points. A realization is shown in Figure 2.13. (a) shows the original points in red. (b) labels points black if there are other points inside the circle of radius R_h. Black points are removed to form the resulting hard core points in (c). If two points have a distance less than the prescribed threshold, any point of two can be chosen to remove in this example. The distance between any two kept points is larger then R_h in (c). The radius of circle is $\frac{R_h}{2}$. In this example, $R_h = 1$.

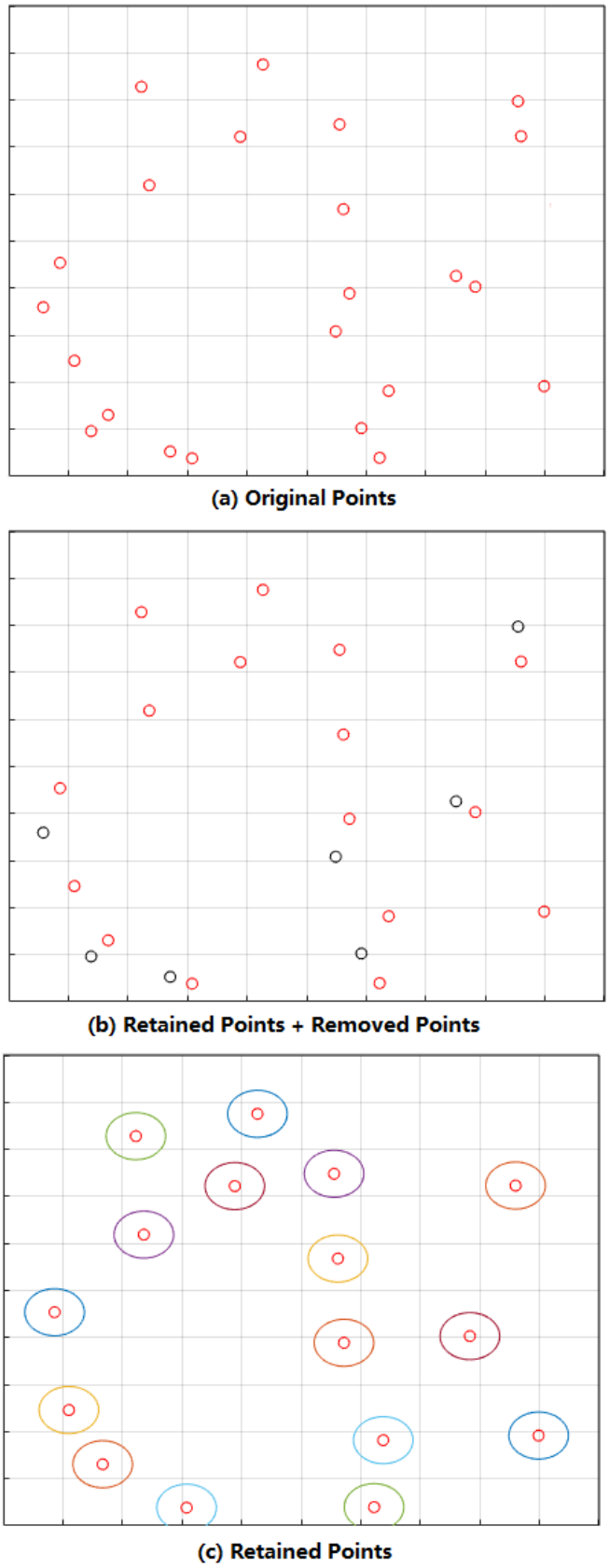

Figure 2.13: Realization of hard core point process

2.3.3.2 Practical Scenarios and Examples

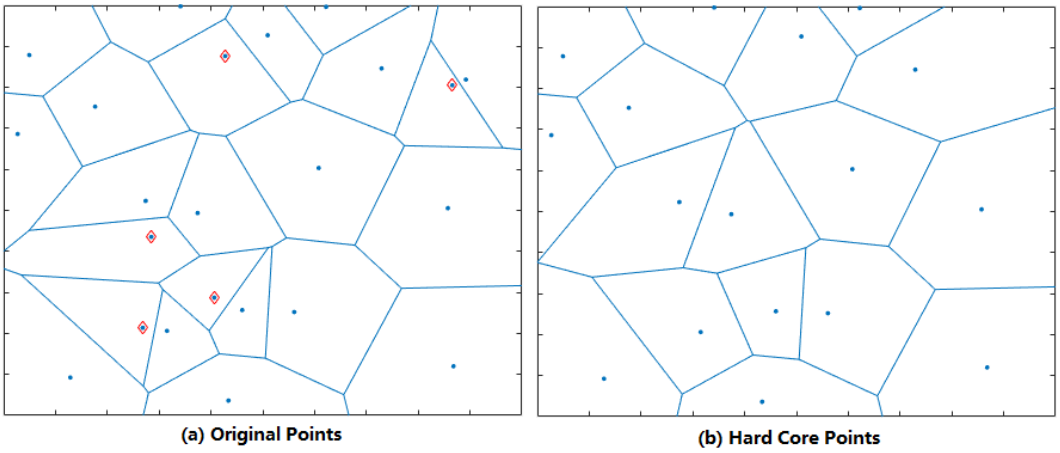

Figure 2.14: Example of hard core point process and their Voronoi region

Figure 2.14 introduces an example of point distribution of hard core point process. If we assume the points as BSs, the labeled red BSs are removed in the right figure since these BSs have a distance of less than a prescribed minimum distance with other BSs in the left figure. It is practical BS distribution because the distance between any two BSs should be more than a prescribed minimum distance while it is possible for any two BSs to have zero distance when BS distribution is PPP.

2.3.4 Poisson Cluster Process (PCP)

2.3.4.1 Poisson Cluster Process Introduction

Poisson cluster process is a random pattern produced by random clusters [48]. PCP generates homogeneous and independent clusters. The PCP has two types of points, parent points and daughter points. Parent points are PPPs and form the center of each cluster. Daughter points are generated spatially around each parent point according to some distribution function. PCP assumes that daughter points are symmetrically, independently, and identically distributed (i.i.d.) around parent points.

There are many types of PDF distribution for daughter points. For example, in a Matern cluster process, daughter points are uniformly distributed around parent points in a circle of a predefined radius R where the PDF is $\frac{1}{\pi R^2}$. In a Thomas cluster process, daughter points are distributed around parent points by an uncorrelated two dimensional normal

distribution with a predefined variance σ where the PDF is $\frac{1}{2\pi\sigma^2}\exp(-\frac{r^2}{2\sigma^2})$. In a linear cluster process, daughter points are distributed around parent points by linearly decreasing probability within a circular disc of predefined radius R where the PDF is $\frac{3}{\pi R^2}(1-\frac{r}{R})$. In an exponential cluster process, daughter points are distributed around parent points by exponentially decreasing probability of predefined rate parameter E where the PDF is $\frac{E^2}{2\pi}\exp(-Er)$. r is the distance between the daughter point and the parent point. In Figure 2.15, an example of the above four PDFs is shown. For Matern cluster process, the radius is $R = 50$ m. For Thomas cluster process, the variance is $\sigma = 40$. For linear cluster process, the radius is $R = 50$ m. For exponential cluster process, the rate is $E = 0.05$.

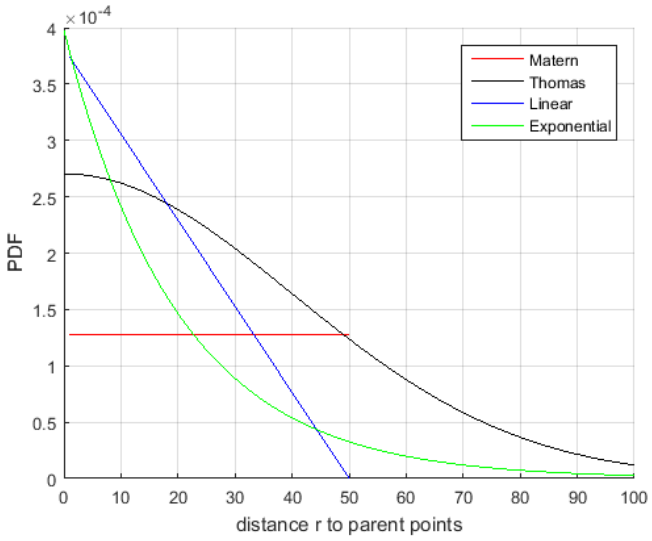

Figure 2.15: PDF distribution example in PCP

Figure 2.16 shows a realization of PCP. (a) shows parent points with PPP. (b) is PCP based on (a). The black points are daughter points and the red points are parent points. The daughter points follow Matern cluster process. The area is 10 m by 10 m.

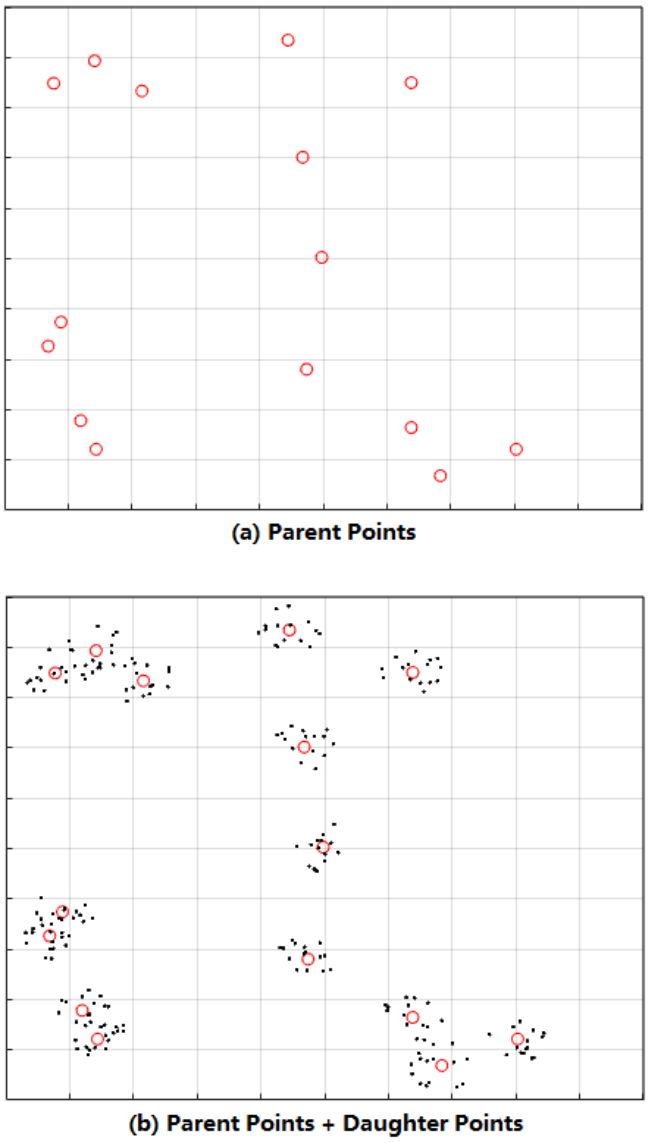

Figure 2.16: Realization of PCP

2.3.4.2 Practical Scenarios and Examples

Figure 2.17 illustrates an example of point distribution of PCP. If we assume the points as BS, this example represents the scenario where users concentrate together and more BSs are deployed around the area where cluster users are distributed so as to serve and support cluster users. The Voronoi region represent the coverage area with closest distance association. In this example, a single tier of BSs is assumed. For situations where multi-tier BSs exist, the coverage area will be different, which will be discussed in the following chapter.

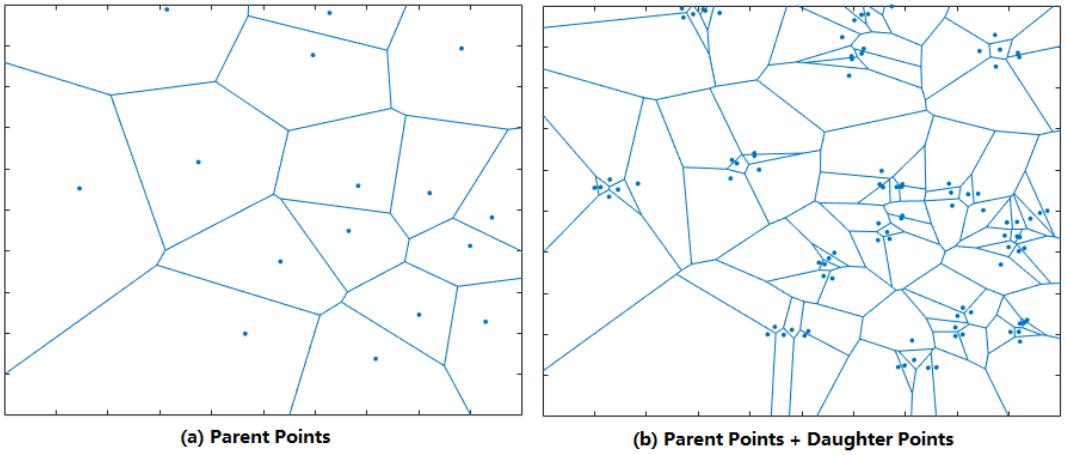

Figure 2.17: Example of PCP and their Voronoi region

2.4 Literature Review of Non-Uniform UE Distribution

The use of spatial random point processes to model UE in HetNet has been considered extensively. In the literature, the user spatial distribution is mostly assumed to be distributed as an PPP (uniform) independent of the distribution of BS. However, in HetNets, users tend to be spatially non-uniform and have an attraction to their associated BSs, especially in small cells [49,50]. Non-uniform spatial distribution of users reflects the user-centric capacity-driven deployment of small cells. The literature focused on non-uniformly distributed users is very limited. In the literature, the performance analysis of the non-uniform user distributions is summarized in the following two categories.

1. The first category of research work are studies where coverage probability is determined through time-consuming system level simulations.

   In [51], the authors uses the doubly stochastic Poisson process (DSPP) to model the user location, which is also known as the Cox process. Cox process considers a second layer of randomness, for example by generalizing the constant user density into a random variable. Coefficient of variation (CoV) is taken as an indication of heterogeneity. The authors of [51] give system level simulations that show that the network performance deteriorates greatly with increased heterogeneity (CoV) of UEs and the non-correlation of the UE location and the BS location. Nevertheless, the performance enhances if small cell BSs are deployed at the centers of the user hot-spots determined by cluster analysis algorithm. The model used in [52] also indicates a similar conclusion that the performance improves when users are clustered

around the BSs in WCDMA networks. While in [53], the model simulates a conventional CDMA system on uniform distributed users and clustered distributed users. It shows that the two distributed users have similar mean values of measured carrier to interference as well as similar outage. The clustered distributed users have higher standard deviation of measured carrier to interference ratio. The work in [54] demonstrates that 3GPP standard body requires users with the high density in the vicinity of small cell BSs. In [55, 56], the performance is obtained through system simulation while the traffic load is a random variable with log-normal or Weibull distribution.

The authors of [57] describe a non-uniformly distributed spatial user model in cellular CDMA systems. The density of users per unit area as a function of the distance from the base station have been modeled in different ways, such as linear exponential, and Gaussian. However, this model is for conventional macro cells, i.e. single tier systems; and the performance analysis and results are obtained by Monte Carlo simulations rather than analysis using stochastic geometry.

A user model for heterogeneous user distribution in heterogeneous wireless cellular networks (thus called HetHetNets) is introduced and discussed in [58]. Users are attracted to social attractors (SAs), such as buildings, bus stations, shopping centers, restaurants, and other social places. Attraction of SAs to BSs is also considered. Performance metrics are determined by simulation methods. This paper considers the correlation between BSs, UEs, and SAs. However, an analytical evaluation is not presented in [58].

2. The second category of research work is performed using the tools of stochastic geometry.

   In [59], we presented a user model, in which the user's position relative to the BS is determined by a parameter p, which varies between 0 and 1. The parameter p represents a correlation between the location of the UE and the BS. For $p = 0$, all UEs are randomly placed in the cell according to a PPP, while when $p = 1$, all UEs are positioned at the BS. Therefore, the model created situations where there are very few UEs near the cell boundaries when p is high. In [60], we deployed a density function as opposed to a correlation parameter p as in [59] to describe the non-uniformity to avoid the unlikely scenarios where there are no users near a cell boundary. The work of [60] provided a general non-uniform user model with heterogeneous PPP, in which the density is dependent on the distance to the associated BS. The density function can be any function, such as monotonically increasing, decreasing, or other trend.

   The authors of [61] presented a random heterogeneous node distribution based on

a neighborhood-dependent thinning of a homogeneous PPP. This user model is heterogeneous and clustered to some degree. However, it is impossible to predict the position of the cluster center. The positions of cluster center in this model are completely random or unrelated to the position of BS. However, rather than being totally random, users in practical HetNets are attracted to BSs. Furthermore, this model is hard to analytically obtain the derived performance metrics, such as the coverage probability.

In [47] another kind of thinning model is described. Each base station is independently retained with probability P_r and thinned (i.e. removed) with probability $1-P_r$. The users inside the coverage of the thinned base station are also thinned. The retained base stations determine the new coverage boundaries. In [47], a tractable performance analysis is given; but again, this model is only for single-tier macro cells. In [47], both user and BS locations are modeled by homogeneous PPPs with different densities in the first step; and heterogeneous user distribution is obtained by conditional thinning of BSs and the corresponding users in the Voronoi cells of thinned BSs. This method facilitates the deduction of analytical expressions. However, the generated user distributions may not be entirely realistic because of the absence of users in the thinned areas and the identical density of users in the remaining areas. Figure 2.10 gives an example of this thinning process.

The research in [23, 24] introduces a case of user-centric deployment, in which the UE locations and BS locations are correlated. The user distribution is a Poisson cluster process (PCP) where cluster centers are BSs. PCP assumes that the users in the cluster are symmetrically, independently, and identically distributed (i.i.d.) around the center. The corresponding performance analysis of the downlink coverage probability is obtained.

In [62], we introduced a mixed traffic model including the uniformly and non-uniformly distributed users at the same time. The non-uniform user distribution follows the same idea as in [59], in addition to which we extend the non-uniform distribution to include mixed distributions.

The authors of [63] provided a simple non-uniform distribution model, which only focuses on indoor communications. More practical non-uniform distribution model over HetNets should also be considered. The networks with the non-uniform user distribution in device-to-device communication is also discussed in [64–68].

The above research focuses on the downlink. In the literature, the uplink is also investigated. In the downlink the interference comes only from BSs of all tiers while

in the uplink the interference comes from all active UEs. The location of BSs is fixed, but the location of UEs is moving. In addition, the uplink power control of UE side should be considered. Covering BS point process and UE point process together into an uplink analysis brings many challenges. In the uplink reference, the uplink coverage probability is obtained over single tier, multi-tier, other fading type, decoupled uplink-donwlink biased cell association, and so on [69–74]. However, the user distribution is still uniform. We extend our non-uniform user distribution to the uplink research in this thesis.

The literature on non-uniform user distribution is very limited. It is especially lacking in research on non-uniform user distribution on heterogeneous networks in both downlink and uplink. Therefore, developing the non-uniform user model framework, delivering the performance analysis in both downlink and uplink, and showing system insight on HetNets is the main goal of this thesis.

Chapter 3

System Model

3.1 Introduction

The performance of HetNets critically depends on the spatial distribution of BSs and UEs, which plays a key role in the research, design, evaluation, and deployment of 5G HetNets. In HetNets, the spatial distribution of BS and UE is generally non-uniform. Analysis of the impact of non-uniform user distribution based on a heterogeneous cellular network is essential for designing efficient HetNets. In this chapter the system model – which deals with BS distribution (Section 3.2), user distribution (Section 3.3), and user connectivity (Section 3.4) – will be explained.

3.2 BS Distribution

3.2.1 Related Work on BS Distribution in the Literature

There are many papers that focus on the research of the spatial distribution of BS with the assumption of uniform user distribution. Some of these papers are:

- The work presented in [20, 21] focuses on the downlink of a heterogeneous cellular network (HCN) consisting of K tiers of randomly located BSs with different cell sizes and capabilities.
- The work in [22, 75–79] extends the idea of K-tier networks to include flexible cell association and load-aware policies.

- The work in [80] considers a K-tier network where the BS distribution includes a minimum distance policy while the work in [81] considers a K-Tier network where the BSs are distributed according to a Matern process.
- The work in [82–84] presents a BS distribution model where small cells are deployed outside of exclusion zones around macro cells. The exclusion zones are referred to as holes and the BS distribution is performed using a Poisson hole process (PHP).
- In [85–89], small cells are modeled by clusters using Poisson cluster process (PCP).
- In [90, 91], the outage probability of BS models with the general point process can be obtained with a fixed positive SINR shift from the PPP model.

3.2.2 BS Distribution Model Used In the Thesis

Throughout this thesis, the basic assumption is that the BS distribution follows the K-tier network described in [20]. In K-tier networks, cells in the same tier have approximately the same BS transmit powers, densities, SINR coverage thresholds, and path loss exponents. However, BSs from different tiers have different transmit powers, densities, SINR coverage thresholds and path loss exponents. The BS distribution in each tier is an independent spatial Poisson point process (SPPP). We assume that BSs in the kth tier are generated by SPPP ϕ_k with the density λ_k, transmit power P_k, SINR coverage threshold T_k, and path loss exponent α_k.

Figure 3.1 gives a realization of a 3-tier BS distribution. Figure 3.1 (a-c) represents a BS realization of 1st tier, 2nd tier and 3rd tier separately, in which each tier is an independent PPP with different BS density. The final BS realization (d) of 3-tier is the superposition of (a), (b), and (c). We name the first tier of BS the macro cell tier, the second tier of BS the pico cell tier, and the third tier of BS the femto cell tier. In Figure 3.1 (e), the BS realization of 3-tier with cell boundaries (blue curves) is given. In (e), the BS transmit power of the macro cell is 10 times greater than that of the cell pico and 100 times greater than that of the femto cell. The area is a square of 1 km by 1 km, in which there are 3 macro BSs, 6 pico BSs, and 18 femto BSs.

Based on the assumption of BS distribution of the above K-tier networks, this thesis proposes the non-uniform user distribution model and the corresponding performance analysis, such as the downlink and the uplink coverage probability using stochastic geometry. The downlink and the uplink coverage probability is obtained by considering the comple-

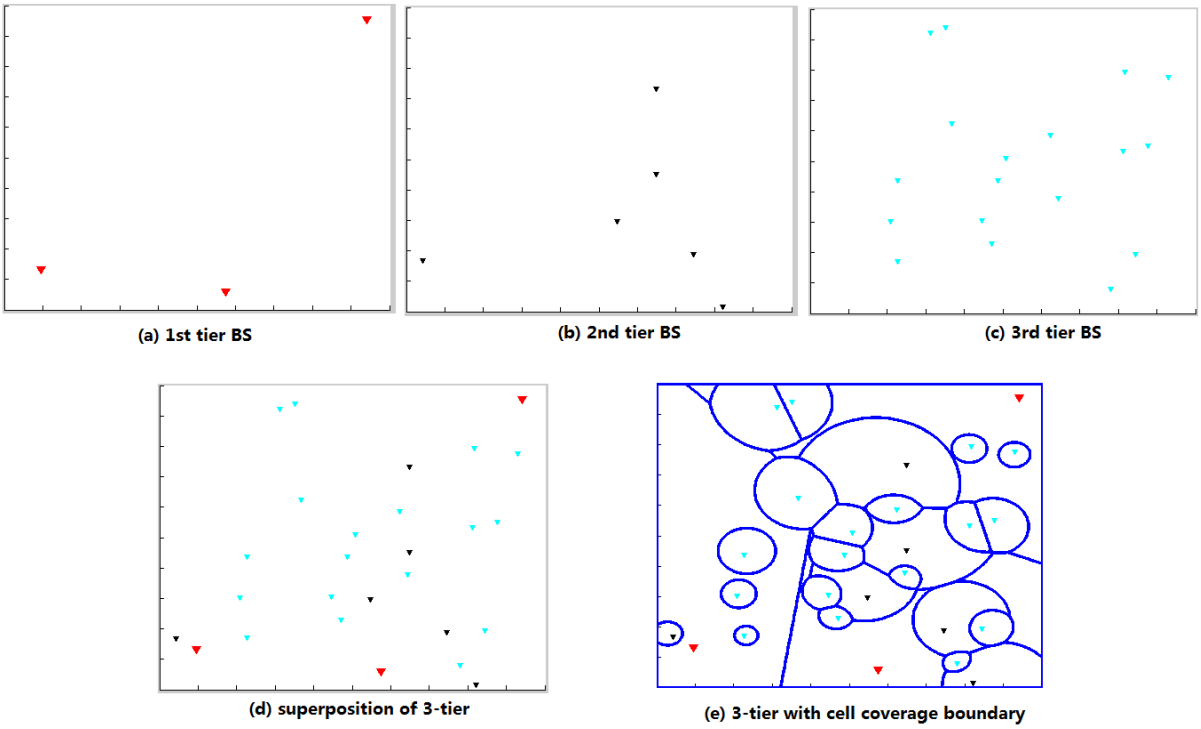

Figure 3.1: A realization of a 3-tier BS distribution

mentary cumulative distribution function (CCDF) of the signal to interference plus noise ratio (SINR).

3.3 User Distribution

Realistic user behavior is hard to model because the motions and positions of people with mobile devices are difficult to predict and control. However, most of the research in the literature is based on uniform user distribution models. We can take the uniform user distribution model as a benchmark. In this section, we introduce the concept of user distribution, including uniform and non-uniform cases, in single tier and multi-tier BS systems. In order to evaluate the benefit of deploying small cells, the simulation results of the coverage probability in the downlink and the uplink are shown in the following subsection.

The parameters of the 1-tier BS system are as follows: There are three macro BSs in the area of a square of 1 km by 1 km, which is equivalent of the macro BS density $\lambda_1 = \frac{3}{10^6}$. The path loss exponent is normally in the range of 2.5 to 4. Here we choose the path loss exponent $\alpha_1 = 3$. According to 3GPP TR 36.942, the maximum transmit power for a 10

MHz channel bandwidth is 46 dBm so we take the macro BS transmit power $P_1 = 45$ dBm.

The parameters of the 2-tier BS systems are as follows: There are three macro BSs and three pico BSs in the area of a square of 1 km by 1 km, which is equivalent to the macro BS density $\lambda_1 = \frac{3}{10^6}$ and the pico BS density $\lambda_2 = \frac{3}{10^6}$. We take the same path loss exponent for both tiers, which is $\{\alpha_1, \alpha_2\} = \{3, 3\}$. Lastly the transmit power of macro BSs is 10 times greater than that of pico BSs, which is $\{P_1, P_2\} = \{45, 35\}$ dBm and $P_1 = 10P_2$.

The parameters of the 3-tier BS system are as follows: There are three macro BSs, three pico BSs and six femto BSs in the area of a square of 1 km by 1 km, which is equivalent to the macro BS density $\lambda_1 = \frac{3}{10^6}$, the pico BS density $\lambda_2 = \frac{3}{10^6}$ and the femto BS density $\lambda_3 = \frac{6}{10^6}$. We take the same path loss exponent for three tiers, which is $\{\alpha_1, \alpha_2, \alpha_3\} = \{3, 3, 3\}$. The transmit power of macro BSs is 10 times greater than that of pico BSs and 100 times greater than that of femto BSs, which is $\{P_1, P_2, P_3\} = \{45, 35, 25\}$ dBm and $P_1 = 10P_2 = 100P_3$.

A procedure of designing the simulation setting of the following figures is given in Appendix C.1 and C.2.

3.3.1 Non-Uniform User Distribution in a Single Tier BS System

3.3.1.1 Set Initial BS Density

The UE distribution pattern of uniform and non-uniform, coverage map and coverage boundaries, and performance based on three macro BSs are shown.

3.3.1.1.1 UE Distribution Pattern

Figure 3.2 shows a uniform UE distribution in (a) and a non-uniform UE distribution in (b), in which the user cluster centers of the non-uniform UEs are distributed randomly and they have not any correlation between BSs and the user cluster centers.

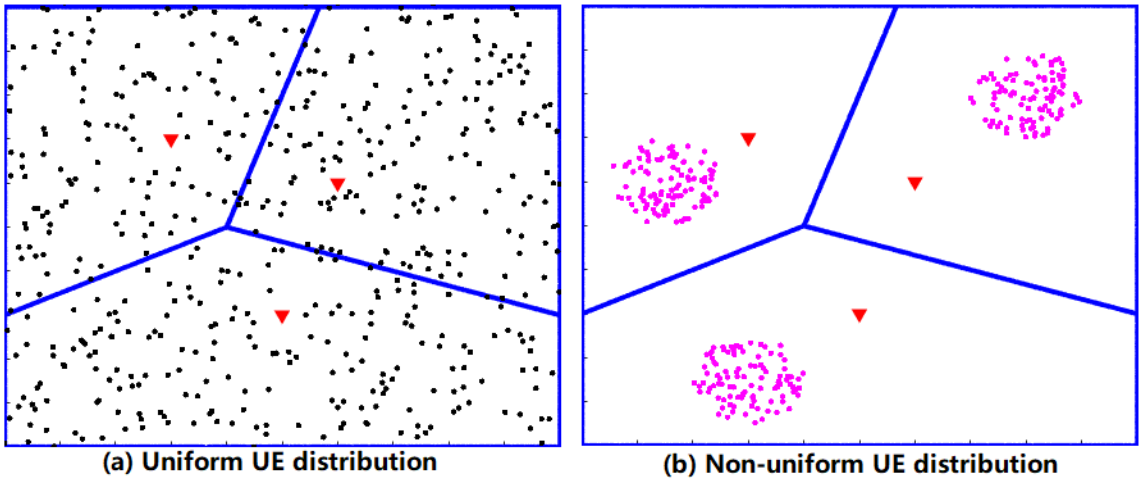

Figure 3.2: UE distribution pattern with uniform UEs and non-uniform UEs. Red triangles are macro BSs. Blue curves are cell boundaries. Black points are uniform UEs in (a) while magenta points are non-uniform UEs in (b).

3.3.1.1.2 Coverage Map and Cell Boundaries

In Figure 3.3, (a) gives the actual cell map with the maximum SINR association rule and (b) indicates the cell boundaries with blue curve. (a) shows the coverage map in which the relative SINR coverage threshold is labeled. The coverage map is the contour with the measured SINR of 0, 10, 20 and 30 dB. If a UE is randomly distributed, it will fall into a BS's associated area. However, the coverage area depends on the SINR coverage threshold. For example, in (a), most area is in coverage if the SINR coverage threshold is 0 dB. In a single tier system, the cell boundaries are the exact same as the Voronoi cell edges if the transmit power of all BSs is the same as shown in Figure 3.3. In Figure 3.4, the transmit power of BS1 is 4 times of the transmit power of BS2 and BS3. The cell boundaries is different with Figure 3.3. In Figure 3.4, we just give one example that the BSs in the same tier transmit with different power. In other figures of this thesis, we assume the BSs in the same tier transmit with the same power.

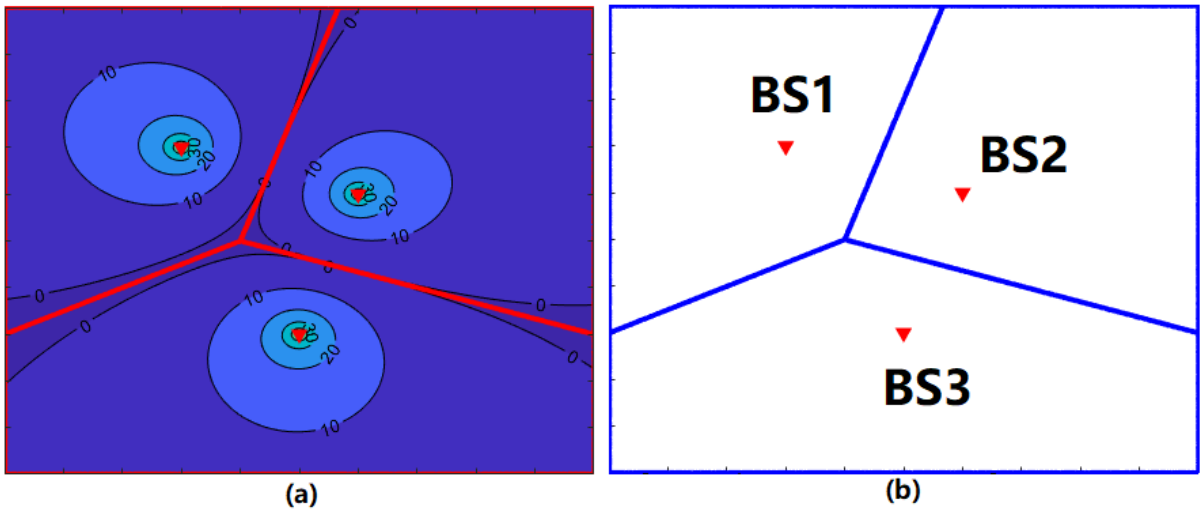

Figure 3.3: Coverage map (a) and cell boundaries (b) in a single tier BS system (3 BSs) where the transmit power of BS1, BS2 and BS3 is the same.

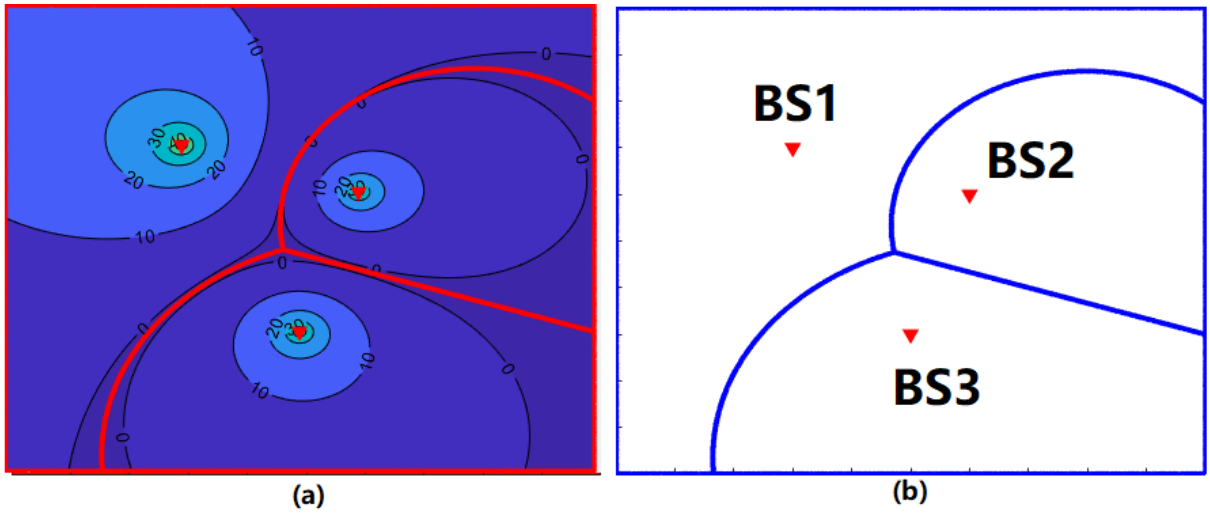

Figure 3.4: Coverage map (a) and cell boundaries (b) in a single tier BS system (3 BSs) where the transmit power of BS2 and BS3 is the same and the transmit power of BS1 is 4 times of the transmit power of BS2 and BS3.

3.3.1.1.3 Performance

Figure 3.5 shows the coverage probability of the downlink and the uplink with uniformly distributed UEs and non-uniformly distributed UEs. The figures present the performance of the uniform UEs is the same as the performance of the non-uniform UEs if the non-uniform UE cluster centers are randomly distributed and do not have any correlation with BSs.

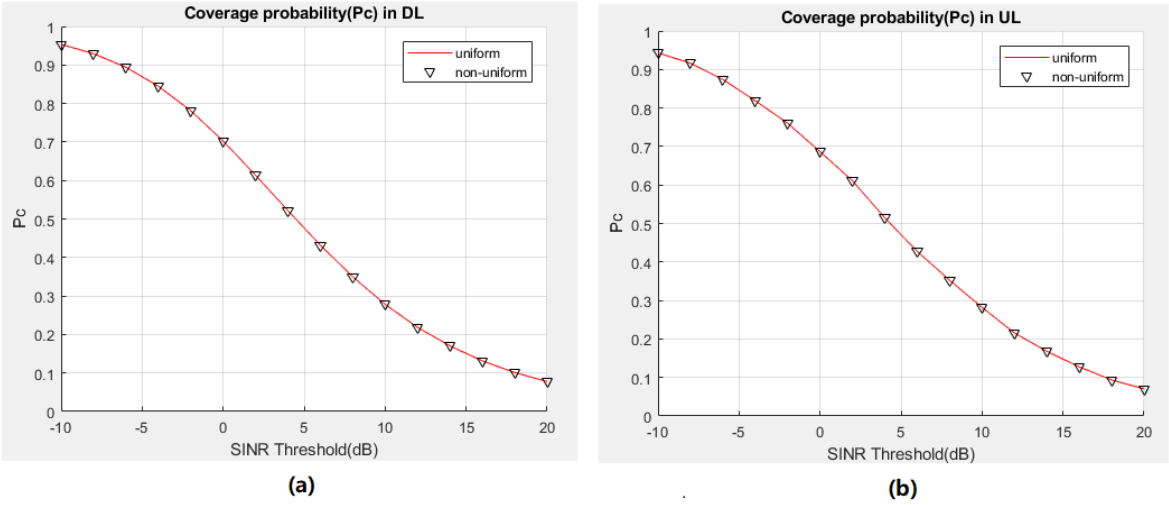

Figure 3.5: Performance of DL and UL in a signal tier (3 macro BSs, the non-uniform UE cluster centers are randomly distributed.).

3.3.1.2 Increasing Macro BS Density

In the following part, we evaluate the benefit by deploying additional macro BSs in the UE cluster centers. In this example, three additional macro BSs are deployed in the cluster centers in order to support the dense UEs.

3.3.1.2.1 UE Distribution Pattern

Figure 3.6 gives UE distribution pattern in which three additional macro BSs are deployed in the UE cluster centers.

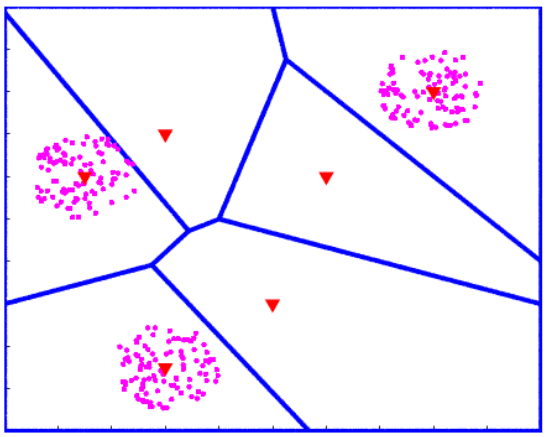

Figure 3.6: UE distribution pattern with non-uniform UEs where three additional macro BSs are deployed in the UE cluster centers.

3.3.1.2.2 Coverage Map and Cell Boundaries

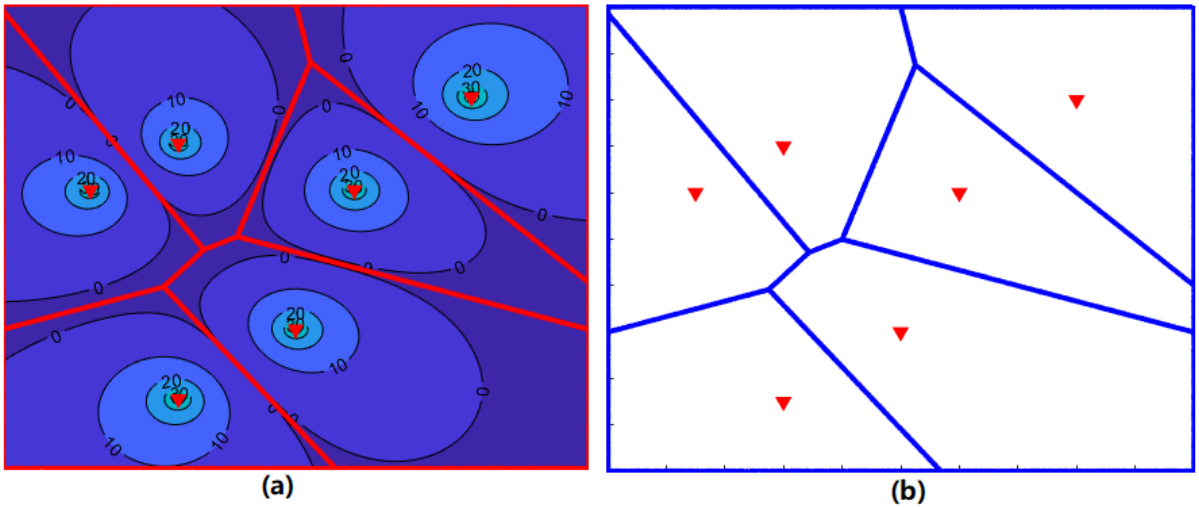

Figure 3.7: Coverage map (a) and cell boundaries (b) in a single tier BS system (6 BSs where 3 macro BSs are put randomly and another 3 macro BSs are put in the user cluster centers)

3.3.1.2.3 Performance

Since three additional macro BSs are deployed in three UE cluster centers, the coverage probability has tremendous improvement in the downlink and the uplink.

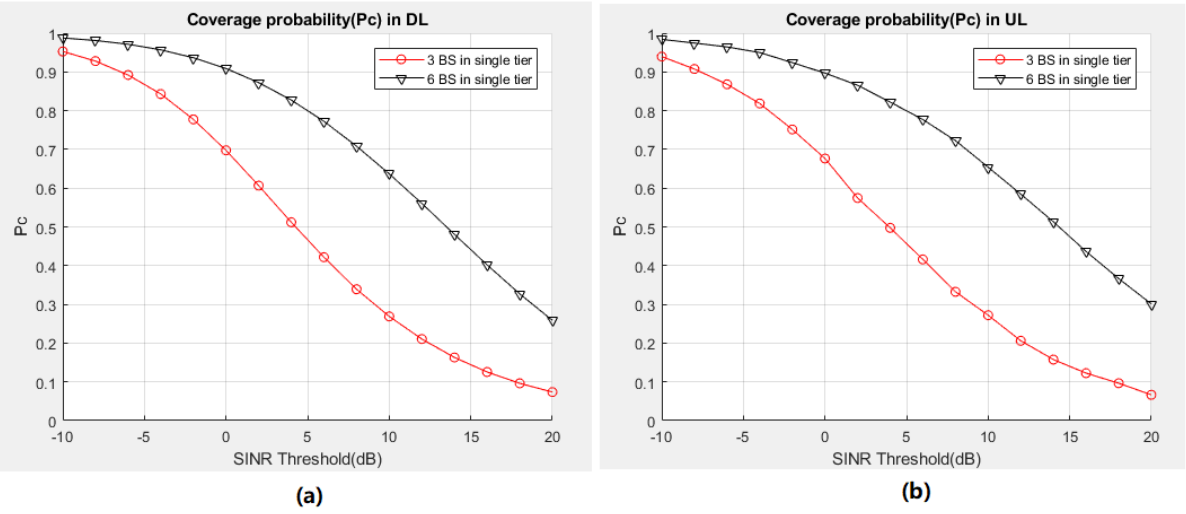

Figure 3.8: Performance of DL and UL in a signal tier (red curve is for 3 macro BSs in a single tier where 3 macro BSs are independent with UE cluster distribution, black curve is for 6 macro BSs in a single tier where 3 macro BSs are independent with UE cluster distribution and another 3 macro BSs are deployed in UE cluster centers.)

3.3.2 Non-Uniform User Distribution in a 2-tier BS System

3.3.2.1 Replacing Macro BSs with Pico BSs

In previous example, macro BSs are deployed in the UE cluster centers. However, due to the small UE cluster radius and power efficiency, it is better to deploy pico BSs rather than macro BSs. The system including macro BSs and pico BSs are named as a 2-tier BS system here.

3.3.2.1.1 UE Distribution Pattern

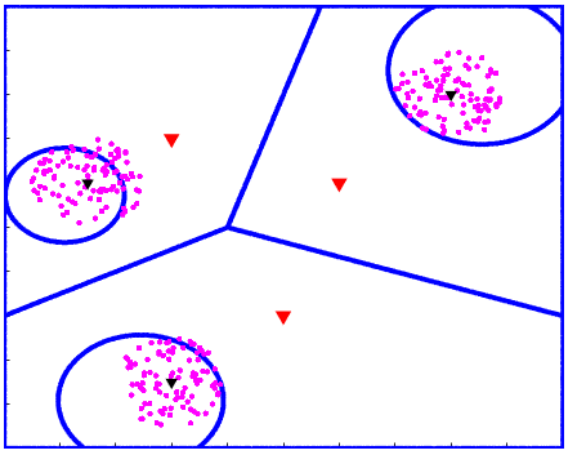

Figure 3.9: UE distribution pattern with non-uniform UEs in which pico BSs are deployed in the UE cluster centers.

3.3.2.1.2 Coverage Map and Cell Boundaries

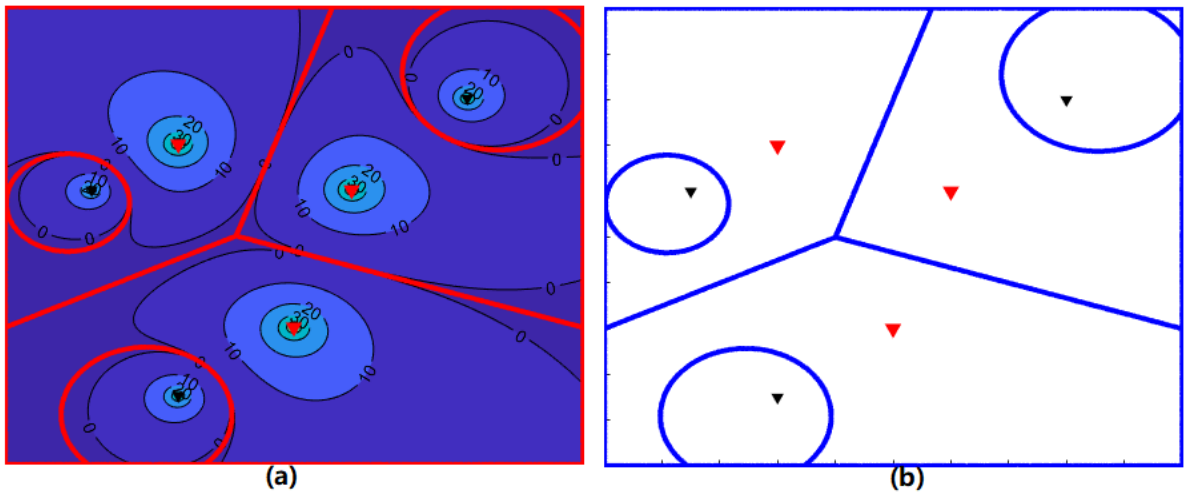

Figure 3.10: Coverage map (a) and cell boundaries (b) in a 2-tier BS system (6 BSs where 3 macro BSs (red triangles) are put randomly and 3 pico BSs (black triangles) are put in the user cluster centers)

3.3.2.1.3 Performance

After replacing macro BSs with pico BSs, the performance decreases as shown in Figure 3.11. But it saves the power consumption and the coverage area of pico BSs is enough to cover the cluster UEs.

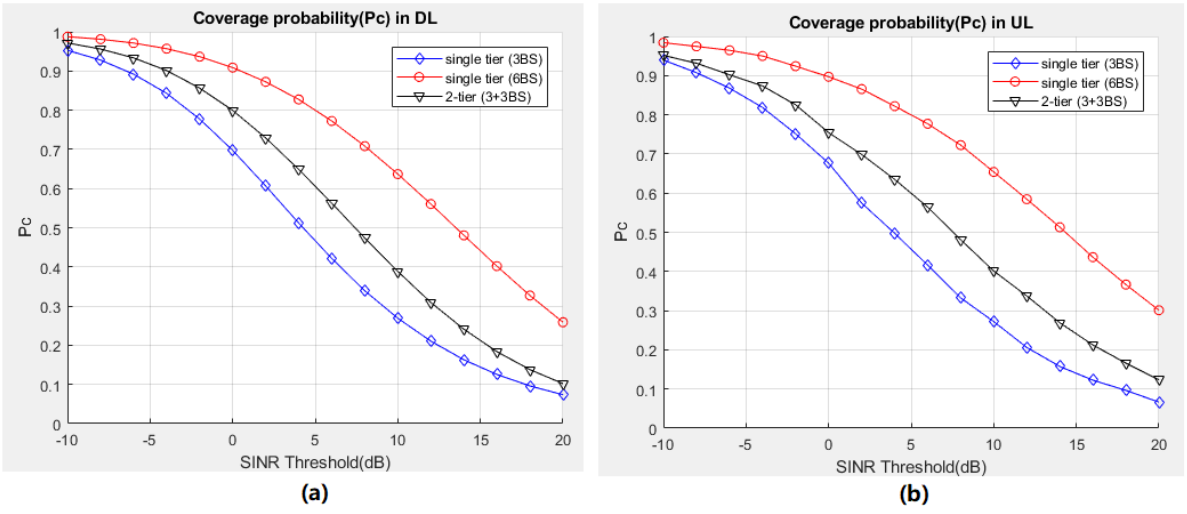

Figure 3.11: Performance of DL and UL (blue curve is for 3 macro BSs in a single tier where 3 macro BSs are independent with UE cluster distribution, red curve is for 6 macro BSs in a single tier where 3 macro BSs are independent with UE cluster distribution and another 3 macro BSs are deployed in UE cluster centers, black curve is for 3 macro BSs and 3 pico BSs in a 2-tier system.)

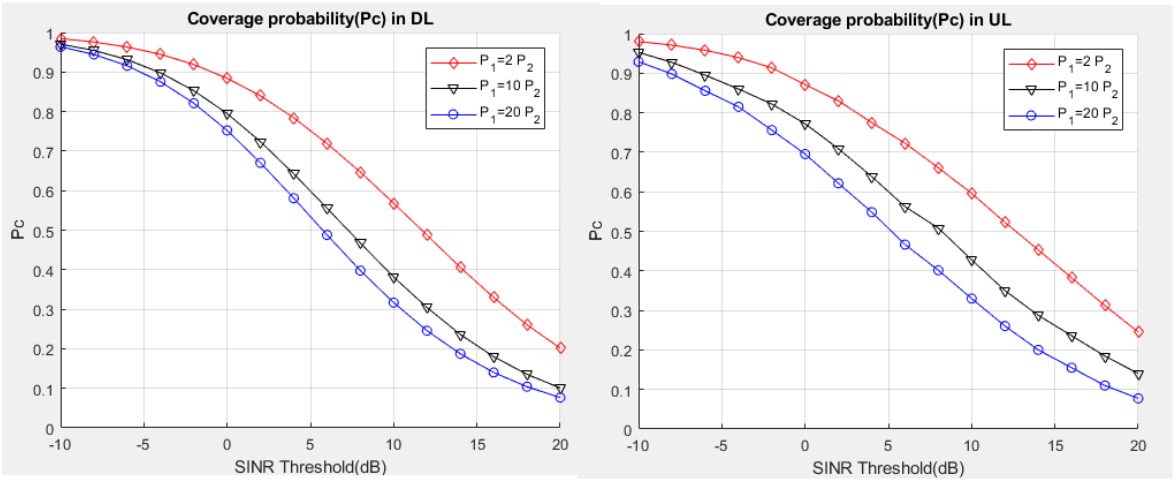

Figure 3.12: Coverage probability of cluster users (magenta points) when $P_1 = 2P_2$, $P_1 = 10P_2$, and $P_1 = 20P_2$ in a 2-tier BS system.

Figure 3.12 shows the coverage probability of a cluster of users with a different power ratio, in which the transmit power of macro BSs is 2 times, 10 times and 20 times greater than the transmit power of pico BSs, respectively. When the power ratio is low, such as $P_1 = 2P_2$, the clustered users are served by pico BS with high SINR so that the coverage probability is higher compared with other two power ratios.

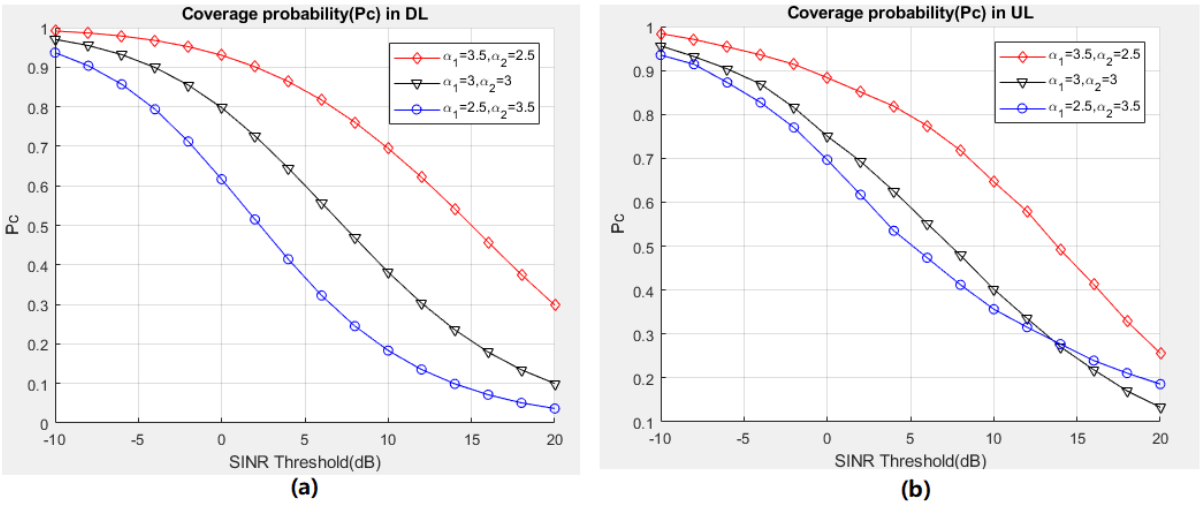

Figure 3.13: Coverage probability of cluster users (magenta points) with different path loss exponents in a 2-tier BS system when $P_1 = 10P_2$.

Figure 3.13 gives the coverage probability of cluster users with different path loss exponents between macro cells and pico cells. When $\alpha_1 = 3.5, \alpha_2 = 2.5$, the cluster users served

by pico cells have higher SINR since $\alpha_1 = 3.5$ results in higher path loss from macro BSs and $\alpha_2 = 2.5$ results in lower path loss from pico BSs so that the cluster users in pico cells have high coverage probability. The users in the macro cells propagate through space with large power attenuation due to the large coverage area and more blocking while the users in the pico cells propagate with low power attenuation due to the small coverage area and less blocking. The users from macro BSs experience the high path loss and the users from pico BSs experience the low path loss. Therefore, the case of $\alpha_1 = 3.5, \alpha_2 = 2.5$ is the most realistic among the three path loss exponent ratios.

3.3.2.2 Increasing Pico BS Density

The additional 6 UE clusters are distributed with smaller radius. In Figure 3.14, these additional 6 UE clusters are labeled with green points.

3.3.2.2.1 UE Distribution Pattern

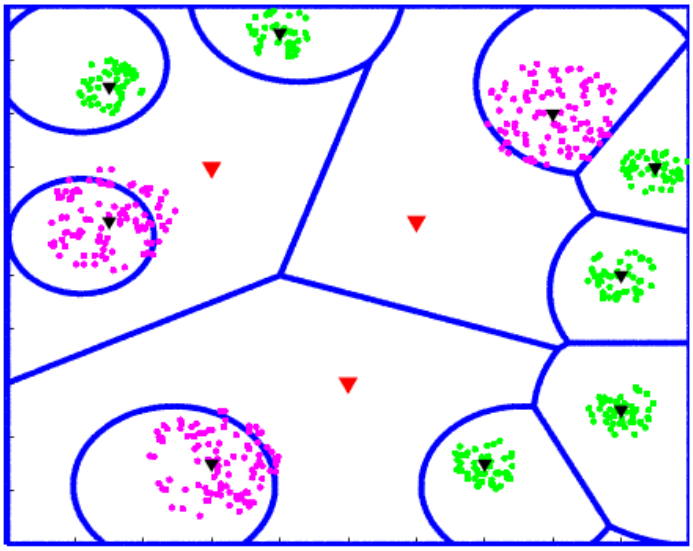

Figure 3.14: UE distribution pattern with non-uniform UEs in which new 6 pico BSs are deployed in these additional 6 UE cluster centers in green.

3.3.2.2.2 Coverage Map and Cell Boundaries

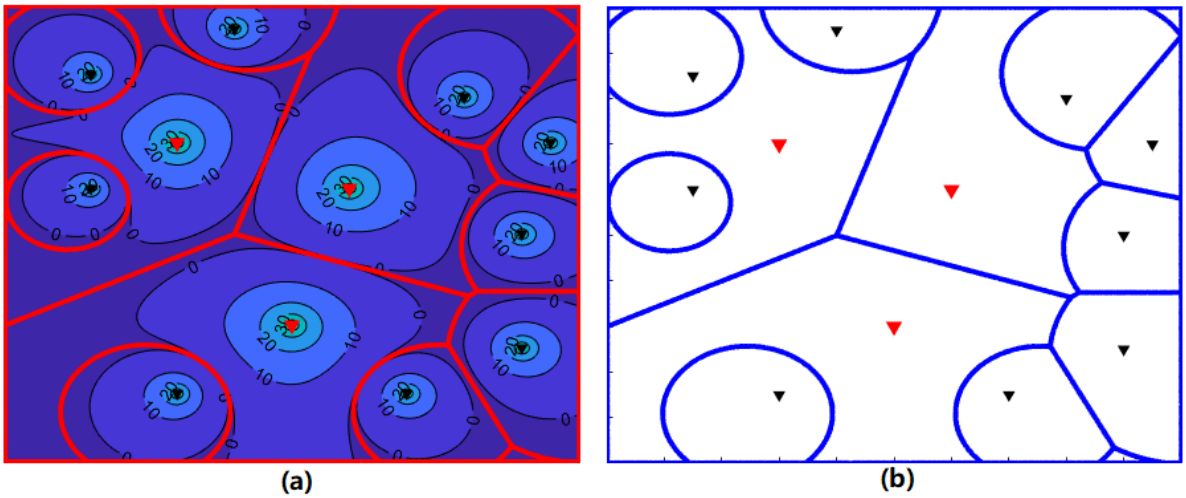

Figure 3.15: Coverage map (a) and cell boundaries (b) in a 2-tier BS system (9 BSs where 3 macro BSs (red triangles) are put randomly, 3 pico BSs (black triangles) are put in the user cluster centers in magenta and 6 pico BS (black triangles) are put in the user clusters in green.)

3.3.2.2.3 Performance

It is obvious that the performance is improved after deploying new 6 pico BSs in these additional 6 small UE clusters in green in Figure 3.14. But due to the number of green cluster limited, the performance improvement is not substantial.

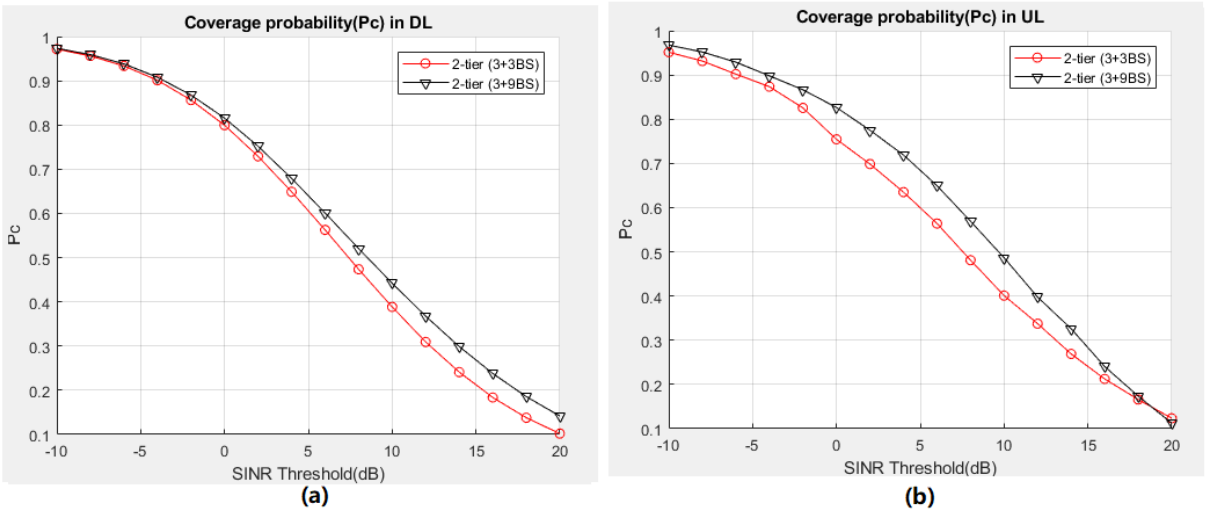

Figure 3.16: Performance of DL and UL in a 2-tier BS system (red curve is for 3 macro BSs and 3 pico BSs in a 2-tier system and black curve is for 3 macro BSs and 9 pico BSs in a 2-tier system.)

3.3.3 Non-uniform User Distribution in a 3-tier BS System

3.3.3.1 Replacing Pico BSs with Femto BSs

Due to the small radius of new green cluster, femto BSs are enough to cover the green UE cluster.

3.3.3.1.1 UE Distribution Pattern

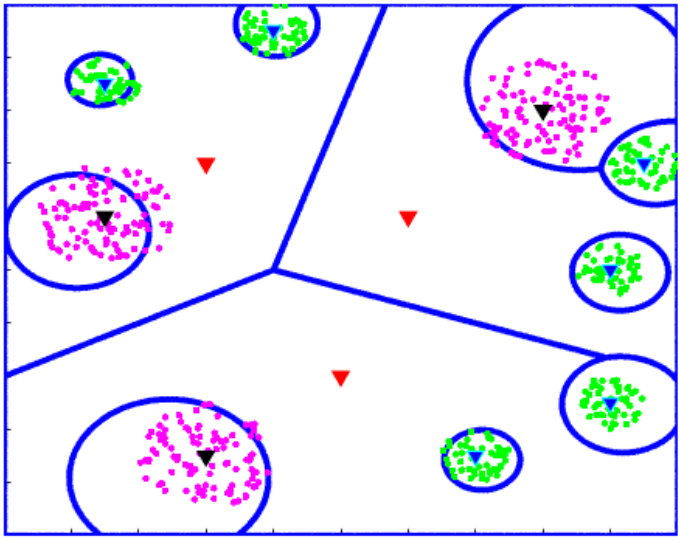

Figure 3.17: UE distribution pattern with non-uniform UEs in which new 6 femto BSs are deployed in these additional 6 UE cluster centers in green. Red triangles are macro BSs. Black triangle are pico BSs. Blue triangles are femto BSs.

3.3.3.1.2 Coverage Map and Cell Boundaries

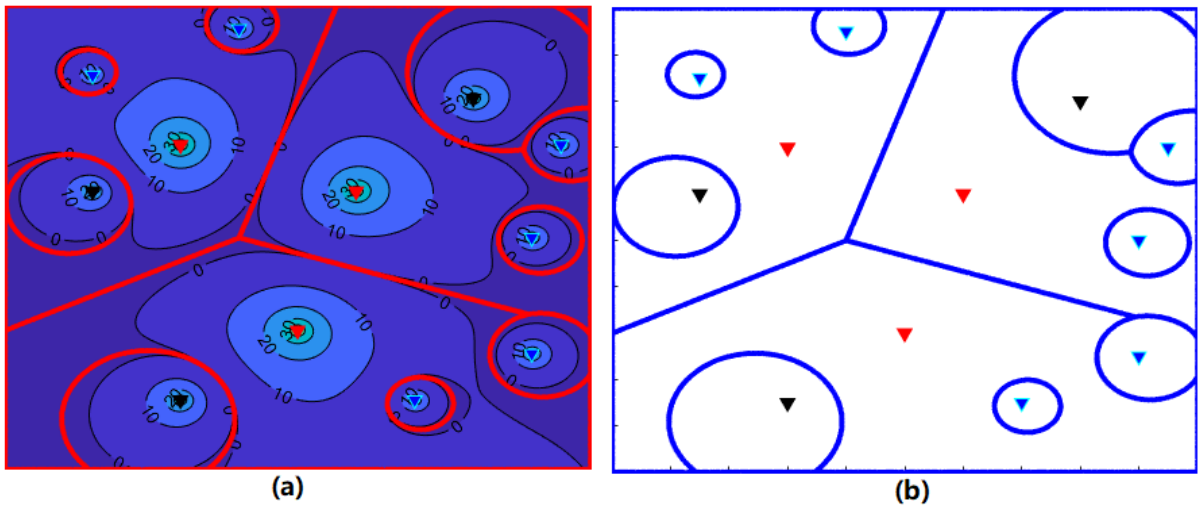

Figure 3.18: Coverage map (a) and cell boundaries (b) in a 3-tier BS system (12 BSs where 3 macro BSs (red triangles) are put randomly, 3 pico BSs (black triangles) are put in the user cluster centers in magenta and 6 femto BSs (blue triangles) are put in the user clusters in green.)

3.3.3.1.3 Performance

After replacing the 6 pico BSs with 6 femto BSs in order to cover small UE clusters in green, the coverage probability decrease. However, femto BSs are enough to cover the small green UE clusters in Figure 3.17 and low power femto BSs would save power consumption.

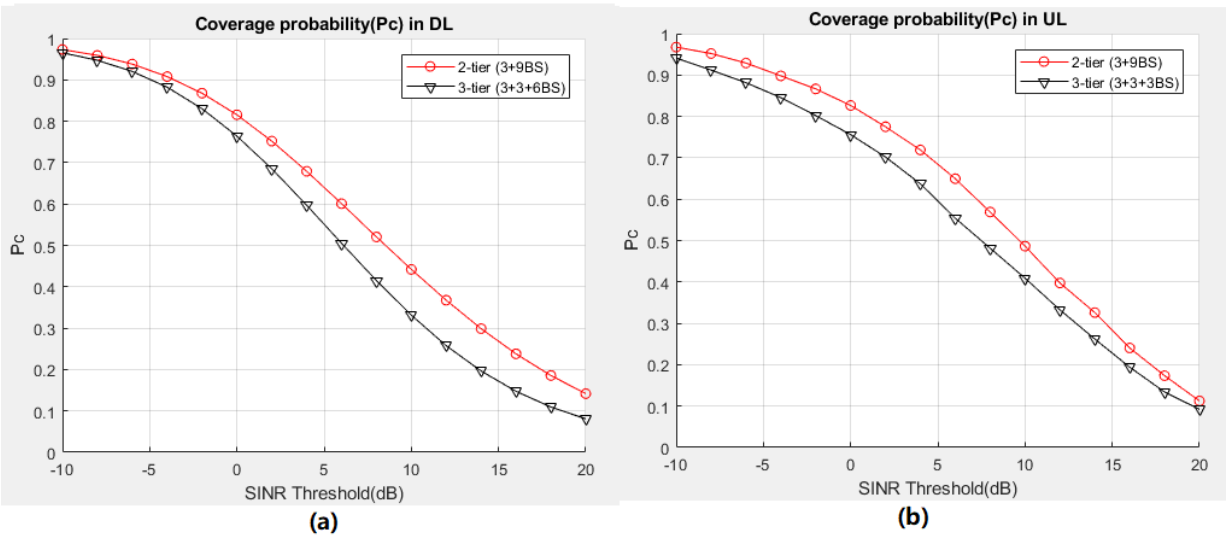

Figure 3.19: Performance of DL and UL in a 2-tier and a 3-tier (red curve is for 3 macro BSs and 9 pico BSs in a 2-tier system and black curve is for 3 macro BSs, 3 pico BS and 6 femto BSs in a 3-tier system.)

3.3.4 Summary of User Distribution

From the above subsection on non-uniform user distribution in a single tier, 2-tier and 3-tier BS system, we summarize that deploying small BSs at the user cluster centers can enhance the capacity (small BSs provide coverage to a cluster of users in a hot spot within macro cells which in turn increases the overall system capacity) and improve the coverage probability. Deploying small BSs with high transmit power will bring more performance improvement for users in small cells, but it may cause high deployment cost and high interference to other users. When the cluster radius is less than 100 m and the transmit power is about 30 dBm, deploying pico cells is a good choice, while when the cluster radius is less than 30 m and the transmit power is about 20 dBm, deploying femto cells is a good choice (referred from the link: *//www.rfwireless-world.com/Tutorials/femtocell-vs-picocell-vs-microcell.html*). In the examples of this chapter, the UE cluster (magenta points) radius in pico cells is 100 m and the UE cluster (green points) radius in femto cells is 50 m

Small BSs are used to improve the cell range, capacity and coverage performance in hot spots or other densely distributed user areas. Therefore, it is reasonable to assume that the user distribution model is that in small cells the users are non-uniformly distributed and clustered around a cluster center. Furthermore, we may extend the discussion to the mixed user distribution, in which uniformly distributed users and non-uniformly distributed users coexist. In mixed user distribution, uniform users are distributed around the whole area, while non-uniform users are distributed with high attraction level in small cells.

3.4 User Connectivity

3.4.1 Connectivity Rule

User connectivity is the process that specifies the BS to which a user is associated with. Usually, the rule of the user connectivity is that a user connects only to one BS at a time. For conventional networks, the user connectivity is normally based on maximum received power or minimum distance. However, such a connectivity rule is not suitable for heterogeneous K-tier networks. In HetNets, one reason for deploying small cells is to expand indoor as well as macro cell edge coverage. Since the transmit power of BSs in small cells is low and the coverage area is small, these cells have lighter loads. Other connectivity rules, such as the bias connectivity rule should be considered to tackle the lighter load issue.

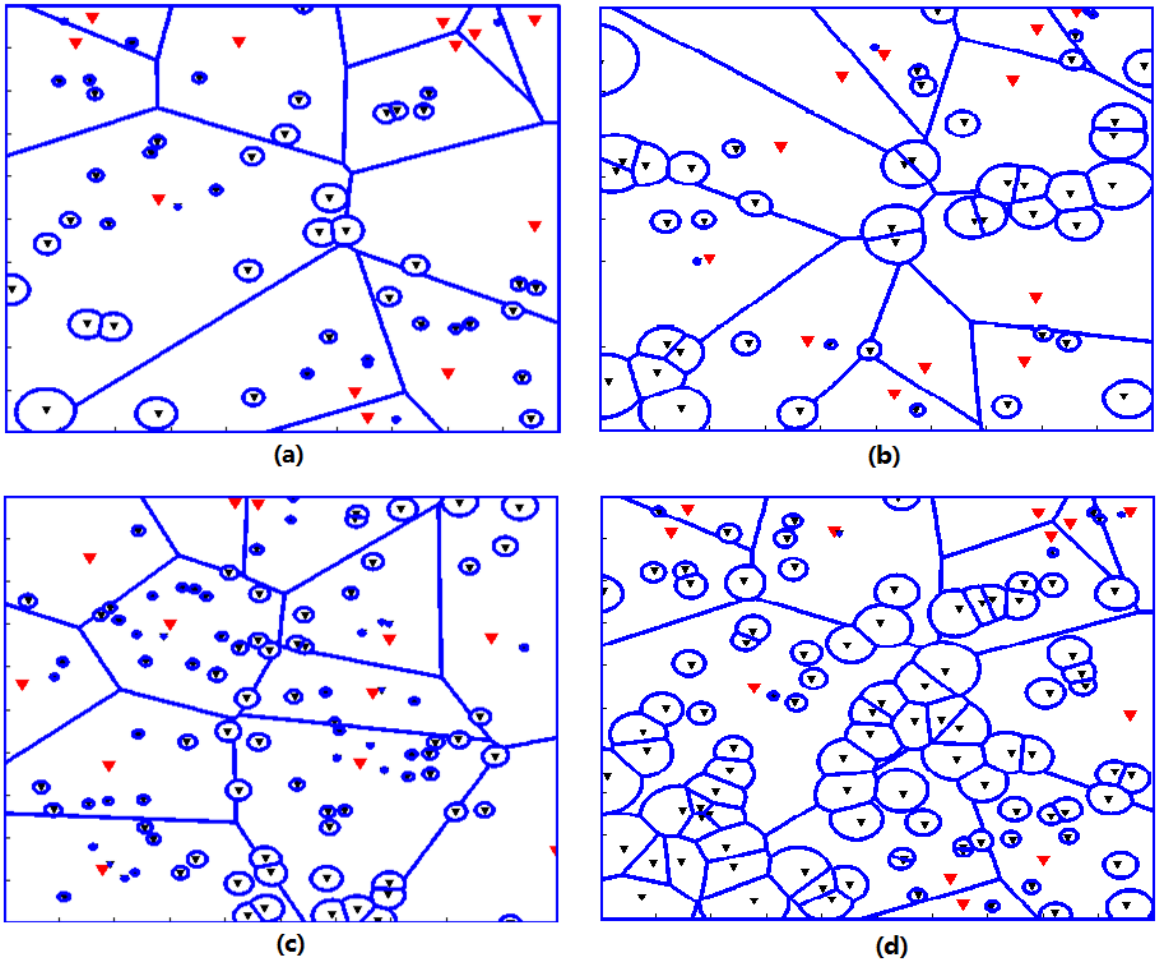

Figure 3.20: Cell coverage boundaries diagram for a 2-tier cellular network based on user connectivity rule of maximum received power. (a) $P_1 = 1000P_2$, $\lambda_1 = 4\lambda_2$. (b) $P_1 = 100P_2$, $\lambda_1 = 4\lambda_2$. (c) $P_1 = 1000P_2$, $\lambda_1 = 8\lambda_2$. (d) $P_1 = 100P_2$, $\lambda_1 = 8\lambda_2$.

In Figure 3.20, we illustrate four examples of the cell coverage boundaries for a 2-tier (macro cells and small cells) HetNets. These examples show the related cells, the distributed users should associate with, according to the user connectivity rule of maximum received power. The macro cell BSs are represented by red triangles, while small cell BSs are represented by black triangles. The BS transmit power in the macro cell, P_1, is assumed to be 1000 or 100 times greater than the BS transmit power in the small cell, P_2. We have considered 2 BS density ratios. In Figure 3.20, the density of the small cells is 4 times greater than the macro cells: $P_1 = 1000P_2$ in (a) and $P_1 = 100P_2$ in (b). In Figure 3.20, the density ratio is 8 for $P_1 = 1000P_2$ in (c) and $P_1 = 100P_2$ in (d). When the BS density is the same, the cell coverage region varies as a function of the transmit power ratio between macro cell BS and small cell BS. As the transmit power ratio drops, the small cells cover

larger areas. The small cell coverage regions are larger when the small cells are located far from the macro cell center.

3.4.2 Connectivity Model

In HetNets, deploying small cells brings the benefits of expanding cell edge coverage. However, the transmit power of BSs in small cells is relatively low and the corresponding coverage area is small, such that these cells have lighter loads. Hence, we need a cell extension bias that enables UE to access the small cells even though UE receives a stronger signal from a macro cell than a small cell. The above rule of associating a user with a bias is controlled by a cell extension bias factor C_j. C_j >1 is used to extend the cell coverage of the jth tier. This bias connectivity rule is called cell range extension (CRE) [22,78,92,93].

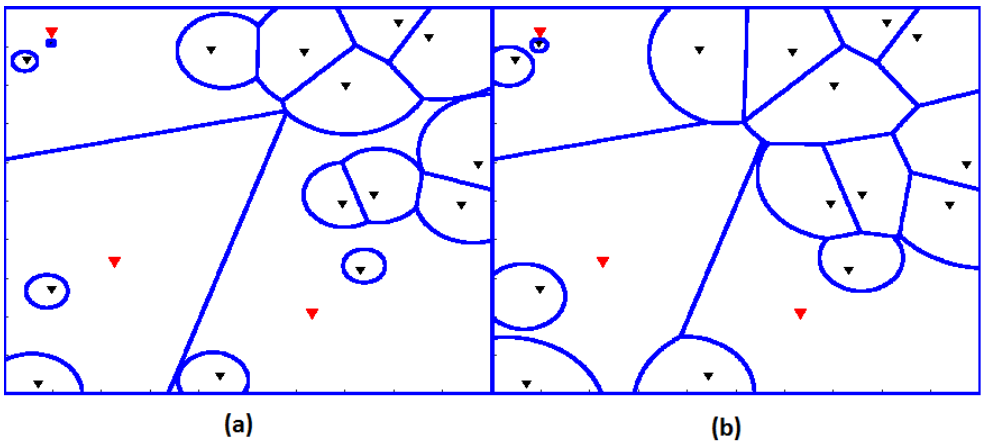

Figure 3.21: Cell extension example. (a) and (b) have the exactly same BS locations. (a) is $\{C_1, C_2\}$=$\{1, 1\}$ without cell extension and (b) is $\{C_1, C_2\}$=$\{1, 6.3\}$ with cell extension. The area is 1 km by 1 km.

In Figure 3.21, the two figures have the exact same BS densities, BS transmit powers and BS locations. In the left figure, there is no cell extension (C_2=1) for small cells. In the right figure, there is cell extension (C_2=6.3) for small cells. In Figure 3.21, the blue curves are the cell boundaries. After changing cell extension bias factor C_2 from 1 to 6.3, the cell coverage areas of the small cells increase. Using the cell extension C_j parameter to enforce a larger coverage area for small cells brings the drawback that the users near the small cell boundary have a lower SINR as opposed to no cell extension. However, the benefit of cell extension is higher capacity in small cells. It is a balance between the users' SINR and small cell capacity. How to find the optimal cell extension parameter C_j is not

covered in this thesis. We will rather give the effect analysis based on cell extension bias factors of small cells in Section 5.3.3 of the downlink and in Section 6.5.3 of the uplink.

Definition 3-1. In this thesis, the maximum average bias received power (BRP) connectivity model [75] is used, which is defined as follows.

The user is associated with the BS, which can provide maximum average bias received power. Let $P_{BRP_j} = P_j C_j r_j^{-\alpha_j}$ (the path loss L_0 at a reference distance 1 m is ignored since it is a constant). The distance between a user and its associated BS is r.

$$r = \arg \ \{ \max_{B_j \in \phi_{BS}} \ \{P_j C_j r_j^{-\alpha_j}\}\}. \tag{3.1}$$

3.5 Conclusions

In this chapter, we introduced the system model used in this thesis, which includes BS distribution, user distribution, and user connectivity. We mainly discussed the non-uniformly distributed users. BS distribution is assumed as a K-tier network, in which each tier of BS is an independent PPP. We also introduced user distributions from a single tier BS system to a 3-tier BS system and from uniform to non-uniform distributions. We showed that deploying small BSs at the user cluster will improve the coverage probability and system capacity such that it is reasonable to assume that the non-uniform users are distributed as a cluster around small BSs. The designed non-uniform user model in this thesis will be introduced in the next chapter. Finally, user connectivity model of the maximum average bias received power is presented. This user connectivity model supports the cell association and it is equivalent to maximum average received power rule when cell extension bias factor $C = 1$. In this thesis, we refer to this maximum average bias received power as the user connectivity rule.

Chapter 4

Designed User Distribution Model and Heterogeneity Analysis

4.1 Introduction

The criteria to design a user distribution model in this thesis is as follows:

- In each tier, user distributions are not uniform as they tend to converge towards social attractors (SAs). Different attraction levels between UEs and SAs should be presented and included.
- In each tier, there should be a parameter that controls spatial dependency or correlation between the location of SAs and BSs. All kinds of dependency should be presented and included.
- In the macro cell tier, the users tend to be distributed with low attraction[1] between UEs and SAs and low dependency[2] between SAs and their BSs.
- In the small cell tier, the users tend to be distributed with high attraction[3] between UEs and SAs and high dependency[4] between SAs and their BSs.

[1]Low attraction means that users have low spatial correlation with their SAs. The user distribution density over the given area is almost the same.

[2]Low dependency means that SAs have low spatial dependency with their BSs. The placement of SAs and BSs is almost independent.

[3]High attraction means that users have high spatial correlation with their SAs. There is a high user density around SAs.

[4]High dependency means that SAs have high spatial dependency with their BSs. The placement of SAs and BSs is dependent.

- Users in different tiers may have different attraction and dependency levels.
- Through the tools of stochastic geometry, the theoretical performance analysis or closed-form equations about performance, such as coverage probability, can be obtained for the designed user model.

Based on the available K-tier BS model, we design a spatially non-uniform user distribution model. Here the non-uniform model (Section 4.2) is a Poisson cluster process (PCP) with the cluster centers located at SAs and SAs have an offset with their BSs. We apply the same user distribution model for each tier. However, in small cells we can choose the user model with high attraction and high dependency while we can choose the user model with low attraction and low dependency for macro cells. Finally, the heterogeneity analysis of non-uniform user distribution is discussed (Section 4.3). All downlink and uplink analysis assume that the channel experiences Rayleigh fading.

4.2 Non-Uniform User Distribution

4.2.1 Definition

Definition 4-1. A non-uniform user distribution in each tier is defined as follows.

- A Poisson cluster process with the cluster centers located at the SAs.
- SAs have a base station offset (BSO) which is the distance between SAs and their BSs.

Figure 4.1 gives an example of this non-uniform user distribution model. Black triangles are BSs of small cells. The blue curves are cell boundaries. Magenta points are users in clusters. Green diamonds are SAs, which are cluster centers. Green circles are the boundaries of clusters with Matern cluster process. D_2 is the base station offset between the SA and its BS in small cells.

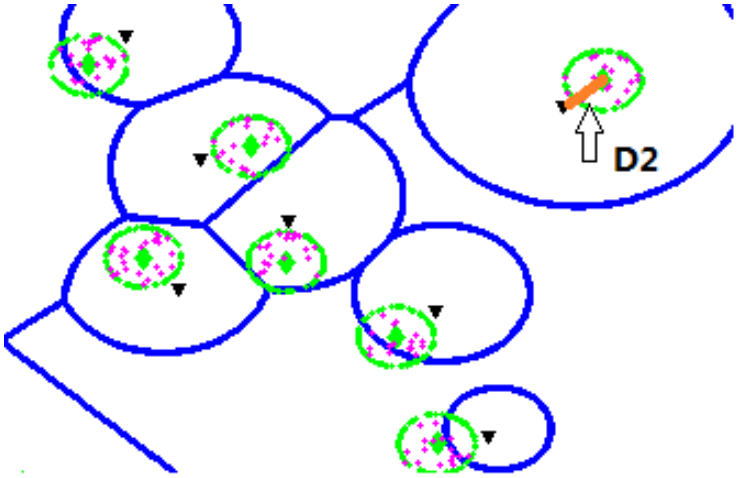

Figure 4.1: Non-uniform user distribution example (D_2 is 55 m with orange line and it is Matern cluster process with radius $R = 40$ m).

4.2.2 Parameters

- Model of UEs Clustering around SAs

UEs in small cells tend to gather in clusters while UEs in macro cells tend to be distributed more uniformly. Our non-uniform user distribution is a PCP with SAs at the cluster centers. We define a subset $\mathbb{S}(\subset \kappa)$ where non-uniform UEs are distributed. The total number of tiers of $\mathbb{S}$ is S. In the kth tier ($k \in \mathbb{S}$), UEs follow our defined non-uniform distribution. It is possible for small cell tiers and macro cell tiers to coexist in the subset $\mathbb{S}$, in which they would have their preferred attraction level depending on different parameters.

We assume that the distribution of a UE's location in a cluster is described by a probability density function (PDF) $f_u(r)$. Here r is the distance of a UE from the cluster center (in our case the SA). $f_u(r)$ in each tier may be different.

We considered four PDFs:

(i) Matern cluster: The density of UEs is uniformly within a circular disc with radius R. Here, R is the parameter to control the level of attraction between UEs and SAs. A small value of R means the attraction level is high, and vice versa.

$$f_u(r) = \frac{1}{\pi R^2} \qquad 0 \leq r \leq R. \tag{4.1}$$

(ii) Thomas cluster: The density of UEs is with Gaussian spatial distribution, in which σ is the standard deviation. Here, σ is the parameter to control the level of attraction between UEs and SAs. A low value of σ means the attraction level is high, and vice versa.

$$f_u(r) = \frac{1}{2\pi\sigma^2} \exp(-\frac{r^2}{2\sigma^2}) \qquad 0 \leq r \leq \infty. \tag{4.2}$$

(iii) Linear cluster: The density of UEs is linearly decreasing within a circular disc with radius R. Here, R is the parameter to control the level of attraction between UEs and SAs. A small value of R means the attraction level is high, and vice versa.

$$f_u(r) = \frac{3}{\pi R^2}(1 - \frac{r}{R}) \qquad 0 \leq r \leq R. \tag{4.3}$$

(iv) Exponential cluster: The density of UEs is exponentially decreasing, in which E is the rate parameter. Here, E is the parameter to control the level of attraction between UEs and SAs. A high value of E means the attraction level is high, and vice versa.

$$f_u(r) = \frac{E^2}{2\pi} \exp(-E \cdot r) \qquad 0 \leq r \leq \infty. \tag{4.4}$$

In this thesis, we design our non-uniform user distribution model with Matern cluster process. It is easy to extend to Thomas cluster, linear cluster and exponential cluster. The Matern cluster radius in the kth tier ($k \in \mathbb{S}$) between UE and its SA is defined as R_k. If R_k is high, the attraction level is low, vice versa. There is the same cluster radius R for each BS in the same tier. R_k is the parameter that determines the attraction level between UE and SA in the kth tier.

- Model of SAs dependent on BSs

Our non-uniform user distribution is modeled by a PCP with the cluster center located at SAs rather than being at BSs. The base station offset between SAs and their BSs represents the dependency level between SAs and BSs.

The base station offset, which is the distance in the kth tier ($k \in \mathbb{S}$) between SAs and their BSs, is defined as D_k. If the base station offset D_k is high, the dependency level is low, and vice versa. There is the same D for each BS in the same tier. Hence, the base station offset D_k is the parameter that determines the dependency level between

SAs and BSs in the kth tier.

- Parameters summary of the user model

  There are two parameters in our designed user distribution model:

  – Cluster radius R
    It is used to control the attraction level between UEs and their SAs.

  – Base station offset D
    It is used to control the dependency level between SAs and their BSs.

  We can choose the combinations of the cluster radius R and base station offset D to create the specific user distribution we need.

4.2.3 Attraction Level and Dependency Level

Figure 4.2: Range of attraction level and dependency level.

4.2.3.1 Attraction Level

The attraction level represents the attraction degree between UEs and SAs. The range of the attraction level is from 0 to 1. The value 0 means that there is no attraction and the distribution of UEs approaches to be uniform. The value 1 means that UEs are extremely attracted to a SA and UEs are located at the same position with the SA.

Let R be the Matern cluster radius of the non-uniform user distribution model. When the cluster radius is large enough, the user distribution converges to a uniform distribution. R_{uni} is the minimum Matern cluster radius where the performance of the non-uniform distribution based on R_{uni} is equivalent to the performance of the uniform distribution. The value of R_{uni} can be measured.

Definition 4-2. The attraction level is defined as follows.

$$\text{Attraction Level} = \begin{cases} 1 - \frac{R}{R_{uni}} & \text{if } R < R_{uni}, \\ 0 & \text{if } R \geq R_{uni}. \end{cases} \tag{4.5}$$

4.2.3.2 Dependency Level

The dependency level we define is used to represent the dependency degree between SAs and BSs. The range of the dependency level is also from 0 to 1. The value 0 means there is no dependency and the position of SAs is randomly and independently distributed with the position of BSs. The value 1 means that SAs are extremely dependent to BSs (SAs and BSs are in the same position).

Let D be the base station offset between SAs and BSs in the non-uniform user distribution model. D_{uni} is the minimum base station offset where the performance of the non-uniform user distribution based on D_{uni} is equivalent to the performance of the uniform distribution. The value of D_{uni} can be measured.

Definition 4-3. The dependency level is defined as follows.

$$\text{Dependency Level} = \begin{cases} 1 - \frac{D}{D_{uni}} & \text{if } D < D_{uni}, \\ 0 & \text{if } D \geq D_{uni}. \end{cases} \tag{4.6}$$

4.2.4 UE Realization

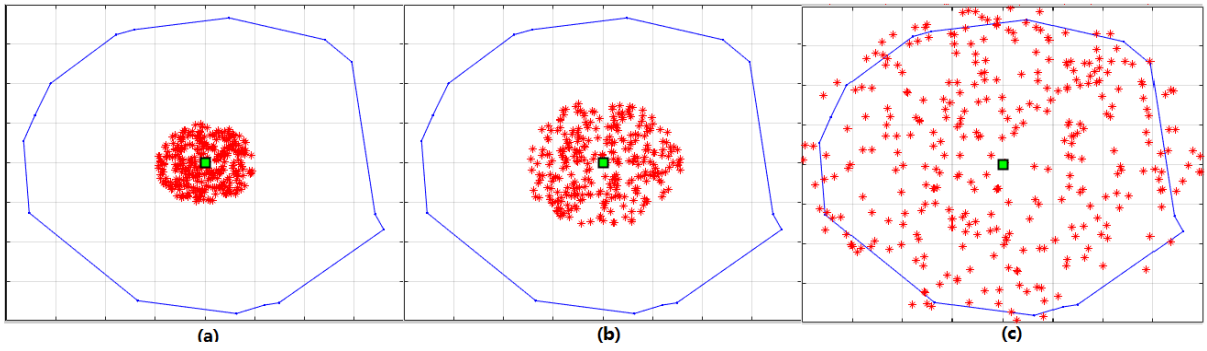

Figure 4.3: A user distribution realization of the non-uniform model (attraction level = 0.75 for (a), attraction level = 0.6 for (b) and attraction level = 0 for (c), dependency level = 1, blue curves are assumed to be cell boundaries).

Figure 4.3 shows examples of user distribution realization. Figure 4.3 is a Matern cluster PDF with the cluster radius parameter $R = 50$ for (a), $R = 80$ for (b) and $R = 200$ for (c). The cluster center is BS and the base station offset is zero between the cluster center (SA) and BS such that the dependency level is 1. We measure $R_{uni} = 200$. Then the attraction level for $R = 50$ is 0.75, the attraction level for $R = 80$ is 0.6, and the attraction level for $R = 200$ is 0. The blue curves are the cell boundaries. The green square is a small BS. The area is 400 m by 400 m. If R is small, such as 50 in (a), there is a high attraction level of 0.75 between the cluster center and UEs, which means that UEs converge to the cluster center, vice versa. UEs are assumed with high attraction level for small cells, such as (a) while UEs are assumed with low attraction level for macro cells, such as (c). The large number of UEs in Figure 4.3, which is just for better visualizing the UE spatial distribution and attraction levels, can be ignored.

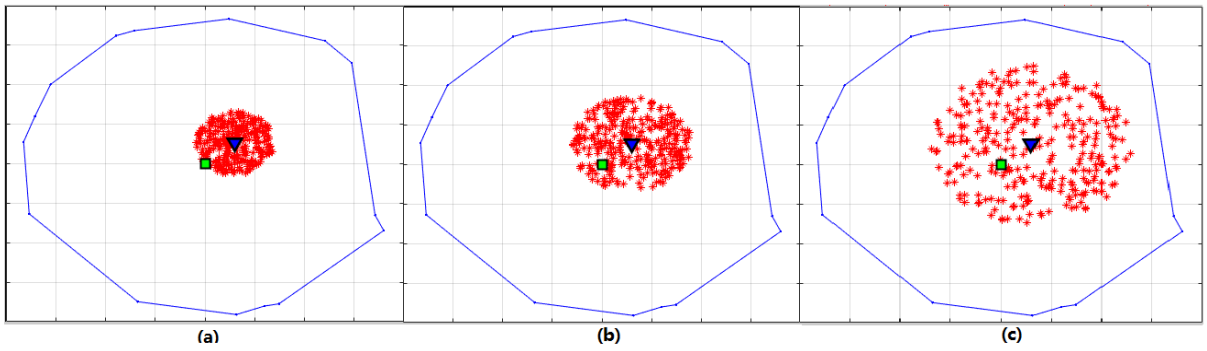

Figure 4.4: A user distribution realization of the non-uniform model with a dependency level is 0.6 (attraction level is 0.8 for (a), attraction level is 0.7 for (b), attraction level is 0.5 for (c), blue curves are assumed to be cell boundaries).

In Figure 4.4, (a) is $R = 40$ m (attraction level is 0.8), (b) is $R = 60$ m (attraction level is 0.7), (c) is $R = 100$ m (attraction level is 0.5). The base station offset between small BS (green square) and cluster center (blue triangle) is 40 m (dependency level is 0.6, measure $D_{uni} = 100$). The area is 400 m by 400 m.

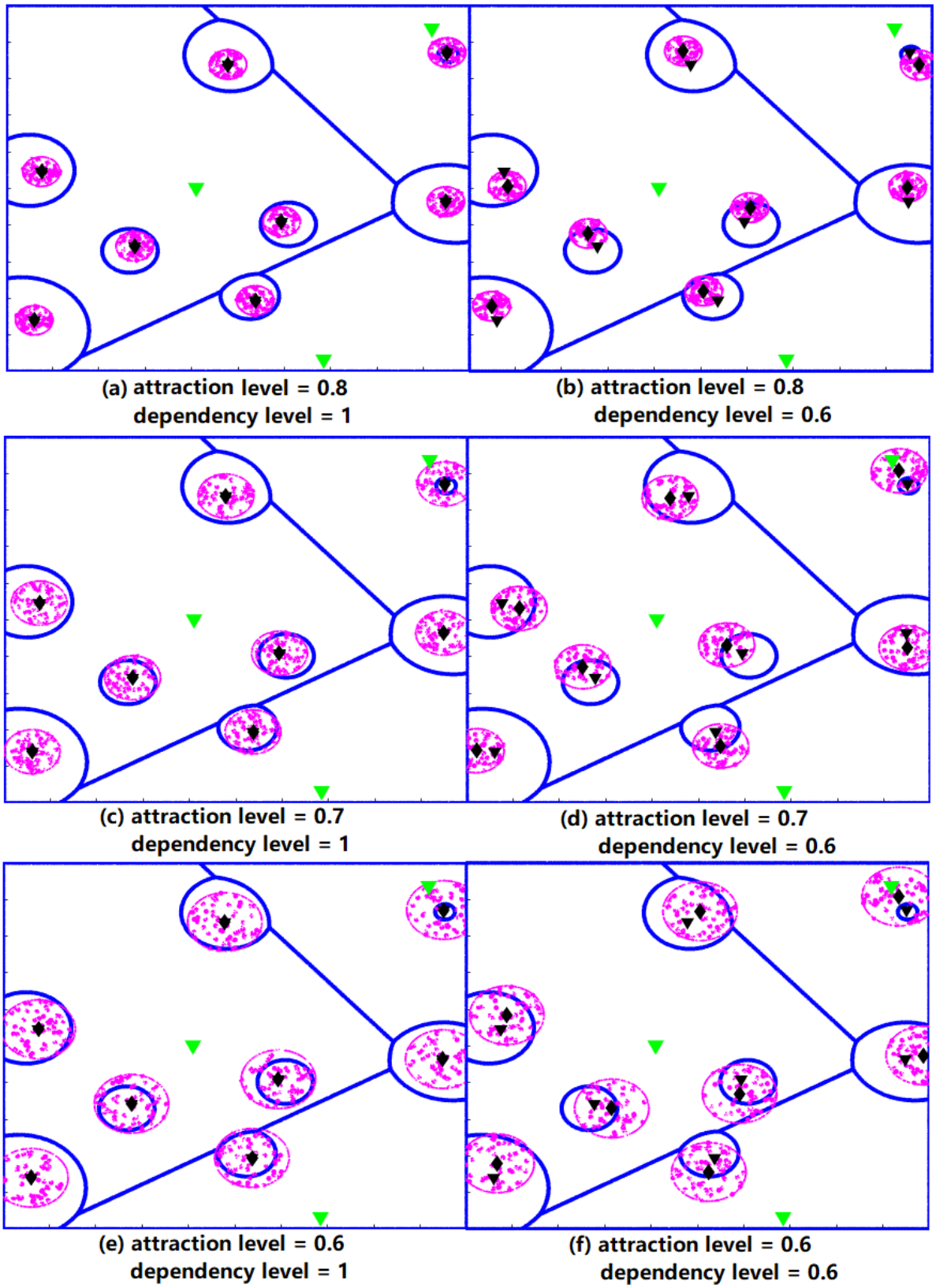

Figure 4.5: Non-uniform user distribution Scenario 1 (a-f). The area is 1 km by 1 km. Green triangles are macro BSs and black triangles are small BSs.

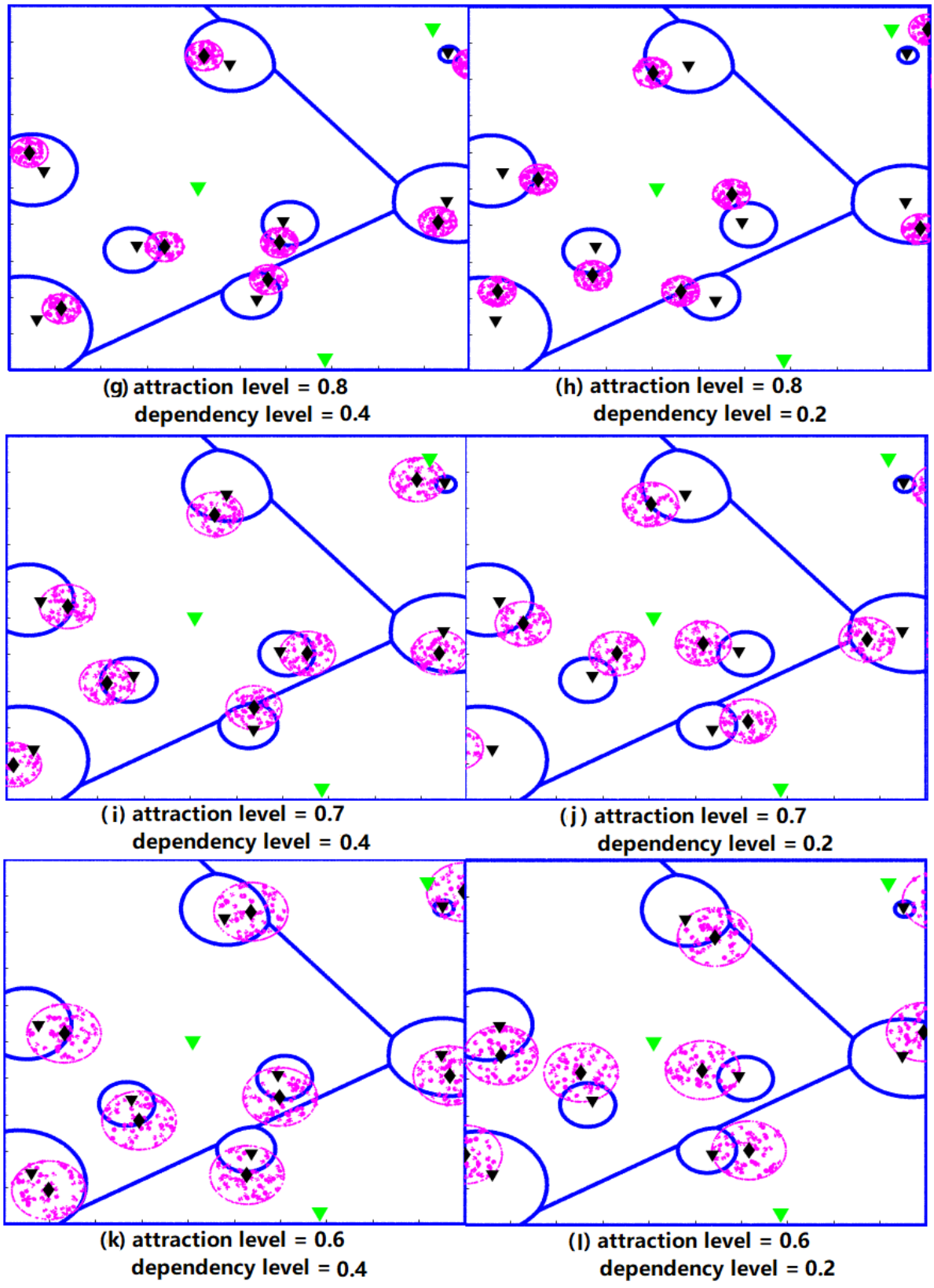

Figure 4.6: Non-uniform user distribution Scenario 1 (g-l). The area is 1 km by 1 km. Green triangles are macro BSs and black triangles are small BSs.

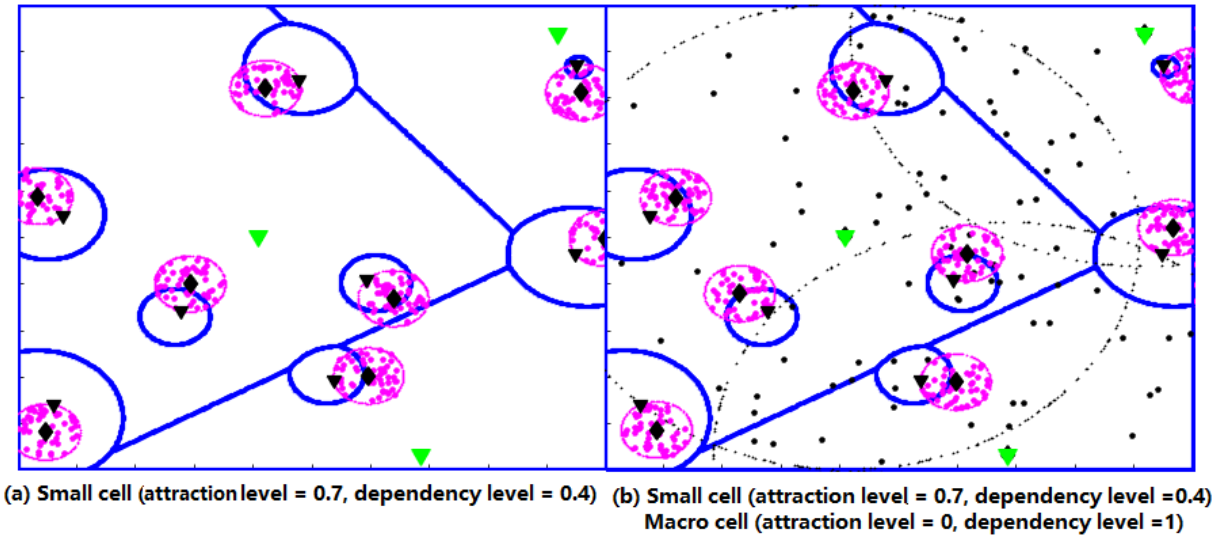

Figure 4.7: Non-uniform user distribution Scenario 2. There are non-uniform cluster users (magenta points) distributed for small cells. Magenta circles are UE cluster boundaries distributed for small cells. Black diamonds are UE cluster centers. There are also almost uniform users (black points) distributed for macro cells in (b). Black circles are UE cluster boundaries for macro cells. The blue curves are the cell boundaries. The area is 1 km by 1 km. Green triangles are macro BSs and black triangles are small BSs.

In Figure 4.5 and Figure 4.6, there are 3 macro BSs and 8 small BSs. Non-uniform UEs (magenta points) are distributed in small cells. The transmit power of macro BSs is 100 times greater than the transmit power of small BSs. We measure $R_{uni} = 200$ and $D_{uni} = 100$. In Figure 4.5 and Figure 4.6, the sub figures in each column have the same base station offset D, such as $D = 0$ (dependency level is 1) for sub figures (a, c, e), $D = 40$ (dependency level is 0.6) for sub figures (b, d, f), $D = 60$ (dependency level is 0.4) for sub figures (g, i, k) and $D = 80$ (dependency level is 0.2) for sub figures (h, j, l). In each column, the radius R from top to bottom is $R = 40$ (attraction level is 0.8), $R = 60$ (attraction level is 0.7) and $R = 80$ (attraction level is 0.6) separately. Each sub figure is a combination of different R and D, which would present plenty of non-uniform user distribution cases.

Figure 4.7 shows the mixed user model. In Figure 4.7 (a) there are non-uniformly distributed users ($R = 60$, $D = 60$, the attraction level is 0.7, and the dependency level is 0.4) with magenta points in small cell and in Figure 4.7 (b) there are almost uniformly distributed users ($R = 500$, $D = 0$, the attraction level is 0, and the dependency level is 1) with black points in macro cells besides the non-uniform users in small cells. It indicates the flexibility that this user model can represent different kinds of attraction levels and

dependency levels in each tier.

4.3 Heterogeneity Analysis of Non-Uniform User Distribution

The attraction and the dependency levels defined above are good indicators of heterogeneity. However, these two levels represent either the relationship between SAs and UEs or the relationship between SAs and BSs. We need another indicator to express the overall heterogeneity. In this section, the heterogeneity analysis is based on the coefficient of variation (CoV). CoV is a good overall indicator of users' spatial heterogeneity. It can be regarded a parameter of user's heterogeneity as path loss exponent in large scale fading.

4.3.1 Definition of CoV (Coefficient of Variation)

For the user distribution model, a suitable statistical measure is required to capture the traffic property, i.e. heterogeneity. Lots of traffic measures exist. In time domain, inter-arrival time is a good measurement. In space domain, there are the density based measures, such as Ripley's K-function and pair correlation function, which measures the user density within a given disc or ring, but it needs to be parameterized by the window size, such as the radius of the given disc. Another popular measurement is distance-based. For example, the nearest-neighbor measurement is the simplest candidate. However, only the nearest neighbor is considered in this measurement. Then there are some other proposed distance-based measures, such as Voronoi cell areas, Delaunay cell edge lengths, and Delaunay cell areas.

4.3.1.1 One Dimension (1D) or Time Domain

In 1D point pattern or the time domain, there are two ways to capture the traffic property.

- The first way is to count the number of arrival points during a specific interval. This is a density-based metric, in which deciding the interval length is challenging. Figure 4.8 (a) shows an example of the first way.
- Second way is Inter-Arrival Time (IAT) $I_k = \text{Time}_{k+1} - \text{Time}_k$, which is a popular measure. The IAT is the consumed time for any point to arrive compared with the

previous point, which is distance-based. Figure 4.8 (b) shows an example of the second way.

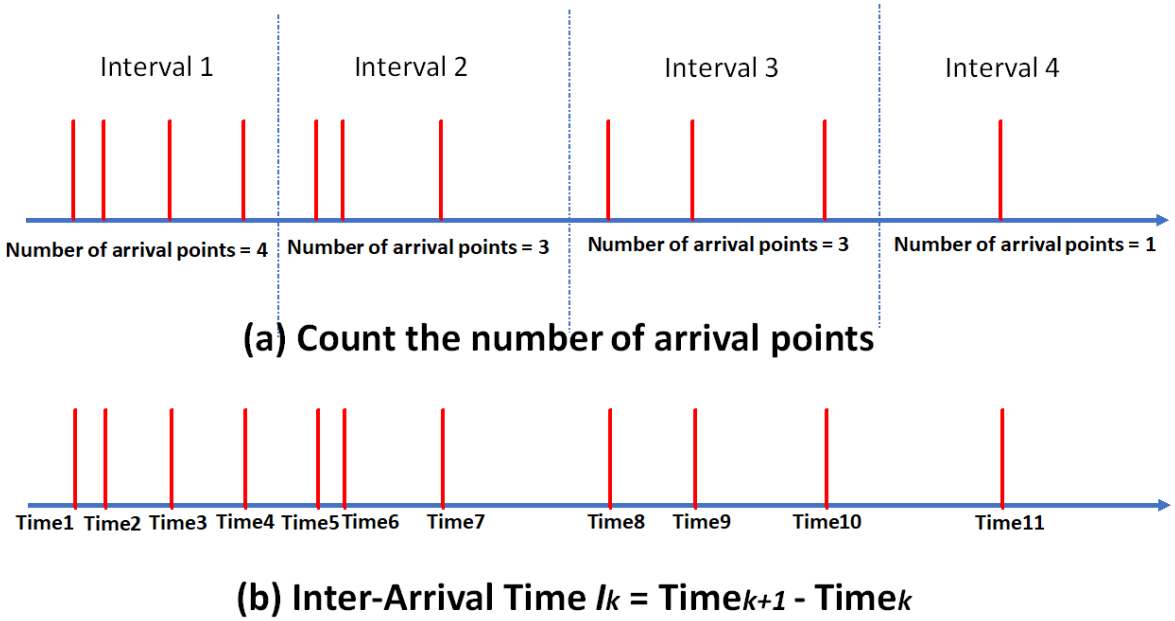

Figure 4.8: Two ways to capture the traffic property in 1D

Define C_I as normalized coefficient of variation (CoV), which is the ratio of standard deviation of I_k and the mean of I_k. For $C_I = 0$, it is 1D lattice distribution. For $C_I = 1$, it is 1D Poisson distribution. For $0 < C_I < 1$, it is sub-Poisson distribution. For $C_I > 1$, it is super-Poisson distribution. Figure 4.9 gives an example of pattern of 1D.

4.3.1.2 Two Dimensions (2D) or Space Domain

Statistics, such as the probability density function (PDF) and auto-correlation function of spatial user are required for good modeling. But it is hard to find a perfect match between the model and the practical scenario. Hence, simplified models only consider the first few moments of the user spatial distribution. The non-uniform user spatial placement in HetNets normally is modeled by two dimension (2D), in which Voronoi cell areas, Delaunay cell edge lengths and Delaunay cell areas [58,94] associated with the points can be measured as equivalents of IAT in the time domain.

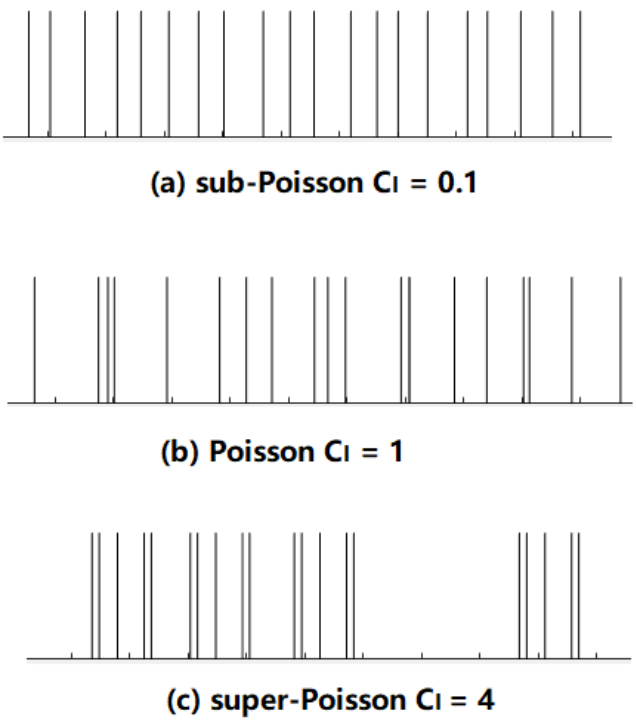

Figure 4.9: Pattern of 1D from left to right with sub-Poisson ($0 < C_E < 1$), Poisson ($C_E = 1$) and super-Poisson ($C_E > 1$)

According to the reference [95], we take C_E, which is a normalized CoV of the second-order as the desired statistics of user model.

$$\text{CoV} = \frac{\sigma_E}{\mu_E}, \tag{4.7}$$

where E is statistic measurement, such as Voronoi cell areas, Delaunay cell edge lengths and Delaunay cell areas. σ_E is the standard deviation of E and μ_E is the mean of E. C_E is normalized second order statistics CoV of user model, which demonstrates the deviation from homogeneity using inter-point distance metrics.

The C_E in 2D is the analog of C_I in 1D to capture heterogeneity of user distribution. It is shown in [94] that for a Poisson distribution $C_E = 1$, for a sub-Poisson distribution (more homogeneous than Poisson) $0 < C_E < 1$, and for a super-Poisson distribution (more heterogeneous than Poisson) $C_E > 1$.

Figure 4.10 gives examples of user distribution pattern. If the pattern is the perfect 2D lattice, the statistic measurement is the same for all points so that $C_E = 0$. Hence a constant distance between points creates the perfect homogeneity. But the Poisson distribution of $C_E = 1$ creates the complete randomness, which is shown in the middle of Figure 4.10. Sub-Poisson pattern is created from a perfect lattice and then apply a random displacement, which is shown in the left of Figure 4.10 with $0 < C_E < 1$. Sub-Poisson pattern is with more homogeneity than Poisson pattern. Super-Poisson pattern is created, such as hierarchical randomness and Markov models. Super-Poisson pattern is with more heterogeneity than Poisson, which is shown in the right of Figure 4.10.

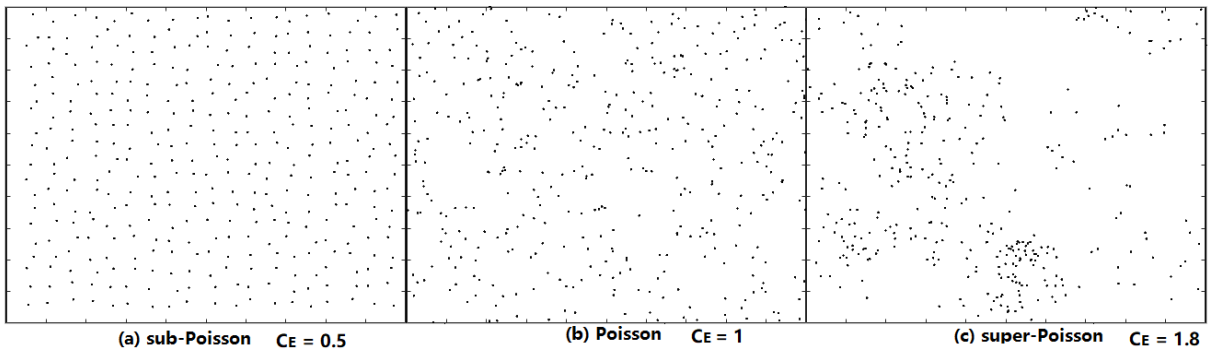

Figure 4.10: Pattern of 2D from left to right with sub-Poisson ($0 < C_E < 1$), Poisson ($C_E = 1$) and super-Poisson ($C_E > 1$)

4.3.2 CoV Measurement

The proposed distance-based measurement is Voronoi cell areas, Delaunay cell edge lengths, and Delaunay cell areas. The definition of Voronoi tessellation and Delaunay tessellation is given in the following.

Definition 4-4. Voronoi tessellation is defined as follows.

For a point pattern $P = \{p_1, p_2, ..., p_k\}$ in a D-dimensional Euclidean space $\mathbb{R}^D$, the Voronoi tessellation $V = \{V_{p_1}, V_{p_2}, ..., V_{p_k}\}$ is the set of cells so that any location $y \in V_{p_i}$ is closer to p_i than any other point in P which has the equation as

$$V_{p_i} = \{y \in \mathbb{R}^D : \mid y - p_i \mid \leq \mid y - p_j \mid \ \ for\ i, j \in 1, ..., k\}. \tag{4.8}$$

Definition 4-5. Delaunay tessellation is defined as follows.

D is space dimension. If $D+1$ Voronoi cells have an intersection, the corresponding Delaunay cell is made up of these $D+1$ points from the pattern $P = \{p_1, p_2, ..., p_k\}$.

Voronoi tessellation and Delaunay tessellation are said to be dual.

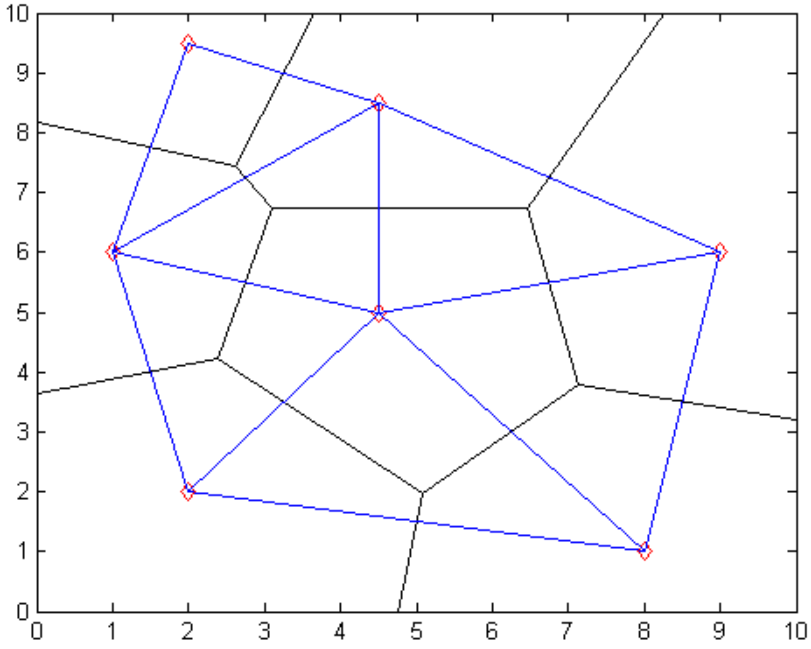

Figure 4.11: Example of Voronoi and Delaunay tessellations (Delaunay cell edges with blue lines and Voronoi cell edges with black lines, and the pattern points with red diamonds).

In the following, we evaluate measured normalized CoV based on Voronoi cell areas, Delaunay cell edge lengths, and Delaunay cell areas. In the simulations, we generate 1000 BS patterns and we then generate the non-uniformly distributed users on each BS pattern where a CoV values based on Voronoi cell areas, Delaunay cell edge lengths, and Delaunay cell areas are calculated separately. Normalized CoV is the measured CoV divided by CoV when PPP. For the detailed simulation setting, please refer to Appendix C.3. The area is a square of 1 km by 1 km. There are 3 macro BSs and 6 small BSs, which is equivalent to $\lambda_1 = \frac{3}{10^6}$ and $\lambda_2 = 2\lambda_1$. The path loss exponent is $\{\alpha_1, \alpha_2\} = \{3.5, 3.5\}$ and the transmit power $\{P_1, P_2\} = \{45, 35\}$ dBm.

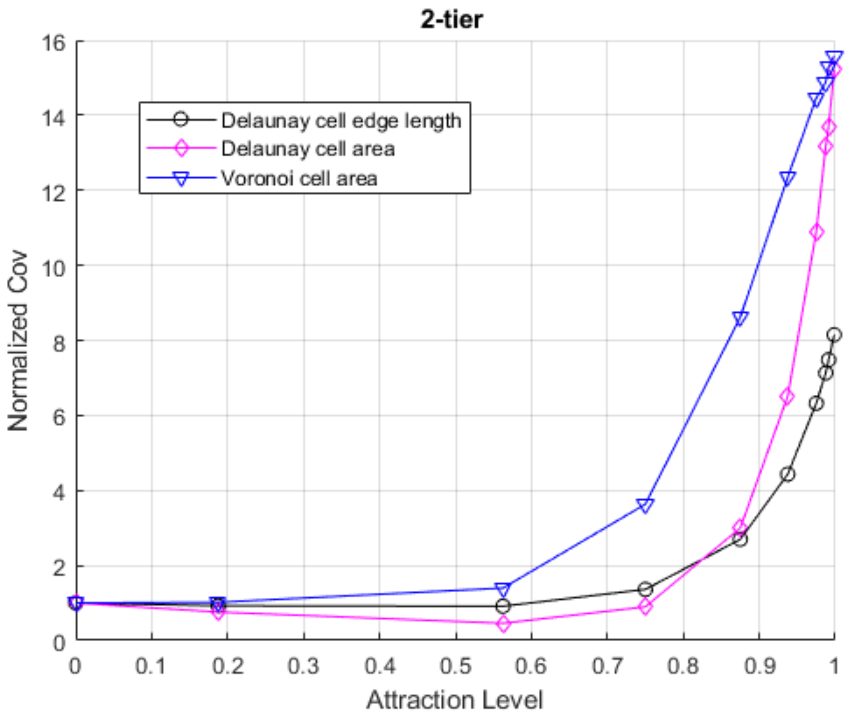

Figure 4.12: Measured normalized CoV for Delaunay cell edge length, Delaunay cell area, and Voronoi cell area (without base station offset between SAs and BSs.)

Figure 4.12 indicates the measured normalized CoV based on the attraction level in our designed user model. This figure shows that normalized CoV is high when the attraction level is high. CoV is a good indicator of users' spatial heterogeneity. High CoV represents high users' spatial heterogeneity, and vice versa. Hence, high attraction level results in high CoV such that high users' spatial heterogeneity. It also shows that Voronoi cell area is preferable to Delaunay cell edge length and Delaunay cell area since there is large CoV range and the slope is moderate. Therefore, Voronoi cell area is used as the traffic CoV statistic measurement in the following simulation results.

4.3.3 CoV Simulation Results

We take the normalized CoV, C_E, as an indication of users' heterogeneity. The relationship between normalized CoV and designed user model's properties, such as the attraction level and the dependency level, is given from Figure 4.13. It can be observed that the dependency level has little impact for normalized CoV and the attraction level has big impact for normalized CoV. Normalized CoV is very high when the attraction level is high. In Figure 4.14, the coverage probability based on the attraction level and the dependency level is

shown. When both the attraction and the dependency are high, the coverage probability is high. Otherwise the performance is almost the same as the uniform case.

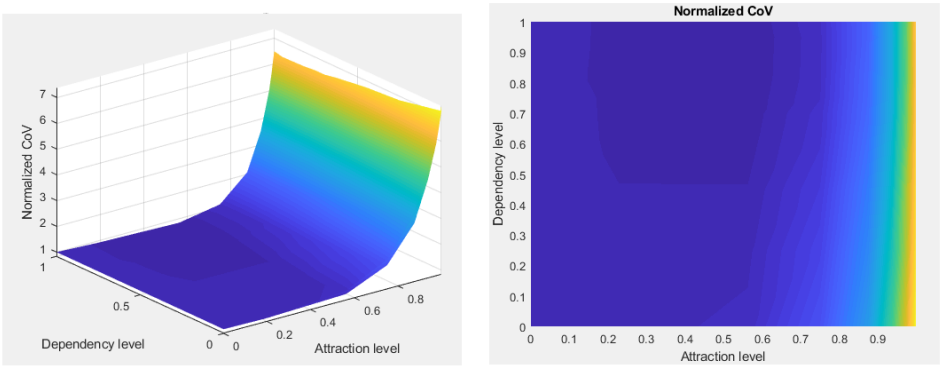

(a) Normalized CoV (b) View from top

Figure 4.13: Measured CoV based on the attraction level and the dependency level

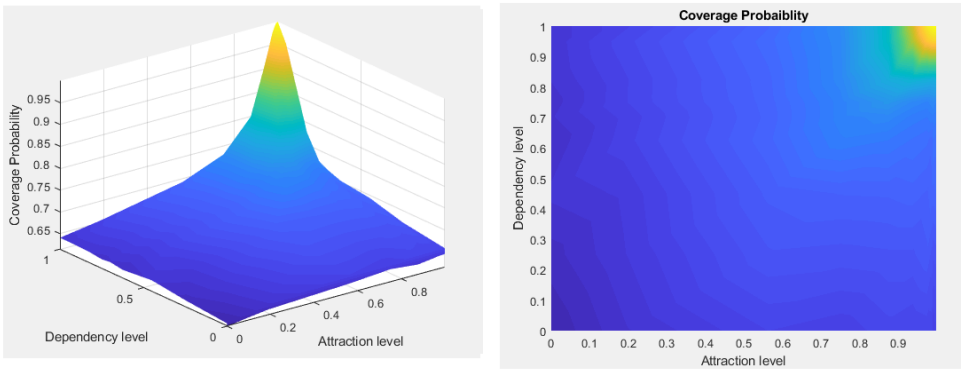

(a) Coverage probability (b) View from top

Figure 4.14: Measured coverage probability based on the attraction level and the dependency level

4.4 Conclusions

In this chapter, we introduced our non-uniform user distribution model. In our model, there is a parameter called the cluster radius R, which controls the attraction level between UEs and SAs. There is also another parameter called the base station offset D, which controls the dependency level between BSs and SAs. This user model is a Poisson cluster process (PCP) with the cluster centers located at the SAs and SAs may have a base station offset with their BSs. UEs in each tier may have their own attraction level and dependency level.

For example, in small cells UEs are non-uniformly distributed with high attraction level and high dependency level while in macro cells UEs are almost uniformly distributed with low attraction level and low dependency level.

The heterogeneity analysis is also given based on the normalized CoV of Voronoi cell area. It shows that the normalized CoV is high when the attraction level is high regardless of the dependency level. However, the coverage probability depends on both the attraction level and dependency level. Hence, high CoV (high heterogeneity) does not result in high coverage probability.

Chapter 5

Downlink Coverage Probability Performance Analysis

5.1 Introduction

In the first part of this chapter, we give the performance analysis of the downlink coverage probability for the designed non-uniform user distribution model. In the second part of this chapter, simulation results are provided to verify the accuracy of the performance analysis derived in the first part of this chapter.

Before we introduce the derivation of the downlink coverage probability, some notations are given:

- In our non-uniform user model, each SA has a base station offset with a BS. A UE cluster is distributed around each SA. The base station offset between each SA and its BS in the same tier is the same. In this thesis, the distance between the SA and its BS is called the base station offset.
- BS_i^j refers to the jth BS in the ith tier.
- Similarly, SA_i^j refers to the SA that has a base station offset D_i with BS_i^j.
- A UE of interest in the cluster is distributed around SA_i^j and SA_i^j has a base station offset D_i with BS_i^j. Since it is not certain that the UE of interest in the cluster has the nearest distance with BS_i^j or the UE of interest is associated with BS_i^j, we can not name BS_i^j as the nearest BS or associated BS and we just name BS_i^j as the BS that the UE of interest belongs to spatially.

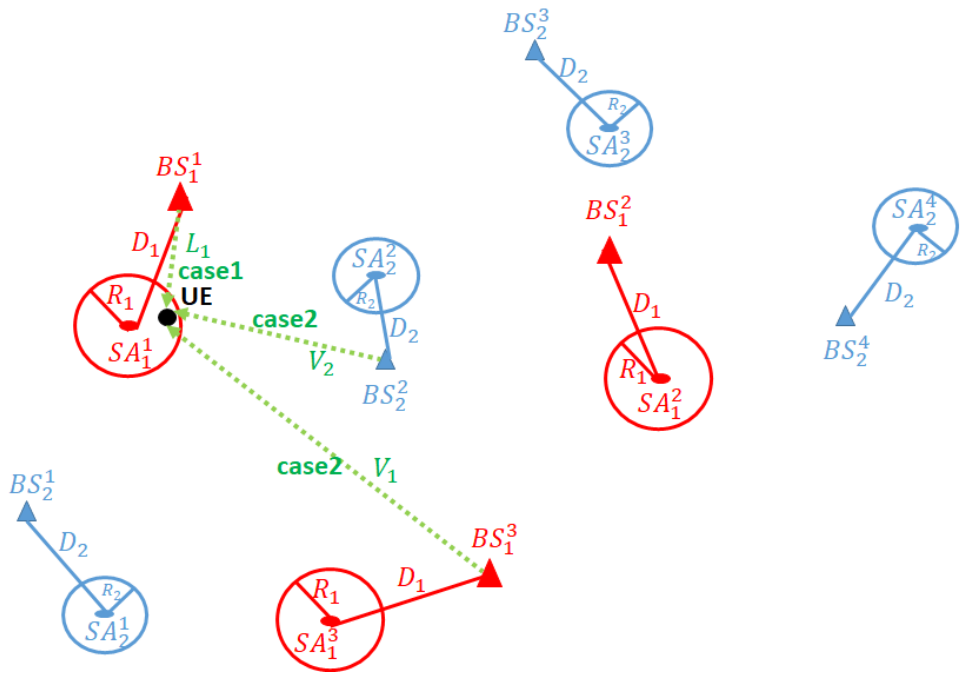

Figure 5.1: Example of spatial distances between UE, BS, and SA and the related notation in a 2-tier downlink system

Figure 5.1 shows an example of spatial distances between UE, BS, and SA and the related notation in a 2-tier downlink system. The 1th tier such as macro cell tier is in red and the 2th tier such as small cell tier is in blue. In the 1th tier, there are three BSs (BS_1^1, BS_1^2 and BS_1^3) and three corresponding SAs (SA_1^1, SA_1^2 and SA_1^3). The three corresponding SAs have a base station offset D_1 with the three BSs. In the 2th tier, there are four BSs (BS_2^1, BS_2^2, BS_2^3 and BS_2^4) and the four corresponding SAs (SA_2^1, SA_2^2, SA_2^3 and SA_2^4). The four corresponding SAs have a base station offset D_2 with the four BSs. In our non-uniform user distribution, a SA has a base station offset D_i with a ith tier BS. D_i is the parameter that determines the dependency level of a SA to its BS in the ith tier. There is a cluster of UE that surrounds each SA. The UEs are distributed uniformly within the disc of the radius R_i in the ith tier, which is called Matern cluster process. R_i is the parameter that determines the attraction level of a UE and its SA in the ith tier. The random variable L_i is the distance between the UE of interest and the BS that the UE belongs to spatially in the ith tier. The random variable V_i is the distance between the UE of interest and its closest BS in the ith tier.

Let us analyze the performance for a UE of interest, which is the black point in Figure 5.1. This black point UE is uniformly distributed inside the red disc with the radius R_1. The BS that the black point UE belongs to spatially is BS_1^1. The UE is distributed around the cluster center SA_1^1. SA_1^1 has a base station offset D_1 to BS_1^1. The possible BS that the

UE of interest will be associated with can be described into two cases. Case1 is that the UE of interest is associated with the BS_1^1 that it belongs to spatially. Case2 is that the UE of interest is associated with other BS, such as BSs in the 1th tier (BS_1^2 and BS_1^3), or BSs in the 2th tier (BS_2^1, BS_2^2, BS_2^3 and BS_2^4). Therefore, let us summarize the two cases of the possible BS that the UE of interest is associated with. The UE of interest in the cluster of SA_i^j may be associated with the BS_i^j (case1) or associated with another BS_m^k (case2). This BS_m^k may be of the same tier as i ($m = i, k \neq j$), or it may be in another tier ($m \neq i$).

Let $m = 1, 2, ...k$ be the tier of interest. The procedure to get the downlink coverage probability $\mathbb{P}_{dl,c}$ is as follows:

- Find the probability density function (PDF) $f_L^{(m)}(l)$ and complementary cumulative distribution function (CCDF) $\bar{F}_L^{(m)}(l) = \mathbb{P}^{(m)}(L > l)$ of random variable L. Let L be the distance between a UE and the BS that the UE belongs to in the mth tier.
- Find the PDF $f_V^{(m)}(v)$ and CCDF $\bar{F}_V^{(m)}(v) = \mathbb{P}^{(m)}(V > v)$ of random variable V. Let V be the distance between a UE and the closest BS in the mth tier.
- The possible BS that the UE of interest (e.g. black point UE in Figure 5.1) in a given mth tier is associated with can be summarized into two cases.
  Case1: associated with the BS to which the UE of interest belongs.
  - Derive $\mathbb{P}^{(m)}(A_{case1})$, which is the probability that a UE of interest is associated with the BS to which the UE belongs. In Figure 5.1, it means that the black point UE is associated with BS_1^1.
  - Derive the downlink coverage probability $\mathbb{P}^{(m)}[SINR_m(l) > T_m | A_{case1}]$ conditioned on the black point UE associated with BS_1^1.
  - Derive the downlink coverage probability $\mathbb{P}_{dl,c,case1}^{(m)} = \mathbb{P}^{(m)}(A_{case1}) * \mathbb{P}^{(m)}[SINR_m(l) > T_m | A_{case1}]$ that the black point UE is associated with BS_1^1 to which this UE belongs.

  Case2: associated with a BS in all tiers except the BS to which UE belongs (e.g. except BS_1^1)
  - Derive $\mathbb{P}^{(m)}(A_{k,case2})$, which is the probability that a UE is associated with a kth tier BS.
  - Derive the downlink coverage probability $\mathbb{P}^{(m)}[SINR_k(v) > T_k | A_{k,case2}]$ conditioned on a UE associated with a kth tier BS.

  - Derive the downlink coverage probability $\mathbb{P}^{(m)}_{dl,ck,case2} = \mathbb{P}^{(m)}(A_{k,case2}) * \mathbb{P}^{(m)}[SINR_k(v) > T_k | A_{k,case2}]$ of associating with a kth tier BS.

  Summary

  - $\mathbb{P}^{(m)}(A_{case1})$ and $\mathbb{P}^{(m)}(A_{k,case2})$ is the probability that a UE of interest in the mth tier is associated with the BS to which UE belongs and a kth tier BS. $\mathbb{P}^{(m)}(A_{case1}) + \sum_{k=1}^{K} \mathbb{P}^{(m)}(A_{k,case2}) = 1$. K is the total number of BS tiers.
  - The downlink coverage probability for a UE distributed in the mth tier is $\mathbb{P}^{(m)}_{dl,c} = \mathbb{P}^{(m)}_{dl,c,case1} + \sum_{k=1}^{K} \mathbb{P}^{(m)}_{dl,ck,case2}$.

- The overall coverage probability of the designed non-uniform distribution model is

$$\mathbb{P}_{dl,c} = \sum_{m \in \mathbb{S}} \frac{N_m \lambda_m}{\sum_{m \in \mathbb{S}} N_m \lambda_m} \mathbb{P}^{(m)}_{dl,c}, \tag{5.1}$$

  where N_m is the average number of users in each cluster of the mth tier. λ_m is the BS density of the mth tier. There are total of S tiers with a subset $\mathbb{S}$ distributed with our designed non-uniform user model.

5.2 Model Performance Analysis

In this section, we derive the downlink coverage probability. The definition of the downlink coverage is as follows.

Definition 5-1. The downlink SINR at a typical UE located at the origin in the kth tier is

$$SINR_k(r) = \frac{P_k G_k r^{-\alpha_k}}{I_r + \frac{\sigma^2}{L_0}}, \tag{5.2}$$

$$I_r = \sum_{j=1}^{K} I_{rj} = \sum_{j=1}^{K} \sum_{B_{ji} \in \phi_j \setminus B_0} P_j G_j r_{ji}^{-\alpha_j}, \tag{5.3}$$

- P_k is BS transmit power in the kth tier.

- G_k denotes the channel random power gain in the kth tier. Let the complex channel coefficient between the kth tier BS and the user be denoted as h_k (Rayleigh fading is assumed in this thesis). Then we define $G_k = |h_k|^2$, which is an exponential distribution with unity mean.
- α_k is the path loss exponent in the kth tier.
- r_{ji} is the distance of the typical user to the ith BS in the jth tier (i.e. B_{ji}).
- I_r is the total received interference from all BSs (except the associated BS at B_0) and I_{rj} is the total received interference from the jth tier (see (5.3)).
- σ^2 is the power of the additive white Gaussian noise (AWGN).
- K is the total number of tiers.
- ϕ_i is SPPP with a density λ_i in the ith tier.
- L_0 is the path loss at a reference distance of 1 m.

Definition 5-2. A UE in the kth tier is in the coverage if the downlink SINR from the associated BS with the maximum downlink average bias received power is more than the coverage threshold T_k ($\boldsymbol{\phi}_j$ is an independent homogeneous PPP).

$$SINR_k = \frac{P_k G_k r^{-\alpha_k}}{\sum_{j=1}^{K} \sum_{B_{ji} \in \phi_j \setminus B_0} P_j G_j {r_{ji}}^{-\alpha_j} + \frac{\sigma^2}{L_0}} > T_k. \tag{5.4}$$

5.2.1 Distance Characterization

5.2.1.1 PDF and CCDF of Random Variable V

V is a random variable that represents the distance between a UE of interest and the closest BS. The distance between the UE of interest and other BSs must be farther than V. Because the BS distribution in each tier is an independent PPP, the probability density function of V is obtained by the conclusion of the null probability of a PPP. The distribution of V is given from [24] and [96].

Remark 5-1. The distribution of V in the mth tier is

$$\text{PDF:} \qquad f_V^{(m)}(v) = 2\pi\lambda_m v \exp(-\lambda_m \pi v^2), \tag{5.5a}$$

$$\text{CCDF:} \qquad \bar{F}_V^{(m)}(v) = \exp(-\lambda_m \pi v^2), \tag{5.5b}$$

where λ_m is the BS distribution density of the mth tier.

5.2.1.2 PDF and CCDF of Random Variable L

L is a random variable that represents the distance between a UE of interest and the BS that the UE of interest belongs to spatially. Matern cluster process has a PDF of $f_u(r) = \frac{1}{\pi R_m^2}$ $(0 \leq r \leq R_m)$, which means that the clustered UEs are uniformly distributed within a circular disc with the radius R_m around the SA in the mth tier. D_m is the base station offset between the surrounded SA and the BS that the UE belongs to in the mth tier.

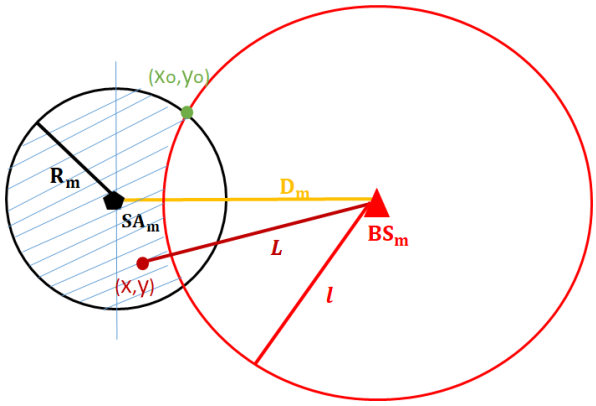

Figure 5.2: Calculation example of PDF and CCDF of Random Variable L in the mth tier

Figure 5.2 gives an example of PDF and CCDF calculation in the mth tier. We assume that SA_m is located at the origin and (x, y) are the coordinates of a UE of interest in the Matern cluster (the black disc with the radius R_m). $L = \sqrt{(x - D_m)^2 + y^2}$ is the random distance variable between the UE of interest and BS_m to which the UE of interest belongs. The red circle is the position where the distance to BS_m is l so that CCDF $\bar{F}_L^{(m)}(l) = \mathbb{P}^{(m)}(L > l)$ is the proportion of the shadowed area to the whole black cluster disc area since the UE of interest is uniformly distributed within the black cluster disc. PDF $f_L^{(m)}(l)$ is the proportion of the red arc length of the shadow part to the whole black cluster disc area.

According to Figure 5.2, we get the following equations of the coordinates (x_0, y_0) of the joint point between the black user cluster disc and the red circle which will be used in the following derivation.

$$\begin{aligned} &{x_0}^2 + {y_0}^2 = R_m^2, \\ &(D_m - {x_0}^2) + {y_0}^2 = l^2, \\ &\Rightarrow x_0 = \frac{{D_m}^2 + R_m^2 - l^2}{2D_m}, \\ &\Rightarrow y_0 = \frac{1}{2D_m}\sqrt{\|4{D_m}^2 R_m^2 - ({D_m}^2 + R_m^2 - l^2)^2\|}. \end{aligned} \tag{5.6}$$

Corollary 5-1. PDF $f_L^{(m)}(l)$ and CCDF $\bar{F}_L^{(m)}(l)$ of the random variable L in the mth tier is in Table 5.1.

For proof of Table 5.1 see Appendix A.1.

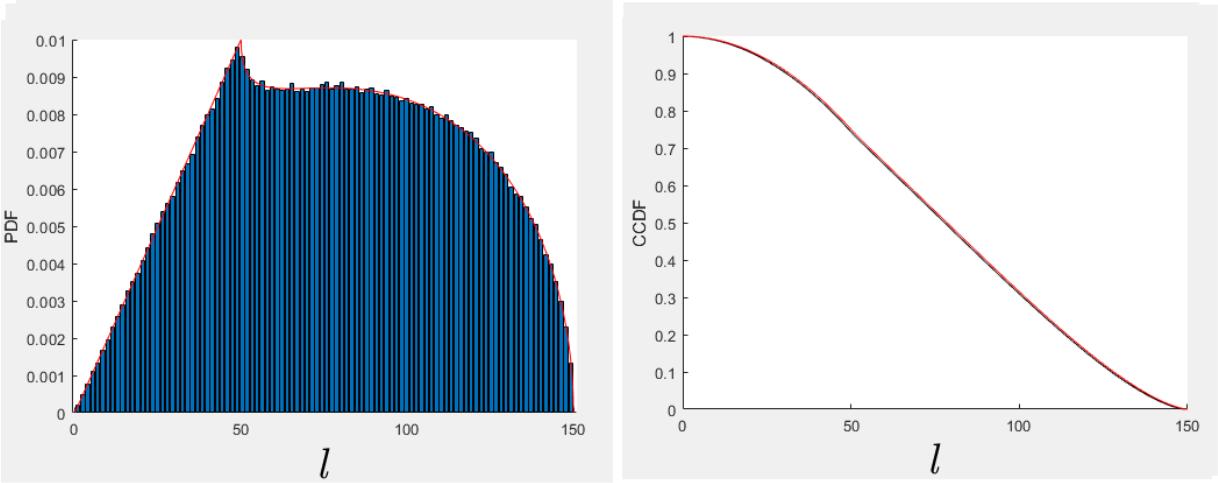

Figure 5.3: PDF and CCDF example of L $(R = 100, D = 50)$

Figure 5.3 shows an example for PDF and CCDF of L. The figure on the left is about PDF where the blue bins are from simulations and the red curve is from the above derived equations in Table 5.1. It shows that the simulations and derivations match closely. The curve on the right is about CCDF where the black curve is from simulations and the red curve is from the above derived equations in Table 5.1. The simulation curves and derivations also match closely.

Table 5.1: PDF and CCDF of the random variable L

	Scope	θ_1	θ_2	$\bar{F}_L^{(m)}(l)$	$f_L^{(m)}(l)$
When $D_m \geq R_m$	$l \leq D_m - R_m$	NA	NA	1	0
	$D_m - R_m < l < D_m + R_m$	$(\arctan\frac{y_0}{x_0}+\pi)\%\ \pi$	$(\arctan\frac{y_0}{D_m-x_0}+\pi)\%\ \pi$	$1-\frac{\theta_1 R_m^2+\theta_2 l^2-D_m y_0}{\pi R_m^2}$	$\frac{2\theta_2 l}{\pi R_m^2}$
	$D_m + R_m \leq l$	NA	NA	0	0
When $D_m < R_m$	$l \leq R_m - D_m$	NA	NA	$1-\frac{l^2}{R_m^2}$	$\frac{2l}{R_m^2}$
	$R_m - D_m < l < R_m + D_m$	$(\arctan\frac{y_0}{x_0}+\pi)\%\ \pi$	$(\arctan\frac{y_0}{D_m-x_0}+\pi)\%\ \pi$	$1-\frac{\theta_1 R_m^2+\theta_2 l^2-D_m y_0}{\pi R_m^2}$	$\frac{2\theta_2 l}{\pi R_m^2}$
	$R_m + D_m \leq l$	NA	NA	0	0
When $D_m = 0$	$l \geq R_m$	NA	NA	0	0
	$l < R_m$	NA	NA	$1-\frac{l^2}{R_m^2}$	$\frac{2l}{R_m^2}$

$x_0 = \frac{{D_m}^2+R_m^2-l^2}{2D_m}$ and $y_0 = \frac{1}{2D_m}\sqrt{\|4{D_m}^2R_m^2-({D_m}^2+R_m^2-l^2)^2\|}$.
$a\%b$ is the remainder when dividing a by b.

5.2.2 Interference Characterization

The total downlink interference of the UE of interest from BSs in all tiers except the associated BS B_0 is

$$I_r = \sum_{j=1}^{K} I_{rj} = \sum_{j=1}^{K} \sum_{B_{ji} \in \phi_j \setminus B_0} P_j G_j r_{ji}^{-\alpha_j}. \tag{5.7}$$

The basic reason that we can analyze the performance theoretically using the tools of stochastic geometry is that the distribution of BS in each tier is an independent PPP. And we can transform the unlimited sum of interference from BSs in one tier into an integral expression utilizing the property of products over PPP (probability generating functional (PGFL)). If ϕ is a PPP with the density λ, this expression is $\mathbb{E}[\prod_{x\in\phi} f(x)] = \exp(-\lambda \int_{\mathbb{R}^2}(1-f(x))dx)$. Specifically, the Laplace transform $\mathscr{L}_x(s) = \mathbb{E}_x[e^{-sx}]$ ($\mathbb{E}_x[*]$ is the expectation of $*$ over x) of the interference is very useful during the theoretical derivation.

Lemma 5-1. Calculate the Laplace transform of the total interference in the jth tier.

$$\begin{aligned}
&\mathscr{L}_{I_{rj}}(s) \\
&= \mathbb{E}_{I_{rj}}[e^{-sI_{rj}}], \\
&= \mathbb{E}_{\phi_j}[e^{-s\sum_{B_{ji}\in\phi_j\setminus B_0} P_j G_j r_{ji}^{-\alpha_j}}], \\
&= \mathbb{E}_{\phi_j}[\prod_{x\in\phi_j} e^{-sP_j G_j r_{ji}^{-\alpha_j}}], \\
&\overset{(a)}{=} \exp(-\lambda_j \int_{\mathbb{R}^2} (1 - \mathbb{E}_{G_j}(e^{-sP_j G_j x^{-\alpha_j}}))dx), \\
&= \exp(-2\pi\lambda_j \int_{d_{min}}^{\infty} (1 - \mathscr{L}_{G_j}(sP_j r^{-\alpha_j}) r dr), \\
&\overset{(b)}{=} \exp(-2\pi\lambda_j \int_{d_{min}}^{\infty} (1 - \frac{1}{1+sP_j r^{-\alpha_j}}) r dr), \\
&= \exp(-2\pi\lambda_j \int_{d_{min}}^{\infty} (\frac{sP_j r^{-\alpha_j}}{1+sP_j r^{-\alpha_j}}) r dr),
\end{aligned} \tag{5.8}$$

where (a) comes from the property of product over PPP (PGFL). (b) follows the Laplace transform of the Rayleigh fading in which the fading power G_j is the exponential distribution with unity gain and the Rayleigh fading envelope is $\sqrt{G_j}$. d_{min} is the distance to the

closest interferer in the jth tier. The above procedure follows the same derivation as [75].

5.2.3 Downlink Coverage Probability for Case1 (associated with the BS to which the UE belongs)

In this subsection, we derive the downlink coverage probability that a UE of interest in a cluster of the mth tier associates with the BS to which the UE belongs. The SA in the cluster center has the distance D_m with the BS to which the UE belongs. In Figure 5.1, it means that a UE of interest (black point) clustered around SA_1^1 is associates with the red triangle BS_1^1.

Lemma 5-2. The probability that a UE of interest in the mth tier is associated with the BS that the UE belongs to is (conditioned on the distance l between the UE of interest and the BS that the UE belongs to)

$$\mathbb{P}_{|l}^{(m)}(A_{case1}) = \prod_{i=1}^{K} \exp(-\lambda_i \pi (\frac{P_i C_i}{P_m C_m})^{\frac{2}{\alpha_i}} \cdot l^{\frac{2\alpha_m}{\alpha_i}}). \tag{5.9}$$

For proof see Appendix A.2.

Lemma 5-3. The coverage probability associated with the BS that a UE of interest belongs to is (conditioned on the distance l between the UE of interest and the BS that the UE belongs to)

$$\begin{aligned} &\mathbb{P}_{|l}^{(m)}[SINR_m(l) > T_m | A_{case1}] \\ &= \exp(-\frac{\sigma^2}{L_0} T_m {P_m}^{-1} l^{\alpha_m}) \cdot \prod_{i=1}^{K} \mathscr{L}_{I_{ri}}(T_m {P_m}^{-1} l^{\alpha_m}), \end{aligned} \tag{5.10}$$

where T_m is SINR coverage threshold in the mth tier. For proof see Appendix A.3.

For the details of $\mathscr{L}_{I_{ri}}(T_m {P_m}^{-1} l^{\alpha_m})$, the reader is referred to Equation 5.8 and [75]. $\mathscr{L}_{I_{ri}}(s)$ is the Laplace transform of the total interference in the ith tier.

$$
\begin{aligned}
&\mathscr{L}_{I_{ri}}(T_m {P_m}^{-1} l^{\alpha_m}) \\
&= \exp(-2\pi\lambda_i \int_{d_{min}}^{\infty} (\frac{T_m {P_m}^{-1} l^{\alpha_m} P_i r^{-\alpha_i}}{1 + T_m {P_m}^{-1} l^{\alpha_m} P_i r^{-\alpha_i}}) r dr), \\
&= \exp(-2\pi\lambda_i \int_{d_{min}}^{\infty} (\frac{1}{1 + (T_m l^{\alpha_m} \frac{P_i}{P_m})^{-1} r^{\alpha_i}}) r dr), \\
&= \exp\{-\pi\lambda_i (\frac{P_i}{P_m})^{\frac{2}{\alpha_i}} \cdot \mathcal{Z}(T_m, \alpha_i, \frac{C_i}{C_m}) \cdot l^{\frac{2\alpha_m}{\alpha_i}}\},
\end{aligned}
\tag{5.11}
$$

where $d_{min} = (\frac{P_i C_i}{P_m C_m})^{\frac{1}{\alpha_i}} \cdot l^{\frac{\alpha_m}{\alpha_i}}$ from Appendix A.2.

$\mathcal{Z}(T_m, \alpha_i, \frac{C_i}{C_m}) = \frac{2T_m}{\alpha_i - 2}(\frac{C_i}{C_m})^{\frac{2}{\alpha_i}-1} \cdot {}_2F_1[1, 1 - \frac{2}{\alpha_i}; 2 - \frac{2}{\alpha_i}, -\frac{T_m C_m}{C_i}]$ from [75].

where ${}_2F_1$ indicates the Gauss hypergeometric function.

Theorem 5-1. The coverage probability that a UE of interest in the mth tier is associated with the BS that the UE of interest belongs to is

$$
\mathbb{P}^{(m)}_{dl,c,case1} = \int_0^{\infty} \mathbb{P}^{(m)}_{|l}[SINR_m(l) > T_m | A_{case1}] \cdot \mathbb{P}^{(m)}_{|l}(A_{case1}) \cdot f^{(m)}_L(l) \cdot \mathbf{d}l, \tag{5.12}
$$

where $f^{(m)}_L(l)$ comes from subsection 5.2.1.2, which is the PDF of L in the mth tier. L is the random distance variable between a UE of interest and the BS that the UE belongs to. Each tier may have their own cluster radius R and base station offset D such that the PDF of L ($f^{(m)}_L(l)$) in each tier may be different.

5.2.4 Downlink Coverage Probability for Case2 (associated with a BS in all tiers except the BS to which UE belongs)

In this subsection, we derive the coverage probability of a UE of interest in a cluster of the mth tier associated with a BS in all tiers except the BS that UE belongs to. In Figure 5.1, it means that a UE of interest (black point) clustered around SA^1_1 is associated with a BS except the red triangle BS^1_1.

Lemma 5-4. The probability that a UE of interest is associated with a BS in the kth tier rather than the BS to which the UE belongs is (conditioned on the distance v between the

UE of interest and the closest BS in the kth tier)

$$\begin{aligned}&\mathbb{P}^{(m)}_{|v}(A_{k,case2})\\&= \bar{F}^{(m)}_{L}((\frac{P_m C_m}{P_k C_k})^{\frac{1}{\alpha_m}} \cdot v^{\frac{\alpha_k}{\alpha_m}}) \cdot \prod_{i=1, i\neq k}^{K} \exp(^{-\lambda_i \pi (\frac{P_i C_i}{P_k C_k})^{\frac{2}{\alpha_i}} \cdot v^{\frac{2\alpha_k}{\alpha_i}}}).\end{aligned} \tag{5.13}$$

For proof see Appendix A.4.

Lemma 5-5. The coverage probability associated with a kth tier BS rather than the BS that the UE of interest belongs to is (conditioned on the distance v between the UE of interest and the closest BS in the kth tier)

$$\begin{aligned}&\mathbb{P}^{(m)}_{|v}[SINR_k(v) > T_k | A_{k,case2}]\\&= \exp(-\frac{\sigma^2}{L_0} T_k {P_k}^{-1} v^{\alpha_k}) \prod_{i=1}^{K} \mathscr{L}_{I_{ri}}(T_k {P_k}^{-1} v^{\alpha_k}).\end{aligned} \tag{5.14}$$

For the proof the reader can refer to Equation 5.10.

Theorem 5-2. The coverage probability that a UE of interest in the mth tier is associated with a kth tier BS rather than the BS that the UE of interest belongs is

$$\begin{aligned}&\mathbb{P}^{(m)}_{dl,ck,case2}\\&= \int_0^\infty \mathbb{P}^{(m)}_{|v}[SINR_k(v) > T_k | A_{k,case2}] \cdot \mathbb{P}^{(m)}_{|v}(A_{k,case2}) \cdot f^{(k)}_V(v)\ \mathbf{d}v,\\&= \int_0^\infty \mathbb{P}^{(m)}_{|v}[SINR_k(v) > T_k | A_{k,case2}] \cdot \mathbb{P}^{(m)}_{|v}(A_{k,case2}) \cdot 2\pi\lambda_k v \exp(-\lambda_k \pi v^2)\ \mathbf{d}v,\end{aligned} \tag{5.15}$$

where $f^{(k)}_V(v) = 2\pi\lambda_k v \exp(-\lambda_k \pi v^2)$ is the PDF of the distance V between the UE of interest and the closest BS in the kth tier with a PPP distribution. $\mathbf{d}v$ is the derivative operation over v.

5.2.5 Overall Downlink Coverage Probability

If the UE of interest is distributed around a SA, which has the base station offset D_m with the BS that the UE of interest belongs to, Equation (5.12) and Equation (5.15) give

the coverage probability associated with the BS that the UE of interest belongs to (case1) or other BS (case2). When $D_m = 0$ m, this special case is the non-uniform user model discussed in [23] and [24].

Lemma 5-6. The downlink coverage probability for a non-uniform UE distributed in a mth tier is

$$\mathbb{P}_{dl,c}^{(m)} = \mathbb{P}_{dl,c,case1}^{(m)} + \sum_{k=1}^{K} \mathbb{P}_{dl,ck,case2}^{(m)}. \tag{5.16}$$

Theorem 5-3. The overall coverage probability is

$$\mathbb{P}_{dl,c} = \sum_{m \in \mathbb{S}} \frac{N_m \lambda_m}{\sum_{m \in \mathbb{S}} N_m \lambda_m} \mathbb{P}_{dl,c}^{(m)}, \tag{5.17}$$

where N_m is the average number of users in each cluster of the mth tier. λ_m is the BS density of the mth tier. There are total of S tiers with a subset $\mathbb{S}$ distributed with our designed non-uniform user model.

5.3 Simulation Results

BSs are deployed in a square area of 2 km by 2 km. A 2-tier system is simulated consisting of macro and small BSs. Different tiers are independent PPPs with their own BS densities, BS transmit powers, and path loss exponents. Define $\kappa = \{1, 2\}$ as the indices of the 2 tiers (macro cell and small cell tiers). Our non-uniform user distribution model is applied over the small cells so that the subset $\mathbb{S} = \{2\}$. The base station offset between SA and its BS in the small cells is defined as D_2. The fading channel between BSs and UEs is assumed to be Rayleigh fading with unity power gain. Firstly, we generate a BS pattern, and then a SA is selected uniformly around the circle with the radius D_2 to each BS. A cluster of UEs is generated with Matern cluster process around each SA. The average number of UEs, N_m, in a cluster is taken as 20. SINR of each UE in the cluster is measured. We repeat to generate BS pattern, SA, and UE cluster and calculate their SINRs until the number of BS pattern reaches 1,000. We then compare the above simulated coverage probability and the theoretical analysis from Equation (5.17). The detailed simulation setting is discussed

in Appendix C.1.

For the parameters, we follow the same setting as [75]. The thermal noise is assumed to be -104 dBm for all cases. The path loss L_0 at a reference distance 1 m is assumed to be -38.5 dB. In the 2-tier BS system, there are 12 macro BSs and 120 small BSs, which is equivalent that the BS density λ_2 of the small cell tier is 10 times more than the BS density λ_1 of the macro cell tier (the BS density of the macro cell tier is $\lambda_1 = \frac{3}{10^6}$). We choose the path loss exponent as 3.5 for both tiers. The transmit power of macro BSs is 100 times greater than the transmit power of small BSs, which is $\{P_1, P_2\} = \{53, 33\}$dBm. As we know the maximum transmit power of LTE on a 10MHz bandwidth is about 46 dBm according to 3GPP TR 36.942, but here we set it to 53 dBm. One reason is that we want to follow the same parameter setting as [75] as our baseline. The other reason is rather than the actual transmit power that determines the coverage probability it is the the power ratio between macro BSs and small BSs. There is no cell extension bias factor for both tiers, which is $\{C_1, C_2\} = \{1, 1\}$. The summary table of used parameters is shown in Table 5.2.

There is no cell extension bias factor in the subsection 5.3.1 and 5.3.2. The effect of cell extension bias factor will be discussed in the subsection 5.3.3. We also discuss the effect of system parameters, such as BS density ratio between small cells and macro cells, and BS transmit power of small cells. For the path loss exponents, it is hard to determine that the path loss exponent of small cells is higher or lower than the path loss exponent of macro cells. Hence, the different relationships of the path loss exponents between the macro cells and the small cells are discussed in the subsection 5.3.3 of effect of system parameters.

Table 5.2: Parameters about BSs of a 2-tier system

	Value
BS density	$\{\lambda_1, \lambda_2\} = \{\frac{3}{10^6}, \frac{3}{10^5}\}$
Path loss exponent	$\{\alpha_1, \alpha_2\} = \{3.5, 3.5\}$
Cell extension bias factor	$\{C_1, C_2\} = \{1, 1\}$
BS transmit power	$\{P_1, P_2\} = \{53, 33\}$ dBm
R_{uni}	200 m
D_{uni}	100 m

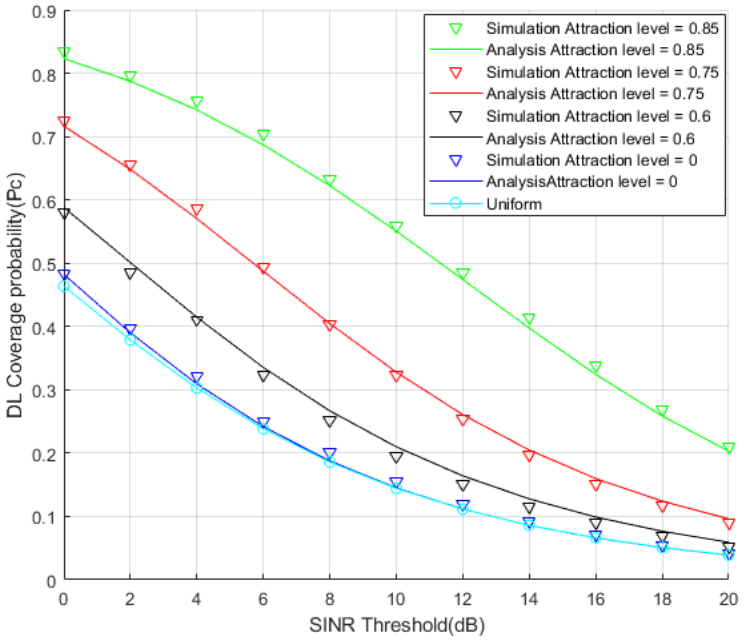

Figure 5.4: Downlink coverage probability of our designed non-uniform user distribution model, in which non-uniform users are distributed in small cells

5.3.1 Matching between Simulation and Theoretical Analysis

Figure 5.4 demonstrates the simulation results and the theoretical results. The theoretical results are obtained from the above Section 5.2. The cluster process is Matern cluster. The attraction level is 0.85 (the UE cluster radius R is 30 m, high attraction, green curve), 0.75 (R is 50 m, high attraction, red curve), 0.6 (R is 80 m, medium attraction, black curve), and 0 (R is 200 m, low attraction, blue curve). The uniform result (cyan curve) has also been included in order to compare with the above non-uniform user distribution. When the attraction level is high, such as 0.85 or 0.75, the coverage probability is high since the user density is high near the cell center. When the attraction level is very low, the coverage probability of the non-uniform user distribution converges to the uniform distribution (cyan curve). The base station offset D_2 is 0 m, which means the dependency level is 1. The effect of the base station offset is discussed in the following subsection 5.3.2. The non-uniform UEs are distributed only in small cells.

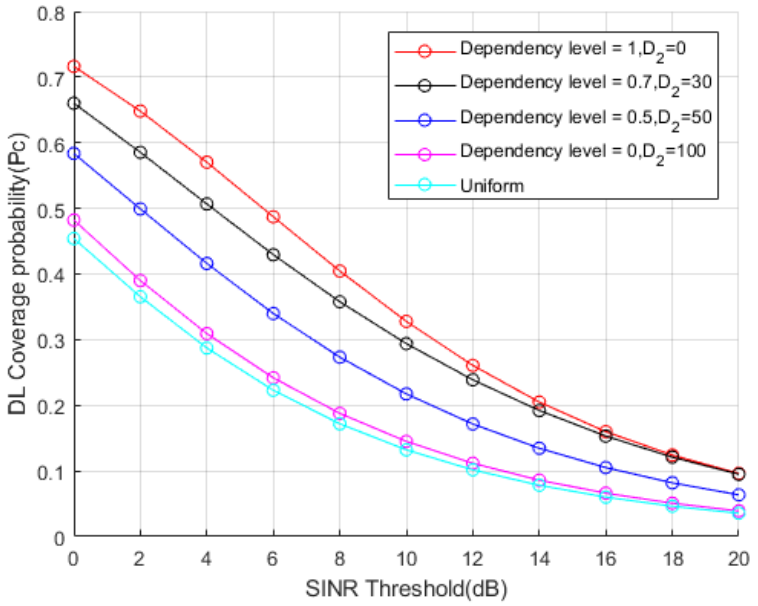

Figure 5.5: Effect of base station offset D_2 on the downlink coverage probability

5.3.2 Effect of Base Station Offset

In this subsection, we keep the user distribution as Matern cluster (attraction level = 0.75, UE cluster radius R = 50 m) and vary the base station offset D_2 as {0, 30, 50, 100} m, which corresponds to the dependency level as {1, 0.7, 0.5, 0}. When the dependency level is high, such as 1 or 0.7, SA has a high dependency with its small BS so that the coverage probability is high. When the dependency level is low, such as 0, the dependency decreases and the coverage probability converges to the uniform case (cyan curve). Figure 5.5 demonstrates these results.

5.3.3 Effect of System Parameters

The non-uniform user distribution model has been introduced and the theoretical analysis of the downlink coverage probability has also been derived in previous Section 5.2. In this subsection, the effect of system parameters, such as BS density ratio between small cells and macro cells, the cell extension bias factor of small BSs and the transmit power of small BSs is given. For the reference and comparison, the performance based on the uniform user model is also included in the following figures. In the literature of the uniform user model, there are some conclusions that give more system insight. Here are two examples. The first example comes from [20], which has the conclusion that "more BSs can be added

in any tier without affecting the coverage and hence the network capacity can be increased linearly with the number of BSs" when SINR threshold is the same in all tiers. The second example is from [75], which concludes "When the low-tier BSs experience higher path loss, the outage and average rate improve as the BSs are added". The above conclusions are true for uniform user cases. However, these conclusions do not hold for the non-uniform user cases. It is essential to give the performance analysis for the non-uniform user model over HetNets, which will provide more system insight and understanding for HetNets design.

We follow the same simulation parameters as the above subsection. When calculating the downlink coverage probability, the SINR coverage threshold is 0 dB. Since we cannot determine the relationship between the path loss exponent of macro cells and the path loss exponent of small cells, we give three curves for each kind of attraction. For each attraction level (uniform, low attraction, medium attraction and high attraction), we show three curves. The first red curve is when the path loss exponent of macro cell is higher than that of small cells ($\{\alpha_1, \alpha_2\} = \{3.5, 3\}$). The second blue curve is when the path loss exponent of macro cell is equal to that of small cells ($\{\alpha_1, \alpha_2\} = \{3.5, 3.5\}$). The third black curve is when the path loss exponent of macro cell is lower than that of small cells ($\{\alpha_1, \alpha_2\} = \{3.5, 4\}$). The base station offset between SAs and BSs is assumed to be 0 m. In the following figures, we set the low attraction level as 0.1, the medium attraction level as 0.6, and the high attraction level as 0.75.

5.3.3.1 Effect of BS Density Ratio between Small Cells and Macro Cells

Table 5.3: Parameters of effect of BS density ratio between small cells and macro cells

	Value
BS density	$\lambda_1 = \frac{3}{10^6}$, $\frac{\lambda_2}{\lambda_1} = 1$(0 dB) to 100 (20 dB)
Path loss exponent	$\{\alpha_1, \alpha_2\} = \{3.5, 3.5\}$
Cell extension bias factor	$\{C_1, C_2\} = \{1, 1\}$
BS transmit power	$\{P_1, P_2\} = \{53, 33\}$ dBm

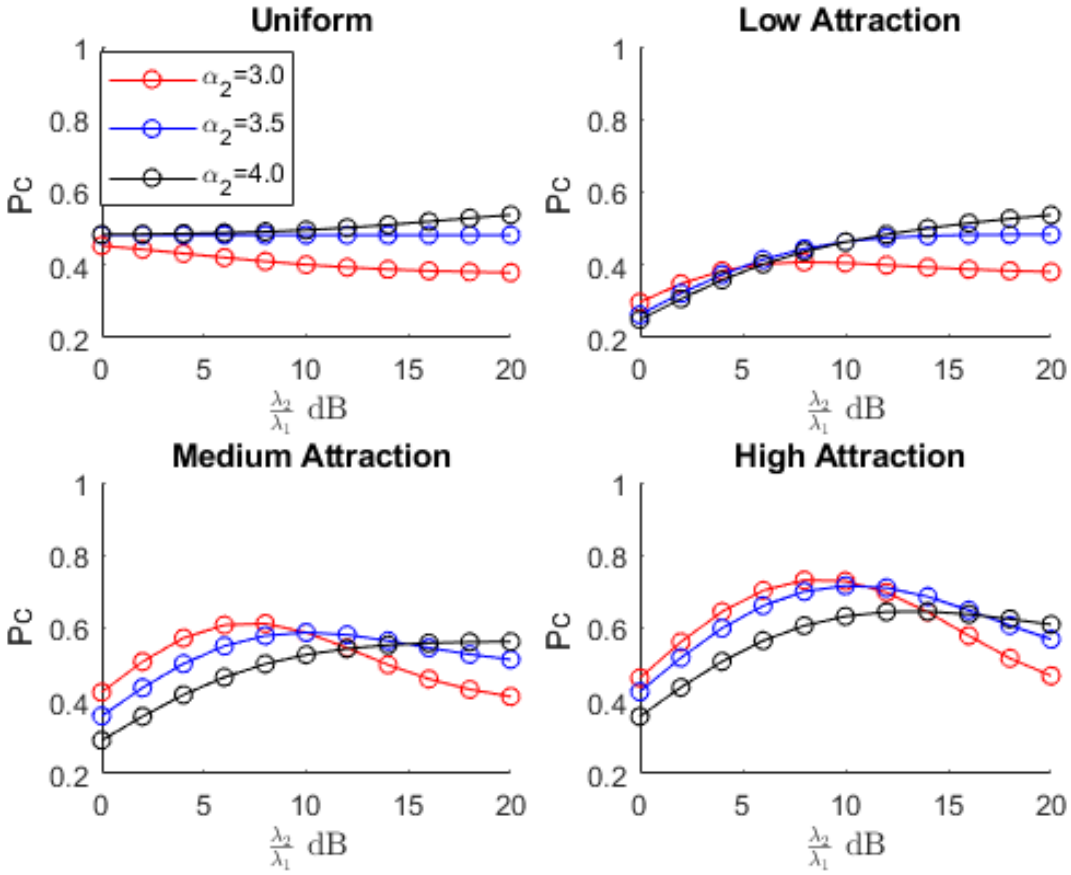

Figure 5.6: Downlink coverage probability as a function of BS density ratio $\frac{\lambda_2}{\lambda_1}$ between small cells and macro cells

The effect of BS density ratio between small cells and macro cells is shown in Figure 5.6.

From Figure 5.6 we can observe:

- When the BS density ratio $\frac{\lambda_2}{\lambda_1}$ between small cells and macro cells is low, such as $0-5$ dB , the case of high attraction has the high coverage probability. Since the coverage area in small cells is large (as shown in Figure 3.20) at the low BS density ratio $\frac{\lambda_2}{\lambda_1}$, the UE cluster may be in the coverage area. Therefore, the high attraction case has high performance.

- When the BS density ratio $\frac{\lambda_2}{\lambda_1}$ between small cells and macro cells is low, such as $0-5$ dB, the case experiencing low path loss exponent in each attraction may have the high coverage probability since the received signal power from the associated BS may be high and the received signal power from interfering BS may be low due to longer distance.

- When the BS density ratio $\frac{\lambda_2}{\lambda_1}$ between small cells and macro cells is high, such as $15 - 20$ dB, all kinds of attraction cases have almost the same performance. When the density ratio is high, the coverage area in the small cells might be small such that all kinds of attraction cases will have the user distribution over the whole coverage area and approach to be uniform.

- When the BS density ratio $\frac{\lambda_2}{\lambda_1}$ between small cells and macro cells is high, such as $15 - 20$ dB, the case experiencing high path loss exponent in each attraction has the high coverage probability.

- For medium attraction and high attraction, the coverage probability increases and then decreases as the BS density ratio increases. The turning point of the BS density ratio from increasing to decreasing is around 12dB in this simulation setting. If deploying small BSs with the same simulation setting for medium attraction and high attraction, the density ratio between small cells and macro cells is preferred to be 12 dB since the coverage probability is optimum at the turning point 12 dB.

- BS deployment suggestion:

  - For low attraction and uniform case experiencing high path loss exponent, the BS density ratio between small cells and macro cells can be increased as much as possible since the coverage probability does not decrease as the increase of the BS density ratio.
  - For medium attraction and high attraction case, the BS density ratio is preferred to be deployed at the density of the turning point (e.g. 12 dB in this simulation setting) since the coverage probability has the optimum or peak value at the turning point.

The summary of the effect of the BS ratio between small cells and macro cells is in the following table.

Summary	**Effect of $\frac{\lambda_2}{\lambda_1}$**	**Effect of Path Loss Exponent**
Low attraction	High path loss: ↑ Same path loss: ↑ Low path loss: ↑	High path loss exponent has high performance.
Medium attraction	High path loss: ↑ Same path loss: ↑→↓ Low path loss: ↑→↓	Low path loss exponent has high performance at low BS density ratio and high path loss exponent has high performance at high BS density ratio.
High attraction	High path loss: ↑→↓ Same path loss: ↑→↓ Low path loss: ↑→↓	Same as medium attraction case.

Note:
↑ means that the coverage probability increases with the increase of BS density ratio $\frac{\lambda_2}{\lambda_1}$.
↑→↓ means that the coverage probability increases, and then decreases with the increase of BS density ratio $\frac{\lambda_2}{\lambda_1}$ after a turning point.

5.3.3.2 Effect of Cell Extension of Small Cells

Table 5.4: Parameters of effect of BS cell extension bias factor of small cells

	Value
BS density	$\{\lambda_1, \lambda_2\} = \{\frac{3}{10^6}, \frac{3}{10^5}\}$
Cell extension bias factor	$C_1 = 1$, $C_2 = 1$ (0dB) to 100 (20dB)
BS transmit power	$\{P_1, P_2\} = \{53, 33\}$ dBm

The effect of BS cell extension bias factor C_2 of small cells is shown in Figure 5.7.

From Figure 5.7 we can observe :

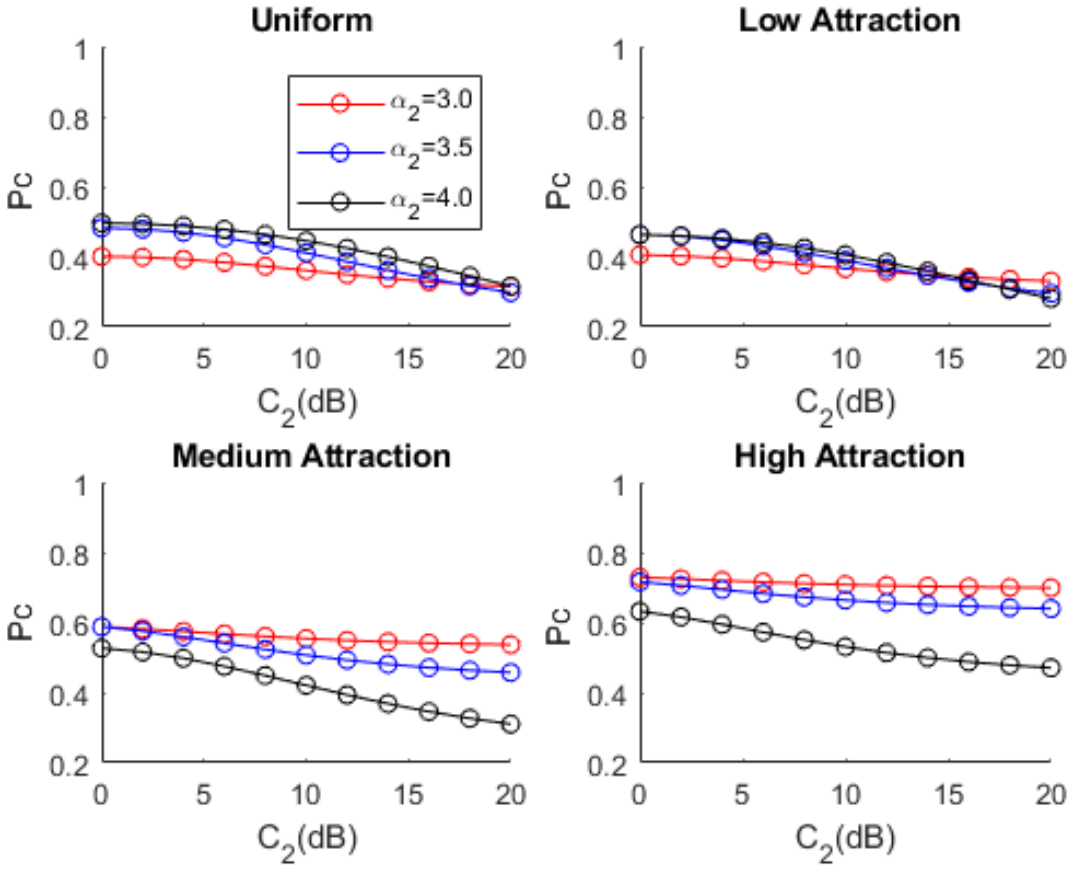

Figure 5.7: Downlink coverage probability as a function of BS cell extension bias factor C_2 in small cells

The effect of BS cell extension bias factor C_2 of small cells is shown in Figure 5.7.

From Figure 5.7 we can observe :

- For low attraction, the performance is almost the same as the uniformly distributed cases.
- For low attraction and medium attraction, the coverage probability decreases with the increase of BS cell extension bias factor C_2 since more users will associate with small cells and this will result in low SINR level.
- For the high attraction, the coverage probability remains almost the same as the increases of C_2 since the users are extremely clustered around the cell center and few users will be impacted by increasing C_2.

- For uniform and low attraction, the case experiencing high path loss exponent has high coverage probability.
- For medium and high attraction, the case experiencing low path loss exponent has high coverage probability.
- BS deployment suggestion:
  - For low attraction, the case experiencing high path loss exponent is preferred since it will have high coverage probability.
  - For medium attraction and high attraction, the case experiencing low path loss exponent is preferred because it will have high coverage probability.
  - For high attraction experiencing low path loss exponent, the cell extension bias factor can be increased as much as possible since the coverage probability still remains the same.

The summary of the effect of BS cell extension bias factor C_2 in small cells is in the following table.

Summary	**Effect of C_2**	**Effect of Path Loss Exponent**
Low attraction	High path loss: $\downarrow$ Same path loss: $\downarrow$ Low path loss: $\downarrow$	High path loss exponent has high performance.
Medium attraction	High path loss: $\downarrow$ Same path loss: $\downarrow$ Low path loss: $\downarrow$	Low path loss exponent has high performance.
High attraction	High path loss: $\sim$ Same path loss: $\sim$ Low path loss: $\sim$	Low path loss exponent has high performance.

Note:
$\downarrow$ means that the coverage probability decreases with the increase of BS cell extension bias factor C_2.
$\sim$ means that the coverage probability does not vary with the increase of BS cell extension bias factor C_2.

5.3.3.3 Effect of BS Transmit Power of Small Cells

Table 5.5: Parameters of effect of BS transmit power of small cells

	Value
BS density	$\{\lambda_1, \lambda_2\} = \{\frac{3}{10^6}, \frac{3}{10^5}\}$
Cell extension bias factor	$\{C_1, C_2\} = \{1, 1\}$
BS transmit power	$P_1 = 53$ dBm, $P_2 = 20$ dBm to 45 dBm

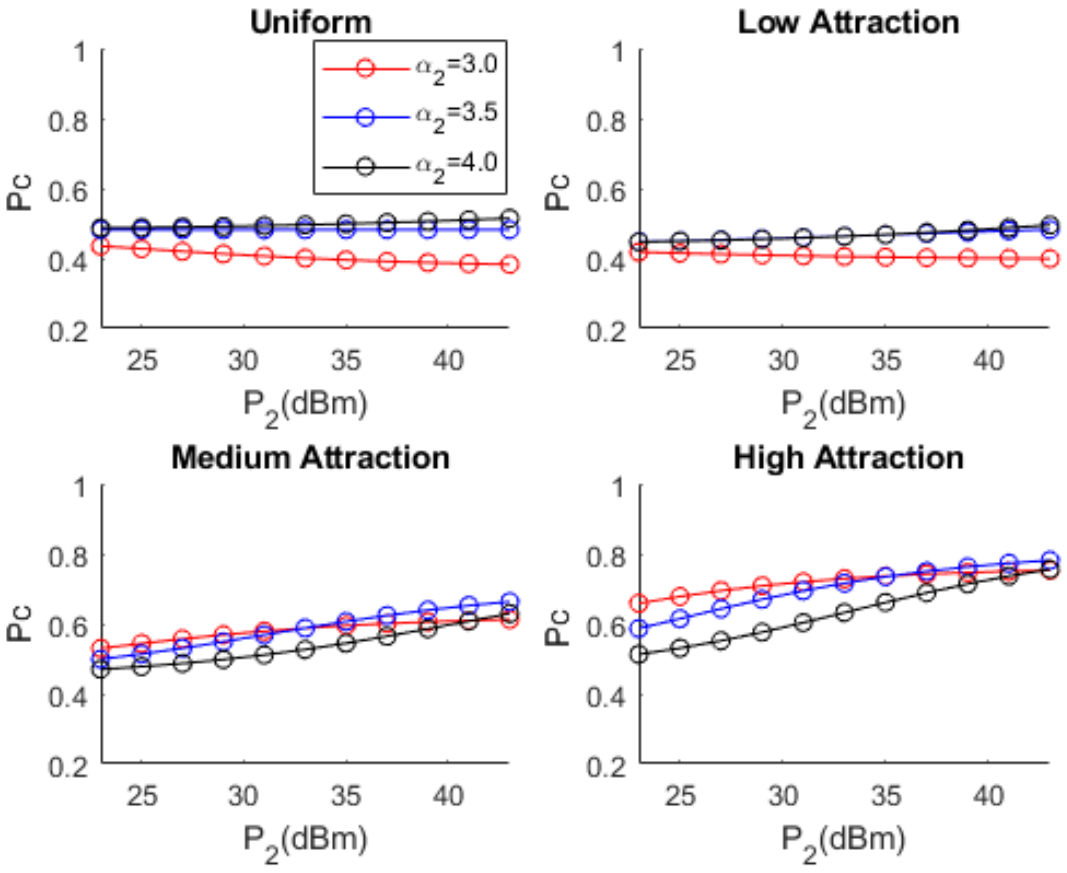

Figure 5.8: Downlink coverage probability as a function of BS transmit power P_2 in small cells

The effect of BS transmit power P_2 of small cells is shown in Figure 5.8.

From Figure 5.8 we can observe :

- The performance of low attraction is almost the same as the uniform case.
- The coverage probability remains the same when experiencing low path loss exponent with low attraction.
- The coverage probability increases with the increase of P_2 when experiencing high or the same path loss exponent with low attraction.
- The coverage probability increases with the increase of BS transmit power P_2 for medium attraction and high attraction.
- The case experiencing low path loss exponent has high coverage probability for medium attraction and high attraction.
- BS deployment suggestion:
  - The transmit power P_2 of small cells can be increased as much as possible since the coverage probability will increase or remain the same with the increase of P_2.

The summary of the effect of BS transmit power P_2 in small cells is in the following table.

Summary	**Effect of P_2**	**Effect of Path Loss Exponent**
Low attraction	High path loss: $\uparrow$ Same path loss: $\uparrow$ Low path loss: $\sim$	High path loss exponent has high performance.
Medium attraction	High path loss: $\uparrow$ Same path loss: $\uparrow$ Low path loss: $\uparrow$	Low path loss exponent has high performance.
High attraction	High path loss: $\uparrow$ Same path loss: $\uparrow$ Low path loss: $\uparrow$	Low path loss exponent has high performance.

Note:
$\uparrow$ means that the coverage probability increases with the increase of P_2.
$\sim$ means that the coverage probability does not vary with the increase of P_2.

5.4 Conclusions

In this chapter, we derived the downlink coverage probability of our designed non-uniform user distribution model. It can be described into two cases. The first case (case1) is to derive the downlink coverage probability when the UE of interest is associated with the BS that the UE of interest belongs to, and the second case (case2) is to derive the downlink coverage probability when the UE of interest is associated with other BS except the BS that the UE of interest belongs to. Then the overall downlink coverage probability is obtained. The simulation results follow the derived performance analysis and confirm that our derived theoretical analysis is very accurate. Hence, the performance can be obtained using our derived equations rather than carrying out time-consuming simulations for any researchers, operators who rely on the non-uniform user model to verify the downlink HetNet system.

The effect of the base station offset between SA and BS is evaluated. It indicates that the performance converges to the uniform case when the base station offset is large enough. The effect of system parameters, such as the BS density ratio between small cells and macro cells, the cell extension bias factor of small cells and the BS transmit power of small cells is also discussed. For example, for the effect of BS density ratio between small cells and macro cells in medium attraction and high attraction case, there is a turning point (here 12 dB) where the coverage probability is optimum so that the operators should consider this turning point as design reference when deploying small BSs. For the effect of cell extension bias factor C_2, the coverage probability could decrease as the increase of C_2 in most cases. However, the performance is not decreased when the path loss exponent of small cells is low and the attraction level is high such that we can consider to increase C_2 when deploying small BSs. For the effect of BS transmit power P_2, the coverage probability increases when the transmit power P_2 increases. Hence, increasing P_2 can bring benefit. But it will bring more interference to other UEs and high power consumption. Then the balance should be taken between increasing the coverage probability and increasing the interference and it will not be covered in this thesis.

Chapter 6

Uplink Coverage Probability Performance Analysis

6.1 Introduction

The downlink analysis is based on the received SINR of a UE from the associated BS with the interference from all other BSs in the downlink direction. The uplink analysis is based on the the received SINR of the associated BS from its active UE with the interference from all other active UEs in the uplink direction. There are more challenges for the uplink analysis than the downlink analysis. The first reason is that the interference in the uplink is coming from the randomly located UEs while the interference in the downlink is coming from the BSs with the fixed placement. The second reason is that there is the uplink power control for the UEs in order to mitigate the near-far effect. This makes the UE transmit power to fluctuate and then an exact characterization of the total uplink interference from all interfering UEs is not available. Hence, we have to make some simplifying assumptions in order to obtain the uplink coverage probability performance using the tools of stochastic geometry. In this chapter, the uplink analysis depends on the same non-uniform UE distribution and the same K-tier BS distribution as the downlink analysis in Chapter 5. The non-uniformly distributed UE model has been introduced in Chapter 4.

The maximum average bias received power connectivity model is assumed for both downlink and uplink in Section 3.4.2. In this connectivity model, UEs are associated or served by the BSs from which the received average bias power is maximum. Figure 6.1 shows a system model example with the above connectivity rule. There are one macro BS and three small BSs, and non-uniform UEs are distributed around small BSs with cluster

center being SAs and SAs have a base station offset with their BSs. Using the maximum average bias received power connectivity model some UEs in the cluster are associated with the BSs that they belong to and other UEs in the same cluster are associated with other BSs. Figure 6.1 has three small BSs, separately represented with a black square, a red square and a blue square, and one macro BS represented with a green square. The UEs are represented as points. The cell boundaries are represented as curves with the same color of the corresponding BS square. For instance, for small BS of black square, there is a UE cluster. The UEs in the cluster associated with the small BS of black square are labeled in black and the remaining UEs in the cluster associated with other BS, such as macro BS of green square are labeled in green. The small BS of black square is the BS that this UE cluster belongs to. In this thesis we assume the UEs are always distributed in cluster. In further research, we propose the non-uniformly distributed clusters as well as the uniformly distributed UEs, i.e. mixed UE distribution should be studied.

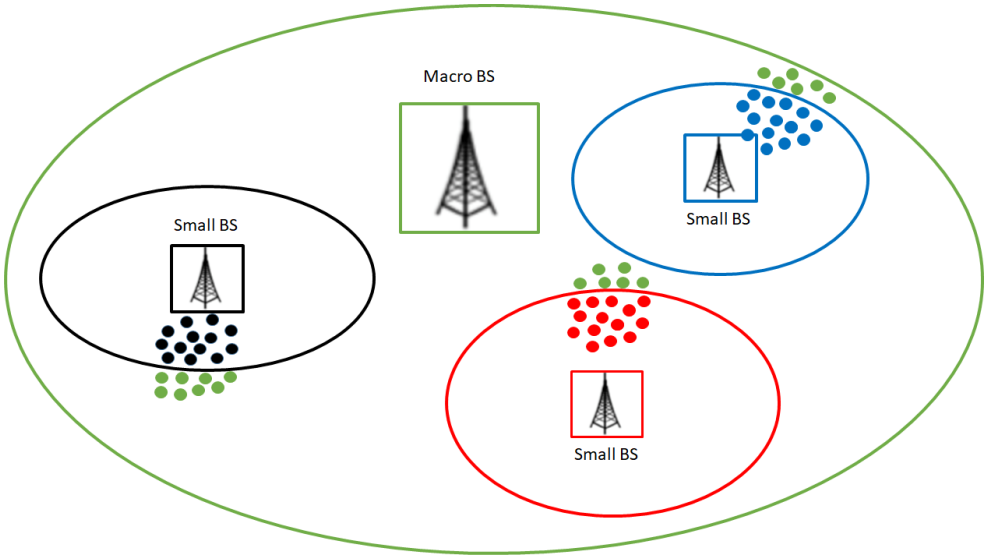

Figure 6.1: System model example with the same cell extension association for both downlink and uplink

Figure 6.2 gives an example with SINR in the downlink. The typical UE receives the signal from its associated small BS of red square with distance L and also receives the interference signals from all interfering BSs with distance V_1, V_2 and V_3. BSs in the same tier have the same downlink transmit power.

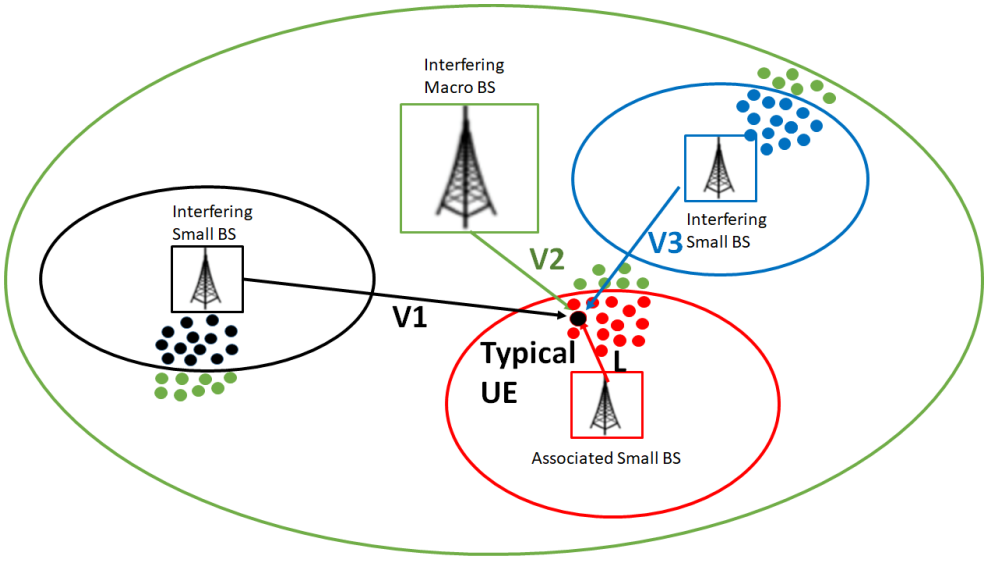

Figure 6.2: System model example with SINR in the downlink

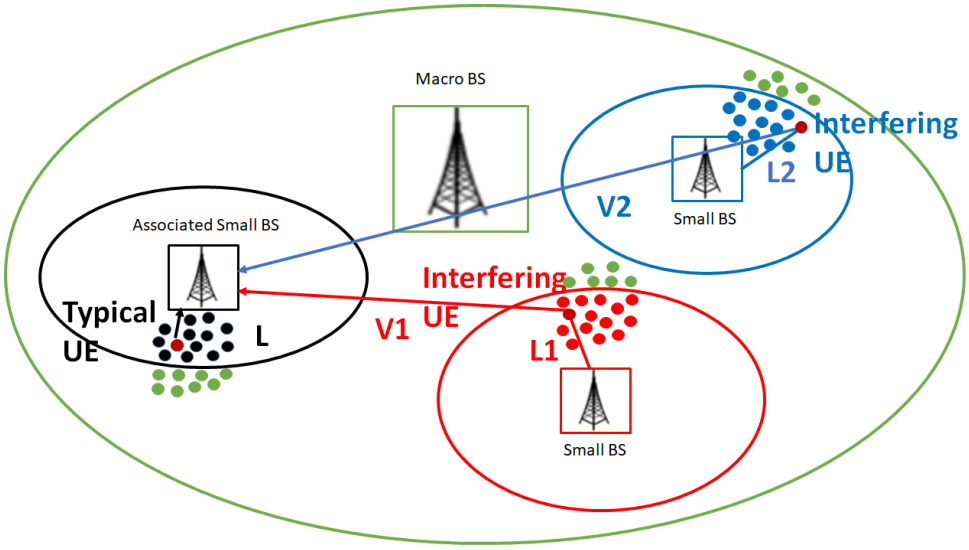

Figure 6.3: System model example with SINR in the uplink

Figure 6.3 shows an example with SINR in the uplink. The associated small BS of black square receives the signal from the typical active UE with distance L and also receives the interference signal from all interfering active UEs with distance V_1 and V_2. In a given resource block of LTE (Long Term Evolution), there is only one active UE in each cell, which is the typical UE or the interfering UEs labeled in maroon in Figure 6.3. The uplink transmit power of each UE is variable. It depends on the power control policy and the distance L_1, L_2, V_1 and V_2, .

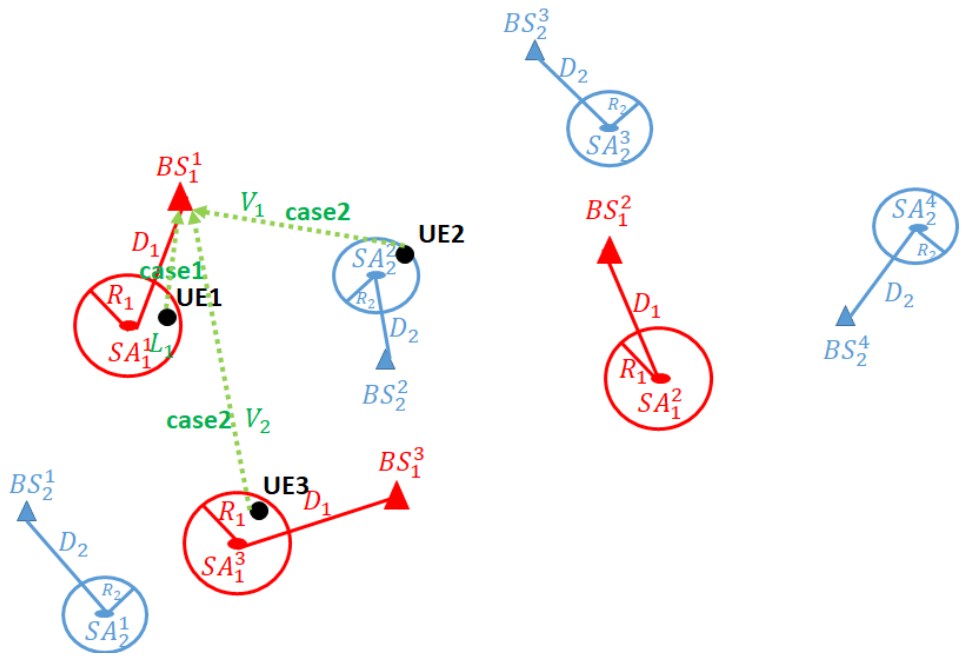

Figure 6.4: Example of spatial distances between UE, BS, and SA and the related notation in a 2-tier uplink system

Figure 6.4 shows an example of spatial distances between UE, BS, and SA and the related notation in a 2-tier uplink system. The 1th tier such as the macro cell tier is in red and the 2th tier such as the small cell tier is in blue. The BS and UE notations are the same as Figure 5.1. In the 1th tier, there are three BSs (BS_1^1, BS_1^2 and BS_1^3) and three corresponding SAs (SA_1^1, SA_1^2 and SA_1^3). The three corresponding SAs have a base station offset D_1 with the three BSs. In the 2th tier, there are four BSs (BS_2^1, BS_2^2, BS_2^3 and BS_2^4) and the four corresponding SAs (SA_2^1, SA_2^2, SA_2^3 and SA_2^4). The four corresponding SAs have a base station offset D_2 with the four BSs.

Let us analyze the uplink performance for a BS of interest, such as BS_1^1 in Figure 6.4. The active UE that is associated with BS_1^1 can be described into two cases. Case1 is that the active UE such as UE1 is located in the cluster around SA_1^1. or we can say the active UE (UE1) belongs to the BS of interest (e.g. BS_1^1). Case2 is that the active UE such as UE2 or UE3 is located in the cluster around other SAs rather than SA_1^1. Therefore, let us summarize the two cases that the possible active UE associated with the BS of interest, BS_i^j, is as follows. The active UE is located in the cluster of SA_i^j (case1) or the active UE is located in the cluster of other SA_m^k (case2). This SA_m^k may be of the same tier as i ($m = i, k \neq j$), or it may be in another tier ($m \neq i$).

Let $m = 1, 2, ...k$ be the tier of interest. The procedure to get the uplink coverage probability $\mathbb{P}_{ul,c}$ is as follows:

- Find the probability density function (PDF) $f_L^{(m)}(l)$ and complementary cumulative distribution function (CCDF) $\bar{F}_L^{(m)}(l) = \mathbb{P}^{(m)}(L > l)$ of random variable L. Let L be the distance between an active UE and its associated BS that the active UE belongs to in the mth tier.

- The BS of interest (e.g. BS_1^1 in Figure 6.4) in a given mth tier can be associated with an active UE in two cases.
  Case1: an active UE that belongs to the BS of interest.

  - Derive $\mathbb{P}^{(m)}(A_{case1})$, which is the probability that the active UE is associated with the BS of interest that the active UE belongs to in the mth tier.
  - Derive the uplink coverage probability $\mathbb{P}^{(m)}[SINR_m(l) > T_m|A_{case1}]$ conditioned on the active UE associated with BS_1^1.
  - Derive the uplink coverage probability $\mathbb{P}_{ul,c,case1}^{(m)} = \mathbb{P}^{(m)}(A_{case1}) * \mathbb{P}^{(m)}[SINR_m(l) > T_m|A_{case1}]$ that the active UE is associated with BS_1^1.

  Case2: an active UE that belongs to other BS rather than the BS of interest.

  - Ignored since a simplifying assumption made in the following section, which is the active UE belongs to the BS of interest.

  Summary

  - $\mathbb{P}^{(m)}(A_{case1})$ is the probability that the active UE that belongs to the BS of interest is associated with the BS of interest.
  - $\mathbb{P}_{ul,c,case1}^{(m)}$ is the coverage probability associated with the BS of interest.
  - The uplink coverage probability for a BS of interest distributed in a mth tier based on the second simplifying assumption that the active UE belongs to the BS of interest is $\mathbb{P}_{ul,c}^{(m)} = \frac{\mathbb{P}_{ul,c,case1}^{(m)}}{\mathbb{P}^{(m)}(A_{case1})}$.
  - The detail of the second simplifying assumption will be explained in the following Section 6.2.

- The overall uplink coverage probability is

$$\mathbb{P}_{ul,c} = \sum_{m \in \mathbb{S}} \frac{N_m \lambda_m}{\sum_{m \in \mathbb{S}} N_m \lambda_m} \mathbb{P}_{ul,c}^{(m)}, \tag{6.1}$$

  where $\mathbb{S}$ is the subset of tiers, in which the non-uniform user is distributed. N_m

is the average number of users in each cluster of a mth tier. λ_m is the BS density of a mth tier.

Section 6.2 introduces the simplifying assumptions of the uplink analysis in this thesis. The uplink power control is shown in Section 6.3. The uplink coverage probability analysis is derived in Section 6.4. Simulation results and the effect of system parameters are presented in Section 6.5.

6.2 Simplifying Assumptions

As mentioned above, the uplink analysis brings more challenges since the uplink power control makes the UE transmit power variable and an exact characterization of the total uplink interference is not available. We have to make some assumptions to simplify the analysis. In Section 6.5, there are the simulation results to demonstrate that the mismatch due to simplified assumptions is less than 1 dB .

The assumptions are as follows:

- In each cell, there is only one active UE.
  LTE of orthogonal multiple access technique is assumed. In a given resource block, there is one active UE in each cell so that the density of the active UE is the same as the density of the BS. The uplink analysis is based on active UEs. In each tier, the density of active UEs in the ith tier is assumed to be λ_i, which is the same as the density of BS in the ith tier.

- An active UE associated with BS_i^j comes from the UEs in the cluster around SA_i^j and other active UEs associated with BS_i^j in the cluster around other SA rather than SA_i^j are not considered in the uplink analysis.

  - In Figure 6.4, SA_1^1 has a base station offset D_1 with BS_1^1. Some UEs in the cluster around SA_1^1 are associated with BS_1^1, and other UEs in the cluster around SA_1^1 are associated with other BSs. Or we cay also say that in the coverage area of BS_1^1, some UEs are from the cluster around SA_1^1 and other UEs are from the cluster around other SAs.
  - We make an assumption that an active UE such as UE1 comes from the cluster around SA_1^1 (and ignore the UE such as UE2 or UE3 from the cluster around other SAs such as SA_2^2 or SA_1^3) when we take BS_1^1 as a BS of interest. The

reason of the above assumption is that the PDF and CCDF of the distance between the UE1 and the BS of interest (e.g. BS_1^1) is available from Section 5.2.1.2. The characterization of the distance between the UE2 (or UE3) and the BS of interest (e.g. BS_1^1) is not available.

– Figure 6.5 gives an example how we assume an active UE in the uplink analysis. In (a), it lists the non-uniformly distributed clusters of our designed user model in small cells. Black points are UEs associated with the small BS1 and green points are UEs associated with other BSs. There are three UE clusters. The center SA1 of UE cluster1 has a base station offset with small BS1. The center SA2 of UE cluster2 (or the center SA3 of UE cluster3) has the base station offset with other BS, which is not included in Figure 6.5. According to our assumption, the active UE is assumed from UE cluster1. The UE cluster2 and UE cluster3 are not considered due to the unavailability of the distance characterization between UEs in UE cluster 2 (or UE cluster 3) and small BS1. An active UE will be got randomly among the black points in (b). These black points from the UE cluster1 are in the coverage area of small BS1. In (c), the active UE is got among black points of (b) randomly.

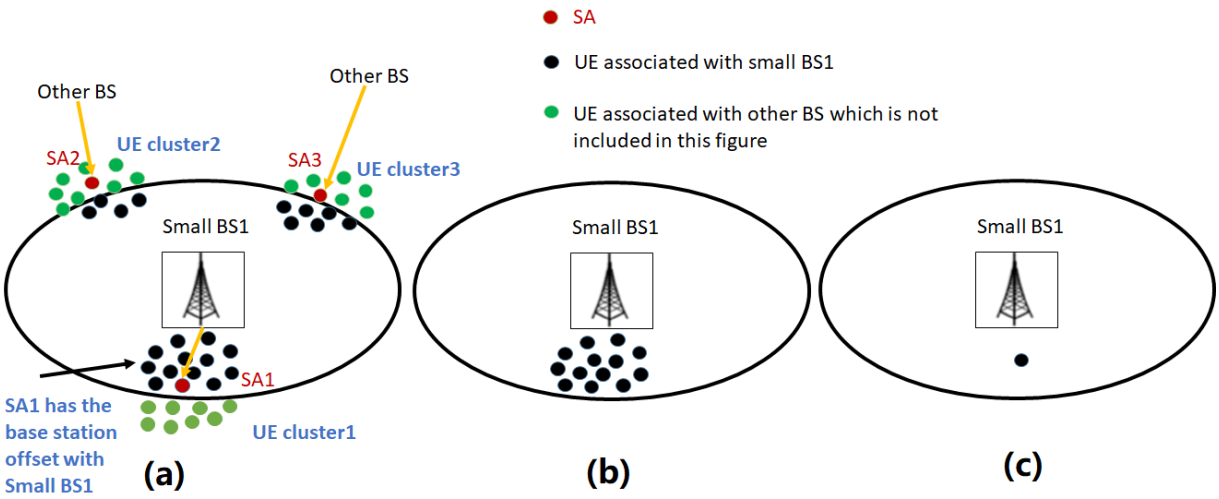

Figure 6.5: Assumption of an active UE

- The base station offset is less than a threshold.
  When the base station offset between SA and its BS is high, most of UEs are located far away from BSs or around the cell edge, which results in the performance will be even worse than the uniform scenario. We assume in the uplink research that the base station offset is less than a threshold. It is reasonable since the scenario

of the non-uniform UE distribution above this threshold will never be deployed by operators.

- Active UEs in each tier form a homogeneous and independent PPP.
  When deriving the characterization of the interference from all interfering active UEs, we make another assumption that the active UEs in each tier form a homogeneous and independent PPP. Since we assume that the distribution of active UEs is PPP, the uplink interference of active UEs can be simplified by the property of probability generating functional (PFGL) using the tools of stochastic geometry.

6.3 Uplink Power Control

Power control is important in the system design of cellular networks. The relevant uplink power control policy is one of the key features of CDMA, UMST or OFDM. The purpose of power control is noted in the following [97–100]:

- Mitigate the near-far problem. If UEs at different locations transmit at the same power, BS potentially fails to decode the signals from the UE far away because the UE close to the BS causes a much higher interference power. This means that the propagation path loss between UEs and BSs should be considered.
- Power control can help save energy cost, which is an important part of green communication. For UEs, the power control is intended to extend battery life through minimum possible power while stable communications are still maintained. For BSs, reasonable power control can maintain interference at a low level while the overall service to UEs are hold.
- Power control provides protection against shadowing and fast fading.

Wireless channels experience both short term and long term fading. We may consider two main power control mechanisms [101].

- Open loop power control:

  The initial power is set at which the UE should transmit considering path loss. The power control has no feedback.

- Closed loop power control:

  - Inner (fast) power control:
    Inner power control is a kind of fast closed loop power control to combat fast fading and short term distortion. Inner fast power control maintain the constant SINR target. This power control happens in high rate.
  - Outer (slow) power control:
    Outer power control is a kind of slow closed loop power control to combat slow fading and long term distortion. Outer slow power control maintain the constant transport block error rate (BLER) target. This power control happens in slow rate.

However, it is difficult to do a tractable analysis of the above power control mechanisms. [102] gives the fractional power control maintaining the constant interference power at BS. The author in [103] proposes an analytical approach depending on the fractional power control. Hence, in this thesis, the fractional power control is considered. The fractional power control proposes a compensation which is proportional to the path loss. The transmit power of the UE using the fractional power control is $r^{\alpha\epsilon}$, where $\epsilon \in [0, 1]$ is the fractional power control factor, r is the distance between the UE and BS, and α is path loss exponent. When a UE is close to the associated BS, the required uplink transmit power decreases while remaining the same received signal power at the associated BS. The uplink power control helps to combat the near-far effect and extends UE device battery life. When $\epsilon = 1$, the fractional power control compensates the complete path loss while when $\epsilon = 0$ there is no power control, UEs transmit with the same power.

6.4 Model Performance Analysis

In this section, we derive the uplink coverage probability. The definition of the uplink SINR and the uplink coverage is as follows. There are total of K tiers of BSs with a subset κ and there are total of S tiers with a subset $\mathbb{S}$ distributed with our designed non-uniform user model.

Definition 6-1. The uplink SINR at an associated BS B_0 located at the origin in the kth tier is

$$SINR_k(L) = \frac{r^{\alpha_k \epsilon} G_k r^{-\alpha_k}}{I_r + \frac{\sigma^2}{L_0}}, \tag{6.2}$$

$$I_r = \sum_{j=1}^{S} I_{rj} = \sum_{j=1}^{S} \sum_{\in \phi_j} l_{ji}^{\alpha_j \epsilon} G_j {r_{ji}}^{-\alpha_j}, \tag{6.3}$$

- r is the distance between the associated BS B_0 and its active UE. l_{ji} is the ith distance between the interfering active UEs and their associated BSs in the jth tier. r_{ji} is the ith distance between the interfering active UEs in the jth tier and the associated BS B_0.
- G_k denotes the random channel power gain in the kth tier. Let the complex channel coefficient between the kth tier BSs and the UEs be denoted as h_k (Rayleigh fading is assumed in this thesis). Then we define $G_k = |h_k|^2$, which is an exponential distribution with unity mean.
- α_k is kth path loss exponent in the kth tier.
- I_r is the total uplink received interference from all interfering active UEs. I_{rj} is the total uplink received interference in the jth tier.
- σ^2 is the power of the additive white Gaussian noise (AWGN).
- S is the total number of tiers distributed with our non-uniform UEs.
- ϕ_j is SPPP with the density λ_j in the jth tier.
- L_0 is the path loss at a reference distance of 1 m.

Definition 6-2. An active UE in the kth tier is in the coverage if the uplink SINR at the BS of interest with the maximum average bias received power is more than the coverage threshold T_k.

$$SINR_K = \frac{r^{\alpha_k \epsilon} G_k r^{-\alpha_k}}{\sum_{j=1}^{S} \sum_{\in \phi_j} l_{ji}^{\alpha_j \epsilon} G_j {r_{ji}}^{-\alpha_j} + \frac{\sigma^2}{L_0}} > T_k. \tag{6.4}$$

6.4.1 Distance Characterization

Based on the assumption that an active UE associated with BS_i^j comes from the UEs in the cluster around SA_i^j, the received signal power of the associated BS from its active UE depends on the random distance variable L between the associated BS and its active UE. L has the same PDF and CCDF as given in Section 5.2.1.2.

6.4.2 Interference Characterization

The uplink total interference from all interfering active UEs in tiers distributed with our designed non-uniform user model is

$$I_r = \sum_{j=1}^{S} I_{rj} = \sum_{j=1}^{S} \sum_{\in \phi_j} l_{ji}^{\alpha_j \epsilon} G_j {r_{ji}}^{-\alpha_j}. \tag{6.5}$$

We have made the assumptions in Section 6.2 that there is an active UE in each cell and active UEs in each tier form a PPP. Then we can use stochastic geometry to simply the uplink interference characterization. So we can change the unlimited sum of interference from all interfering active UEs into an integral expression utilizing the property of products over PPP (probability generating functional (PGFL)), which is $\mathbb{E}[\prod_{x\in\phi} f(x)] = \exp(-\lambda \int_{\mathbb{R}^2}(1-f(x))dx)$ if ϕ is PPP. Specifically, the Laplace transform $\mathscr{L}_x(s) = \mathbb{E}_x[e^{-sx}]$ ($\mathbb{E}_x[*]$ is the expectation of $*$ over x) of the interference is very useful.

Lemma 6-1. Calculate the Laplace transform of the total uplink interference in the jth tier distributed with our non-uniform UE model.

$$
\begin{aligned}
&\mathscr{L}_{I_{rj}}(s) \\
&= \mathbb{E}_{I_{rj}}[e^{-sI_{rj}}], \\
&= \mathbb{E}_{\phi_j}[e^{-s\sum_{\in\phi_j} l_{ji}^{\alpha_j\epsilon} G_j r_{ji}^{-\alpha_j}}], \\
&= \mathbb{E}_{\phi_j,l_j}[\prod_{\in\phi_j} e^{-s l_{ji}^{\alpha_j\epsilon} G_j r_{ji}^{-\alpha_j}}], \\
&\overset{(a)}{=} \mathbb{E}_{l_j}[\exp(-\lambda_j \int_{\mathbb{R}^2} (1 - \mathbb{E}_{G_j}(e^{-s l_j^{\alpha_j\epsilon} G_j x^{-\alpha_j}}))dx)], \\
&= \mathbb{E}_{l_j}[\exp(-2\pi\lambda_j \int_{d_{min}}^{\infty} (1 - \mathscr{L}_{G_j}(s l_j^{\alpha_j\epsilon} r^{-\alpha_j}))rdr)], \\
&\overset{(b)}{=} \mathbb{E}_{l_j}[\exp(-2\pi\lambda_j \int_{d_{min}}^{\infty} (1 - \frac{1}{1 + s l_j^{\alpha_j\epsilon} r^{-\alpha_j}})rdr)], \\
&= \mathbb{E}_{l_j}[\exp(-2\pi\lambda_j \int_{d_{min}}^{\infty} (\frac{s l_j^{\alpha_j\epsilon} r^{-\alpha_j}}{1 + s l_j^{\alpha_j\epsilon} r^{-\alpha_j}})rdr)],
\end{aligned}
\tag{6.6}
$$

where (a) comes from the property of product over PPP (PGFL). (b) follows the fading power G_j of the exponential distribution with the unity gain. d_{min} is the distance to the closest interferer in the jth tier, which is the same as the downlink case. This Laplace transform is the expectation over l_j, which is the random distance variable between UEs and their associated BSs in the jth tier.

6.4.3 Uplink Coverage Probability

Based on the simplifying assumptions we made in Section 6.2, the active UE associated with the BS of interest is in the cluster around a SA, which has a base station offset with the BS of interest. We call that this active UE belongs to the BS of interest spatially. It means that we only consider the case1 and ignore the case2 (case1 and case2 are discussed at the beginning of this chapter). In Figure 6.4, if we take BS_1^1 as the BS of interest, UE1 is assumed as the active UE associated with the BS of interest rather than UE2 and UE3.

Lemma 6-2. The probability that the active UE is associated with the BS of interest that the active UE belongs in the mth tier (conditioned that the distance between the active UE and the BS of interest is l) is

$$
\mathbb{P}_{|l}^{(m)}(A_{case1}) = \prod_{i=1}^{K} \exp(^{-\lambda_i \pi (\frac{P_i C_i}{P_m C_m})^{\frac{2}{\alpha_i}} \cdot l^{\frac{2\alpha_m}{\alpha_i}}}), \tag{6.7}
$$

where l is the random distance variable between the active UE and the BS of interest that the active UE belongs to in the mth tier. For proof it is the same as Equation 5.9 since the downlink and the uplink analysis use the same user connectivity rule, which is the downlink maximum average bias received power.

Lemma 6-3. The probability that the active UE is associated with the BS of interest that the active UE belongs to in the mth tier

$$\begin{aligned}\mathbb{P}^{(m)}(A_{case1}) &= \int_0^\infty \mathbb{P}^{(m)}_{|l}(A_{case1}) \cdot f_L^{(m)}(l) \cdot \mathbf{d}l, \\ &= \int_0^\infty \prod_{i=1}^{K} \exp(^{-\lambda_i \pi (\frac{P_i C_i}{P_m C_m})^{\frac{2}{\alpha_i}} \cdot l^{\frac{2\alpha_m}{\alpha_i}}}) \cdot f_L^{(m)}(l) \cdot \mathbf{d}l,\end{aligned} \tag{6.8}$$

where $f_L^{(m)}(l)$ comes from subsection 5.2.1.2.

Lemma 6-4. The coverage probability of the BS of interest conditioned on the distance between the active UE and the BS of interest as l is

$$\begin{aligned}&\mathbb{P}^{(m)}_{|l}[SINR_m(l) > T_m | A_{case1}], \\ &= \exp(-\frac{\sigma^2}{L_0} T_m l^{\alpha_m(1-\epsilon)}) \cdot \prod_{i=1}^{S} \mathscr{L}_{I_{ri}}(T_m l^{\alpha_m(1-\epsilon)}),\end{aligned} \tag{6.9}$$

where T_m is SINR coverage threshold in the mth tier. For proof see Appendix B.1.

For the details of $\mathscr{L}_{I_{ri}}(T_m l^{\alpha_m(1-\epsilon)})$ the reader is referred to Equation 6.6. $\mathscr{L}_{I_{ri}}(s)$ is the Laplace transform of the uplink interference in the ith tier.

$$\begin{aligned}&\mathscr{L}_{I_{ri}}(T_m l^{\alpha_m(1-\epsilon)}) \\ &= \mathbb{E}_{l_i}[\exp(-2\pi\lambda_i \int_{d_{min}}^\infty (\frac{T_m l^{\alpha_m(1-\epsilon)} l_i^{\alpha_i \epsilon} r^{-\alpha_i}}{1 + T_m l^{\alpha_m(1-\epsilon)} l_i^{\alpha_i \epsilon} r^{-\alpha_i}}) r \mathbf{d}r)], \\ &= \exp(-2\pi\lambda_i \int_0^\infty \int_{d_{min}}^\infty (\frac{T_m l^{\alpha_m(1-\epsilon)} l_i^{\alpha_i \epsilon} r^{-\alpha_i}}{1 + T_m l^{\alpha_m(1-\epsilon)} l_i^{\alpha_i \epsilon} r^{-\alpha_i}}) r f_L^{(i)}(l_i) \mathbf{d}r \mathbf{d}l_i.\end{aligned} \tag{6.10}$$

Theorem 6-1. The coverage probability associated with the BS of interest in the mth

tier, in which the active UE belongs to the BS of interest is

$$\mathbb{P}^{(m)}_{ul,c,case1} = \int_0^\infty \mathbb{P}^{(m)}_{|l}[SINR_m(l) > T_m | A_{case1}] \cdot \mathbb{P}^{(m)}_{|l}(A_{case1}) \cdot f^{(m)}_L(l) \cdot \mathbf{d}l, \tag{6.11}$$

where $f^{(m)}_L(l)$ comes from subsection 5.2.1.2 and L is the random distance variable between the UE and the BS of interest in the mth tier. Each tier may have different parameters of the radius R and the base station offset D such that PDF of L, $f^{(m)}_L(l)$, in each tier may be different.

6.4.4 Overall Uplink Coverage Probability

Lemma 6-5. The uplink coverage probability for a BS of interest distributed in a mth tier with the simplifying assumption that the active UE belongs to the BS of interest is

$$\mathbb{P}^{(m)}_{ul,c} = \frac{\mathbb{P}^{(m)}_{ul,c,case1}}{\mathbb{P}^{(m)}(A_{case1})}, \tag{6.12}$$

where $\mathbb{P}^{(m)}(A_{case1})$ comes from Equation 6.8 and $\mathbb{P}^{(m)}_{ul,c,case1}$ comes from Equation 6.11.

Theorem 6-2. The overall uplink coverage probability is

$$\mathbb{P}_{ul,c} = \sum_{m \in \mathbb{S}} \frac{N_m \lambda_m}{\sum_{m \in \mathbb{S}} N_m \lambda_m} \mathbb{P}^{(m)}_{ul,c}, \tag{6.13}$$

where $\mathbb{S}$ is the subset of tiers, in which the non-uniform UE is distributed. N_m is the average number of UEs in each cluster of the mth tier. λ_m is the BS density of the mth tier.

6.5 Simulation Results

A 2-tier system consists of macro and small BSs. Each tier BS is deployed as an independent PPP with the specific BS density, BS transmit power and path loss exponent. The channels between all BSs and the UEs are independent Rayleigh fading. The average fading power

gain is unity. We generate a BS and UE pattern. According to the maximum downlink average bias received power, we choose an active UE in each cell. We repeat the above steps until the number of BS patterns reaches 1,000 and measure the SINR of the BS of interest in each pattern. Then we calculate the simulated uplink coverage probability using the above recorded SINR and compare with the analytical results of the designed non-uniform UE distribution model in Equation 6.13. For detail simulation setting and method, please refer to Appendix C.2.

For the parameters, we follow the same setting as the downlink case in the previous chapter (Table 5.2) and [75] except that $D_{uni} = 80$ m.

6.5.1 Matching between Simulation and Theoretical Analysis

Figure 6.6 gives the simulation results and theoretical results obtained from the above Section 6.4. The solid lines are for analysis using Equation 6.13. The dash lines are for the simulations. It shows that the analysis and simulation results have some discrepancy because of our simplifying assumptions made in Section 6.2. One assumption is that an active UE associated with BS_i^j comes from the UEs in the cluster around SA_i^j. Another assumption is that the active UEs form a PPP. These assumptions can help us achieve the theoretical performance analysis. But they also cause some mismatch. From Figure 6.6, we can observe that the mismatch between analysis and simulation is less than 1 dB. The analytical method still can be regarded as a reference if the system requirement is not very strict.

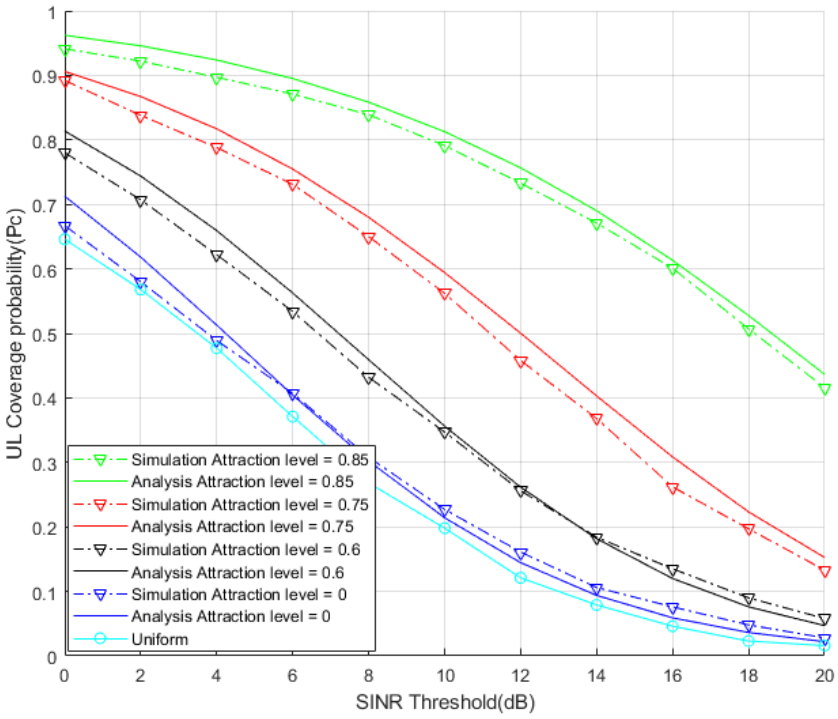

Figure 6.6: Uplink Coverage probability of our designed non-uniform UE distribution model, in which non-uniform UEs are distributed in small cells (fractional power control factor $\epsilon = 0.5$)

The cluster process is Matern cluster. The attraction level is 0.85 (the radius R is 30 m, green curve), 0.75 (the radius R is 50 m, red curve), 0.6 (the radius R is 80 m, black curve) and 0 (the radius R is 200 m, blue curve). The uniform result (cyan curve) has been also included in order to compare with the above non-uniform UE distribution. When the attraction level is high, such as 0.85 or 0.75, the uplink coverage probability is high since the active UE is chosen near the cell center. When the attraction level is low, the coverage probability of non-uniform UE distribution converges to uniform distribution (cyan curve). The base station offset D_2 is 0 m which means the dependency level is 1. The effect of the base station offset is discussed in the following subsection. In order to evaluate the performance of our designed non-uniformly distributed UE model, we put non-uniform UEs only in small cells.

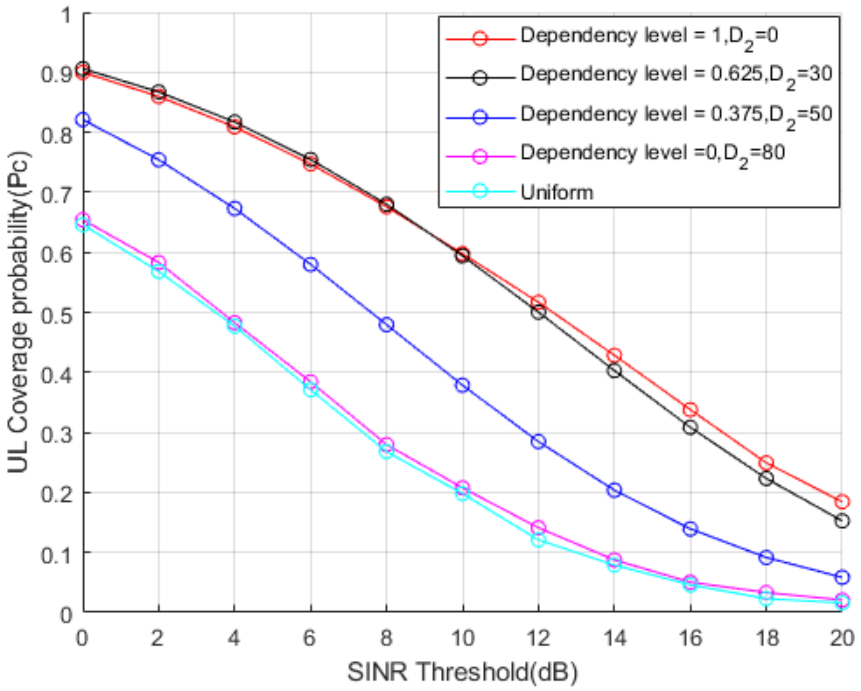

Figure 6.7: Effect of the base station offset D_2 on the uplink coverage probability

6.5.2 Effect of Base Station Offset

In this subsection, we show that the effect of the base station offset D_2 in the uplink coverage probability. We remain the UE distribution as Matern cluster (the attraction level = 0.75, $R = 50$ m) and vary the distance D_2 from {0, 30, 50, 80} m, which corresponds to the dependency level from {1, 0.625, 0.375, 0}. We can observe that there is no obvious difference between $D_2 = 0$ m and $D_2 = 30$ m. However, in the downlink analysis from Figure 5.5, the downlink coverage probability of $D_2 = 30$ m is obviously worse than that of $D_2 = 0$ m. It is due to the fact that the active UE position is almost the same when the base station offset D_2 is less than the Mater cluster radius R (here $D_2 = 0$ m, 30 m and $R = 50$ m) in the uplink analysis. When $D_2 = 50$ m in the uplink, the dependency decreases and then the uplink coverage probability also decreases. And the coverage probability converges to the uniform case (cyan curve) when $D_2 = 80$ m in the uplink. In the downlink, the overall performance for the whole cluster UEs are considered while only an active UE in one cell are considered in the uplink. The clustered UEs are located around the cell edge when the base station offset is high, such as $D_2 = 80$ m. If we still continue to increase the base station offset, such as $D_2 = 100$ m, the uplink coverage probability would be worse than the uniform case. The scenario of the high base station offset doesn't bring any

benefits and it will also never be deployed by operators. Then we assume that an active UE associated with BS_i^j comes from the UEs in the cluster around SA_i^j with reasonable base station offset between BS_i^j and SA_i^j (for example, the base station offset is less than $D_2 = 80$ m in the above simulation setting).

6.5.3 Effect of System Parameters

The theoretical analysis of the uplink coverage probability has been derived. This subsection describes the effect of system parameters, such as the BS density ratio between small cells and macro cells, the cell extension bias factor of small cells, the transmit power of small BSs, and the fractional power control factor.

We follow the same simulation parameters as the downlink case. When calculating the uplink coverage probability, the SINR coverage threshold is 0 dB and the fractional power control factor ϵ is 0.5. Since we cannot determine the relationship between the path loss exponent of macro cells and the path loss exponent of small cells, we give three curves for each kind of attraction. For each attraction (uniform, low attraction, medium attraction and high attraction), we show three curves. The first red curve is that the path loss exponent of macro cell is higher than that of small cells ($\{\alpha_1, \alpha_2\} = \{3.5, 3\}$). The second blue curve is that the path loss exponent of macro cell is equal to that of small cells ($\{\alpha_1, \alpha_2\} = \{3.5, 3.5\}$). The third black curve is that the path loss exponent of macro cell is lower than that of small cells ($\{\alpha_1, \alpha_2\} = \{3.5, 4\}$). The base station offset between SAs and BSs is assumed to be 0 m. In the following figures, the low attraction level is assumed as 0.1, the medium attraction level is assumed as 0.6, and the high attraction level is assumed as 0.75.

6.5.3.1 Effect of BS Density Ratio between Small Cells and Macro Cells

The parameter of effect of BS density ratio between small cells and macro cells are the same as Table 5.3 in the downlink case.

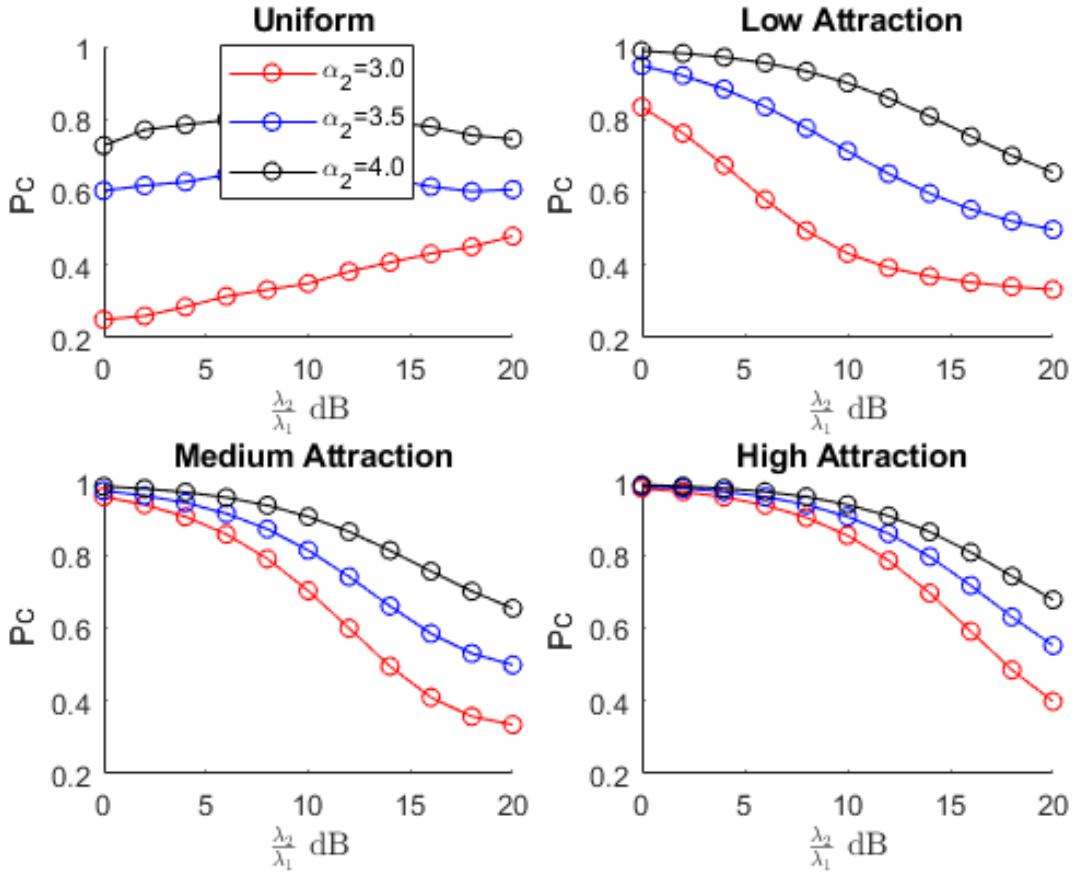

Figure 6.8: Uplink coverage probability as a function of BS density ratio $\frac{\lambda_2}{\lambda_1}$ between small cells and macro cells

The effect of BS density ratio between small cells and macro cells is shown in Figure 6.8.

From Figure 6.8 we can observe:

- When the BS density ratio $\frac{\lambda_2}{\lambda_1}$ between small cells and macro cells is low, such as $0-5$ dB, the number of small cells or the number of active UEs is also low. This results in less interference to the BS of interest such that the uplink coverage probability might be very high.

- When the BS density ratio $\frac{\lambda_2}{\lambda_1}$ between small cells and macro cells is high, such as $15-20$ dB, the density of small cells may be very high and then the coverage area of small cell is small. So the cases of low attraction, medium attraction and high attraction converge to the uniform case when the BS density ratio is high.

- The case experiencing high path loss exponent always has the high uplink coverage probability.
- The general trend is that the uplink coverage probability decreases as $\frac{\lambda_2}{\lambda_1}$ increases.
- The uplink coverage probability of low attraction does not converge to that of the uniform case when the BS density ratio is low. When the BS density ratio is low, the coverage area of small cells is very large and the equivalent radius of the coverage area may be more than the UE cluster radius of low attraction in this simulation setting. Hence, the performance of the uniform case will be worse than the performance of low attraction when the BS density ratio is low.
- BS deployment suggestion:
  - Deploying small cells with the low BS density ratio will have high uplink coverage probability.
  - Deploying the case experiencing high path loss exponent will have high uplink coverage probability.

The summary of the effect of BS density ratio between small cells and macro cells is in the following table.

Summary	**Effect of $\frac{\lambda_2}{\lambda_1}$**	**Effect of Path Loss Exponent**
Low attraction	High path loss: ↓ Same path loss: ↓ Low path loss: ↓	High path loss exponent has high performance.
Medium attraction	High path loss: ↓ Same path loss: ↓ Low path loss: ↓	High path loss exponent has high performance.
High attraction	High path loss: ↓ Same path loss: ↓ Low path loss: ↓	High path loss exponent has high performance.

Note:
↓ means that the coverage probability decreases with the increase of the BS density ratio $\frac{\lambda_2}{\lambda_1}$.

6.5.3.2 Effect of Cell Extension of Small Cells

The parameter of effect of BS cell extension of small cells are the same as Table 5.4 in the downlink case.

The effect of BS cell extension bias factor C_2 of small cells is shown in Figure 6.9.

From Figure 6.9 we can observe:

- The case experiencing high path loss exponent always has the high uplink coverage probability. In the case experiencing high path loss exponent, the active interfering UEs might generate less interference so that the uplink coverage probability might be high in this simulation setting.
- For low attraction, the uplink coverage probability decreases as the increase of C_2. When C_2 increases, the coverage area in small cells increases. So the active UEs may have long distance with their associated BSs. Long distance may cause high transmit power from interfering active UEs in uplink depending on the uplink power control policy. Hence, they might raise high interference such that the uplink coverage probability may decrease.
- For medium attraction and high attraction, the uplink coverage probability remains the same as the increase of C_2. When C_2 increases, the coverage area in small cells increases. However, the UE cluster is still in the coverage, the position of the active UE may not be changed so that the uplink coverage probability remains.
- BS deployment suggestion:
  - Deploying small cells with high attraction will have high uplink coverage probability.
  - Deploying the case experiencing high path loss exponent will have high uplink coverage probability.
  - Deploying low attraction with low C_2 will have high coverage probability.

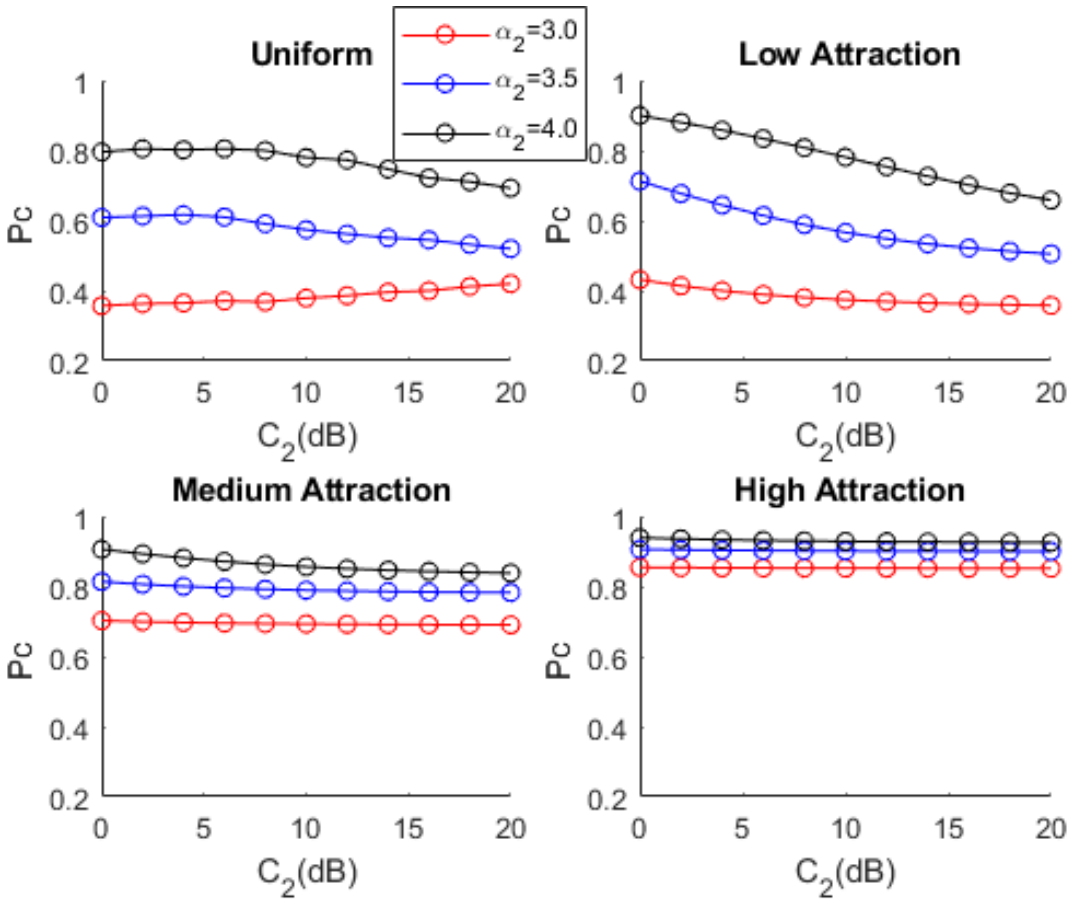

Figure 6.9: Uplink coverage probability as a function of BS cell extension bias factor C_2 in small cells

The summary of the effect of BS cell extension bias factor C_2 in small cells is in the following table.

Summary	**Effect of C_2**	**Effect of Path Loss Exponent**
Low attraction	High path loss: $\downarrow$ Same path loss: $\downarrow$ Low path loss: $\sim$	high path loss exponent has high performance.
Medium attraction	High path loss: $\sim$ Same path loss: $\sim$ Low path loss: $\sim$	high path loss exponent has high performance.
High attraction	High path loss: $\sim$ Same path loss: $\sim$ Low path loss: $\sim$	high path loss exponent has high performance.

Note:
↓ means that the coverage probability decreases with the increase of BS cell extension bias factor C_2.
∼ means that the coverage probability does not vary with the increase of BS cell extension bias factor C_2.

6.5.3.3 Effect of BS Transmit Power of Small Cells

The parameter of effect of BS transmit power of small cells are the same as Table 5.5 in the downlink case.

The effect of BS transmit power P_2 of small cells is shown in Figure 6.10.

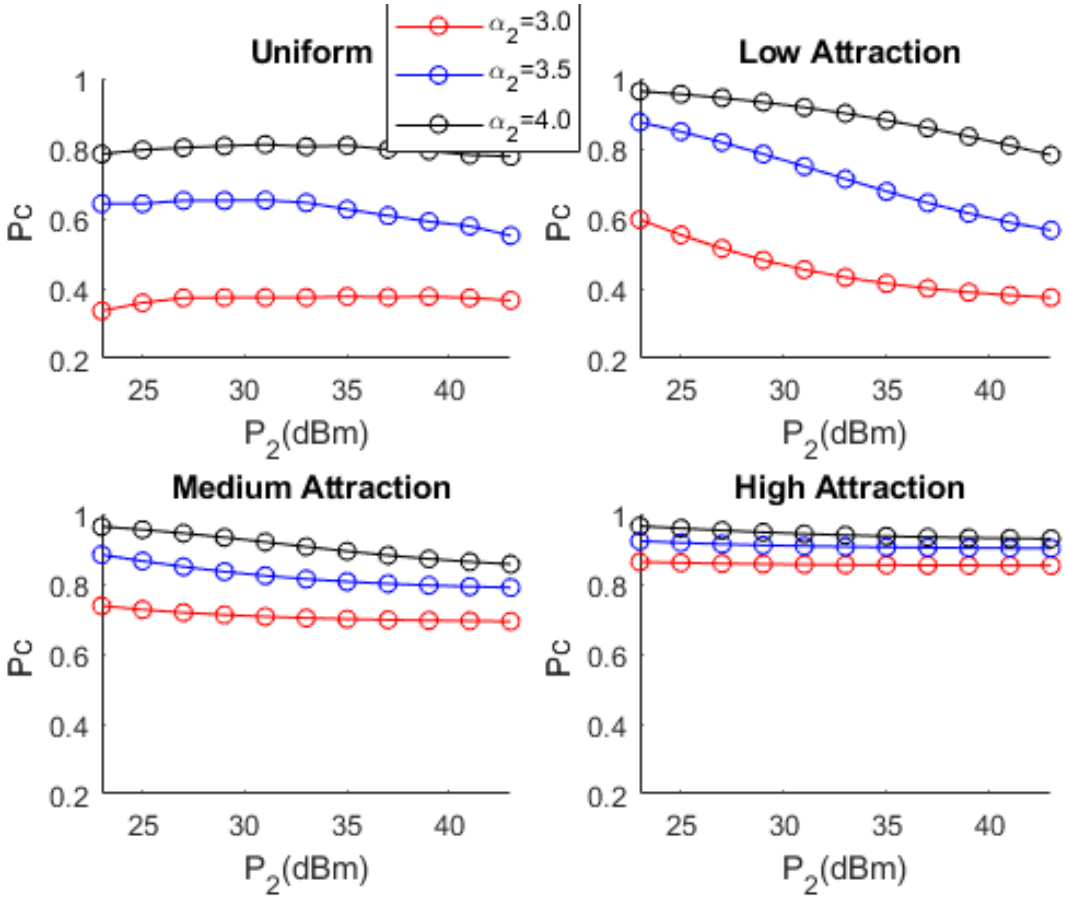

Figure 6.10: Uplink coverage probability as a function of BS transmit power P_2 in small cells

From Figure 6.10 we can observe :

- Increasing P_2 is equivalent to increase C_2. For instance, increasing P_2 will cause the larger coverage area which has the same result as the increase of C_2.
- It can be observed that Figure 6.9 and Figure 6.10 have the almost same curve.
- Hence, the observation and BS deployment suggestion is the same for the effect of BS cell extension bias factor C_2 and the effect of BS transmit power P_2.

The summary of the effect of BS transmit power P_2 in small cells is in the following table.

Summary	**Effect of P_2**	**Effect of Path Loss Exponent**
Low attraction	High path loss: $\downarrow$ Same path loss: $\downarrow$ Low path loss: $\sim$	High path loss exponent has high performance.
Medium attraction	High path loss: $\sim$ Same path loss: $\sim$ Low path loss: $\sim$	High path loss exponent has high performance.
High attraction	High path loss: $\sim$ Same path loss: $\sim$ Low path loss: $\sim$	High path loss exponent has high performance.

Note:
$\downarrow$ means that the coverage probability decreases with the increase of BS transmit power P_2.
$\sim$ means that the coverage probability does not vary with the increase of BS transmit power P_2.

6.5.3.4 Effect of Fractional Power Control Factor

For the parameters, we follow the same setting as the downlink case in the previous chapter (Table 5.2) and [75]. Matern cluster process is with the radius $R = 50$ m and the base station offset is $D = 0$ m.

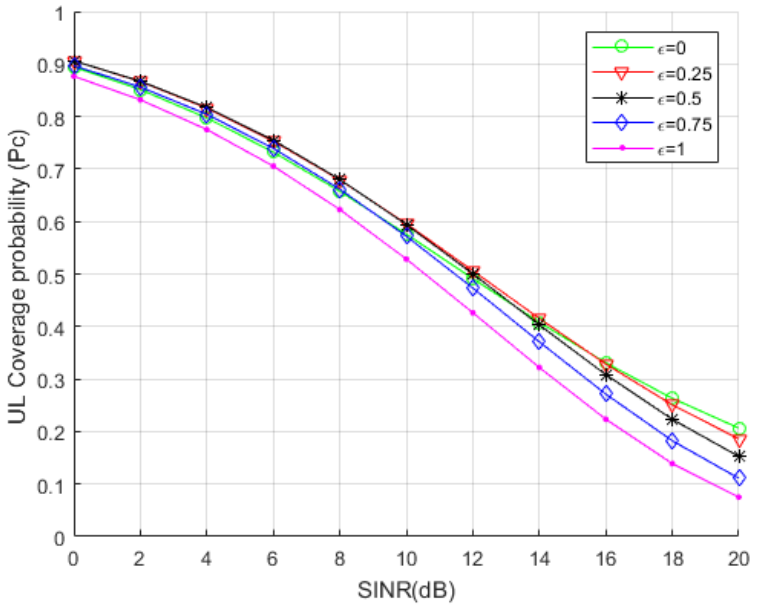

Figure 6.11: Uplink coverage probability as a function of fractional power control ϵ

Figure 6.11 gives the effect of fractional power control ϵ. When $\epsilon = 0$, it represents the fixed transmit power. The case of $\epsilon = 0$ has the highest uplink coverage probability when SINR is high, such as SINR $>$ 14 dB in this simulation setting. The cases of $\epsilon = 0.25$ and $\epsilon = 0.5$ have the highest uplink coverage probability when SINR is low, such as SINR $<$ 14 dB. The difference between $\epsilon = 0.25$ and $\epsilon = 0.5$ is negligible when SINR is low, such as SINR $<$ 14 dB. The uplink coverage probability of $\epsilon = 0.25$ is a little higher than that of $\epsilon = 0.5$ when SINR is high, such as SINR $>$ 14 dB. The case of $\epsilon = 0.75$ is almost the same as the case of fixed transmit power $\epsilon = 0$ when SINR is low, such as SINR $<$ 10 dB. The case of $\epsilon = 0.75$ has lower uplink coverage probability than the case of $\epsilon = 0$, $\epsilon = 0.25$ and $\epsilon = 0.5$ when SINR is high, such as SINR $>$ 10 dB. The case of full path loss compensation $\epsilon = 1$ provides the lowest uplink coverage probability across all SINR coverage thresholds. Hence, the coverage probability of $\epsilon = 0$ is the best when SINR $>$ 14 dB while the coverage probability of $\epsilon = 0.25$ or $\epsilon = 0.5$ is the best when SINR $<$ 14 dB.

6.6 Conclusions

In this chapter, we derived the uplink coverage probability of our designed non-uniform UE distribution. The uplink analysis is more complex than the downlink analysis since the uplink power control makes the UE transmit power variable and the characterization of the

uplink interference from all interfering active UEs is not available. Therefore, we propose some assumptions in order to make our analysis using the tools of stochastic geometry. One assumption is that an active UE associated with BS_i^j comes from the UEs in the cluster around SA_i^j. Then the above assumption makes it possible to get the PDF and CCDF of the distance between the BS of interest and the associated active UE. The uplink coverage probability is derived based on the proposed assumptions. The simulation results do not match closely with the derived analysis because of the simplifying assumptions we made. However, the mismatch between the analysis and the simulation is less than 1 dB. This shows that our assumptions are acceptable if the system requirement is not very strict. Hence, we can obtain the performance using our derived equations rather than carrying out time-consuming simulations for the designed non-uniform user model to verify uplink HetNet performance.

The effect of the base station offset between SA and BS is evaluated. It shows that there is no obvious difference when the base station offset D is less than the Matern cluster radius R. If we still continue to increase the base station offset, the uplink coverage probability would be worse than the uniform case. The operators will never deploy small cells with high base station offset since it will not bring any benefits. So we make an assumption that the base station offset is less than a threshold. The effect of system parameters, such as the BS density ratio between small cells and macro cells, the BS cell extension bias factor of small cells, the BS transmit power of small cells, and the fractional power control factor are also discussed. For example, for the effect of BS density ratio, when the BS density ratio is low, such as $0-5$ dB between small cells and macro cells, the number of small cells or the number of active UEs is also low. This results in less interference so that the uplink coverage probability might be very high. For the effect of BS cell extension bias factor C_2, the case experiencing high path loss exponent always has the high uplink coverage probability. The case experiencing high path loss exponent will generate less interference so that the uplink coverage probability might be high in this simulation setting. For the effect of BS transmit power P_2, increasing P_2 will increase the coverage area, which is equivalent to increase C_2. Finally, the effect of different fractional power control factor is introduced.

Chapter 7

Analysis Comparison between Downlink and Uplink

7.1 Introduction

In this chapter, the analysis comparison between the downlink and the uplink is summarized from the work covered in the previous two chapters. Firstly, Section 7.2 introduces the proposed non-uniform UE model used in the downlink and the uplink analysis. Then Section 7.3 represents the coverage probability performance analysis including the coverage probability definition, the assumptions, the coverage probability derivations and the simulation results. Finally, Section 7.4 indicates the effect of system parameters.

7.2 Non-uniform UE Model

In this thesis, a non-uniform UE model is introduced. This non-uniform UE model is a Poisson cluster process with the cluster centers located at SAs. SAs have the base station offset with their BSs. There are two parameters in this UE distribution model. They are the cluster radius R and the base station offset D. R is used to determine the attraction level between UEs and their SAs. D is used to determine the dependency level between SAs and their BSs. The combination of the attraction level and the dependency level can cover most of the non-uniform scenarios. When operators carry out the evaluation of HetNet design based on the non-uniform UE model, they can choose any combination of two parameters to create the specific non-uniform UE distribution. In our designed non-uniform UE model, different cell tier may have different parameters. In this thesis, we

focus our designed non-uniform UE model with a user's location in a cluster with a PDF of Matern cluster process. It is easy to extend to other PDFs. Our non-uniform UE model is introduced in Chapter 4.

The heterogeneity of this non-uniform UE model is also shown in Chapter 4. The heterogeneity analysis is based on coefficient of variation (CoV). Voronio cell area is used as the CoV statistic measurement of inter-point distance metrics. In this thesis, Cov is defined as the standard deviation of Voronio cell area measurement divided by the mean of Voronio cell area measurement. CoV is a good indication of user's spatial heterogeneity. From Chapter 4, the dependency level has little impact for the heterogeneity and the attraction level has big impact for heterogeneity.

The downlink coverage probability performance analysis in Chapter 5 and the uplink coverage probability performance analysis in Chapter 6 are all based on the non-uniform user model introduced in Chapter 4.

7.3 Coverage Probability Performance Analysis

Based on our designed non-uniform UE distribution model, the downlink and the uplink coverage probability performance analysis are derived step by step. During the evaluation that researchers or operators carry out on HetNets based on the non-uniform UEs, the derived equations of the downlink coverage probability (Equation 5.17) and the uplink coverage probability (Equation 6.13) can be used directly rather than time consuming simulations. The same connectivity rule is applied for the downlink and the uplink analysis, which is the downlink maximum average bias received power. We also set the same simulation parameters (e.g., BS density ratio, BS transmit power, BS cell extension bias factor) in the downlink of Chapter 5 and the uplink of Chapter 6 in order to demonstrate clear difference between them.

7.3.1 Coverage Probability Definition

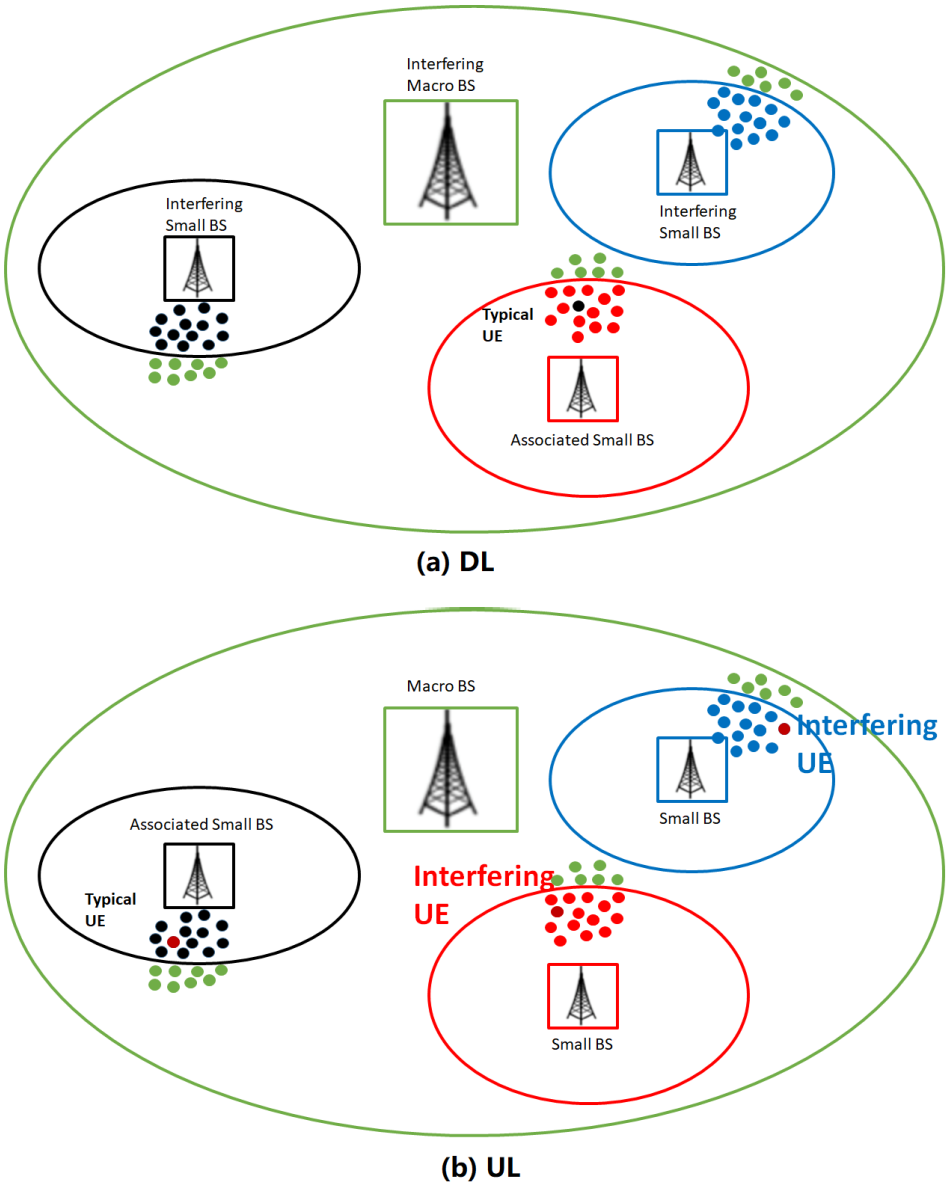

Figure 7.1: Example of coverage probability definition

The downlink and the uplink research is carried out based on K-tier BS system. Figure 7.1 shows an example of coverage probability definition.

7.3.1.1 Downlink

The downlink coverage probability is defined as the average coverage probability over all UEs in the downlink. Firstly, find the associated BS for each UE. Secondly, calculate

the received signal from the associated BS and the total interference power from all other interfering BSs. Thirdly, calculate the downlink SINR for each UE. Finally, the downlink coverage probability is obtained by the complementary cumulative distribution (CCDF) of all calculated SINR. In Figure 7.1 (a), it is an example of the downlink. There are one macro BS (in green) and three small BSs (in black, blue and red). UEs are represented as points and are labeled by the color that is the same as the associated BS. A downlink SINR is calculated in Figure 7.1 (a), in which a black point user is called as the typical UE. The received signal power of the typical UE comes from the associated BS in red and the interference power of the typical UE experiencing comes from the other two small BSs and the macro BS. All UEs will do the same calculation of SINR. The downlink coverage probability is the average coverage probability over all UEs from the BSs in the downlink.

7.3.1.2 Uplink

The uplink coverage probability is defined as the average coverage probability over all BSs in the uplink. Firstly, find the active UE for each BS and there is only one active UE in each cell in a given resource block since LTE of orthogonal multiple access technique is assumed. Secondly, calculate the received signal from the active UE and total interference power from all other active UEs. Thirdly, calculate the uplink SINR for each BS. Finally, the uplink coverage probability is obtained by the complementary cumulative distribution (CCDF) of all calculated SINR. In Figure 7.1 (b), it is an example of the uplink. In each cell, an active UE in maroon is chosen randomly. An uplink SINR is calculated in Figure 7.1 (b), in which there is a typical UE. The received signal power of the associated BS comes from the typical UE and the interference power comes from the other two interfering active UEs. All BSs will do the same calculation of SINR. Hence, the uplink coverage probability is the average coverage probability over all BSs from the active UEs in uplink.

7.3.1.3 Difference

The non-uniform UEs are from our designed non-uniform UE model with specific parameters. All UEs are used to calculate the downlink coverage probability while only active UEs are used to calculate the uplink coverage probability.

7.3.2 Assumptions

The assumptions of the performance analysis are summarized as follows.

7.3.2.1 Downlink

- The channel is Rayleigh fading.

7.3.2.2 Uplink

- The channel is Rayleigh fading.
- In each cell, there is one active UE.
- An active UE associated with BS_i^j comes from the UEs in the cluster around SA_i^j and other active UEs associated with BS_i^j in the cluster around other SA rather than SA_i^j are not considered.
- The base station offset is less than a threshold.
- Active UEs in each tier form a homogeneous and independent PPP.

7.3.2.3 Difference

There are more assumptions in uplink since the positions of UEs are totally random and the uplink power control makes the uplink transmit power of UEs to fluctuate.

7.3.3 Coverage Probability Derivation

7.3.3.1 Downlink

Let $m = 1, 2, ...k$ be the tier of interest. The procedure to get the downlink coverage probability $\mathbb{P}_{dl,c}$ is as follows:

- Find the probability density function (PDF) $f_L^{(m)}(l)$ and complementary cumulative distribution function (CCDF) $\bar{F}_L^{(m)}(l) = \mathbb{P}^{(m)}(L > l)$ of random variable L. Let L be the distance between a UE and the BS that the UE belongs to in the mth tier.
- Find the PDF $f_V^{(m)}(v)$ and CCDF $\bar{F}_V^{(m)}(v) = \mathbb{P}^{(m)}(V > v)$ of random variable V. Let V be the distance between a UE and the closest BS in the mth tier.
- The UE of interest (e.g. block point UE in Figure 5.1) in a given mth tier can be associated with a possible BS into two cases.
  Case1: associated with the BS to which the UE of interest belongs.

- Derive $\mathbb{P}^{(m)}(A_{case1})$, which is the probability that a UE of interest is associated with the BS to which the UE belongs. In Figure 5.1, it means that the black point UE is associated with BS_1^1.
- Derive the downlink coverage probability $\mathbb{P}^{(m)}[SINR_m(l) > T_m|A_{case1}]$ conditioned on the black point UE associated with BS_1^1.
- Derive the downlink coverage probability $\mathbb{P}^{(m)}_{dl,c,case1} = \mathbb{P}^{(m)}(A_{case1}) * \mathbb{P}^{(m)}[SINR_m(l) > T_m|A_{case1}]$ that the black point UE is associated with BS_1^1 to which this UE belongs.

Case2: associated with a BS in all tiers except the BS to which UE belongs (e.g. except BS_1^1)

- Derive $\mathbb{P}^{(m)}(A_{k,case2})$, which is the probability that a UE is associated with a kth tier BS.
- Derive the downlink coverage probability $\mathbb{P}^{(m)}[SINR_k(v) > T_k|A_{k,case2}]$ conditioned on a UE associated with a kth tier BS.
- Derive the downlink coverage probability $\mathbb{P}^{(m)}_{dl,ck,case2} = \mathbb{P}^{(m)}(A_{k,case2}) * \mathbb{P}^{(m)}[SINR_k(v) > T_k|A_{k,case2}]$ of associating with a kth tier BS.

Summary

- $\mathbb{P}^{(m)}(A_{case1})$ and $\mathbb{P}^{(m)}(A_{k,case2})$ is the probability that a UE of interest in the mth tier is associated with the BS to which UE belongs and a kth tier BS. $\mathbb{P}^{(m)}(A_{case1}) + \sum_{k=1}^{K} \mathbb{P}^{(m)}(A_{k,case2}) = 1$. K is the total number of BS tiers.
- The downlink coverage probability for a UE distributed in the mth tier is $\mathbb{P}^{(m)}_{dl,c} = \mathbb{P}^{(m)}_{dl,c,case1} + \sum_{k=1}^{K} \mathbb{P}^{(m)}_{dl,ck,case2}$.

7.3.3.2 Uplink

Let $m = 1, 2, ...k$ be the tier of interest. The procedure to get the uplink coverage probability $\mathbb{P}_{ul,c}$ is as follows:

- Find the probability density function (PDF) $f_L^{(m)}(l)$ and complementary cumulative distribution function (CCDF) $\bar{F}_L^{(m)}(l) = \mathbb{P}^{(m)}(L > l)$ of random variable L. Let L be the distance between an active UE and its associated BS that the active UE belongs to in the mth tier.

- The BS of interest (e.g. BS_1^1 in Figure 6.4) in a given mth tier can be associated with an active UE in two cases.
  Case1: an active UE that belongs to the BS of interest.
  - Derive $\mathbb{P}^{(m)}(A_{case1})$, which is the probability that the active UE is associated with the BS of interest that the active UE belongs to in the mth tier.
  - Derive the uplink coverage probability $\mathbb{P}^{(m)}[SINR_m(l) > T_m|A_{case1}]$ conditioned on the active UE associated with BS_1^1.
  - Derive the uplink coverage probability $\mathbb{P}^{(m)}_{ul,c,case1} = \mathbb{P}^{(m)}(A_{case1}) * \mathbb{P}^{(m)}[SINR_m(l) > T_m|A_{case1}]$ that the active UE is associated with BS_1^1.

  Case2: an active UE that belongs to the other BS rather than the BS of interest.
  - Ignored since the simplifying assumption, which is the active UE belongs to the BS of interest.

  Summary
  - $\mathbb{P}^{(m)}(A_{case1})$ is the probability that the active UE that belongs the BS of interest is associated with the BS of interest.
  - $\mathbb{P}^{(m)}_{ul,c,case1}$ is the coverage probability associated with the BS of interest.
  - The uplink coverage probability for a BS of interest distributed in a mth tier with the simplifying assumption that the active UE belongs to the BS of interest is $\mathbb{P}^{(m)}_{ul,c} = \frac{\mathbb{P}^{(m)}_{ul,c,case1}}{\mathbb{P}^{(m)}(A_{case1})}$.

7.3.3.3 Difference

A UE has associated with a BS into two cases. The first case is that the UE is associated with the BS that the UE belongs to (case1) and the second case is that the UE is associated with other BSs (case2). For downlink analysis, both case1 an case2 are considered. For uplink analysis, only case1 is considered due to the simplifying assumptions.

7.3.4 Simulation Results

For the downlink and the uplink analysis, the simulation results and the theoretical results are based on the same simulation parameters.

7.3.4.1 Downlink

In the downlink, the simulation results and the theoretical results match closely, which proves that our analysis is accurate. For effect of the base station offset, the low base station offset has the high downlink coverage probability while the high base station offset has the low downlink coverage probability and converges to the uniform case.

7.3.4.2 Uplink

The simulation results and the theoretical results do not match closely because of the assumptions made in the uplink performance analysis. However, the gap is less than 1 dB, which proves that our assumptions are acceptable if the system requirement is not very strict. For effect of the base station offset, we can observe that there is no obvious difference between the low base station offset. And the coverage probability converges to the uniform case when the base station offset arrives a threshold in uplink. If we still continue to increase the base station offset, such as $D = 100$ m in our simulation setting, the uplink coverage probability would be worse than the uniform case. Therefore, we have an assumption that the base station offset is less than a threshold.

7.3.4.3 Difference

The theoretical analysis in the downlink is the accurate performance and the theoretical analysis in uplink is the estimated performance. The downlink and the uplink analysis have different effect from the base station offset since all UEs are calculated in the downlink and only an active UE in one cell is calculated in the uplink.

In the following, we indicate the comparison of the downlink and the uplink performance.

- Comparison with the reference literature [69]
  Based on our theoretical analysis, Figure 7.2 gives the performance of the downlink and the uplink, which has the same simulation setting as [69] in a single tier system. In Figure 7.2, the UE distribution converges to be uniform and the coverage probability based on the analysis in this thesis matches with the results in [69]. It confirms that our simulation method and theoretical analysis are solid and we can extend our research to multi-tier system.

The interference in the downlink comes from all interfering BSs and the interference in uplink comes from all interfering active UEs. From Figure 7.2, we can observe that the coverage probability of the downlink is higher than that of the uplink.

Another observation from Figure 7.2 is that the effect of the fractional power control factor ϵ. Low ϵ has the high coverage probability, which aligns with the results of Subsection 6.5.3.4.

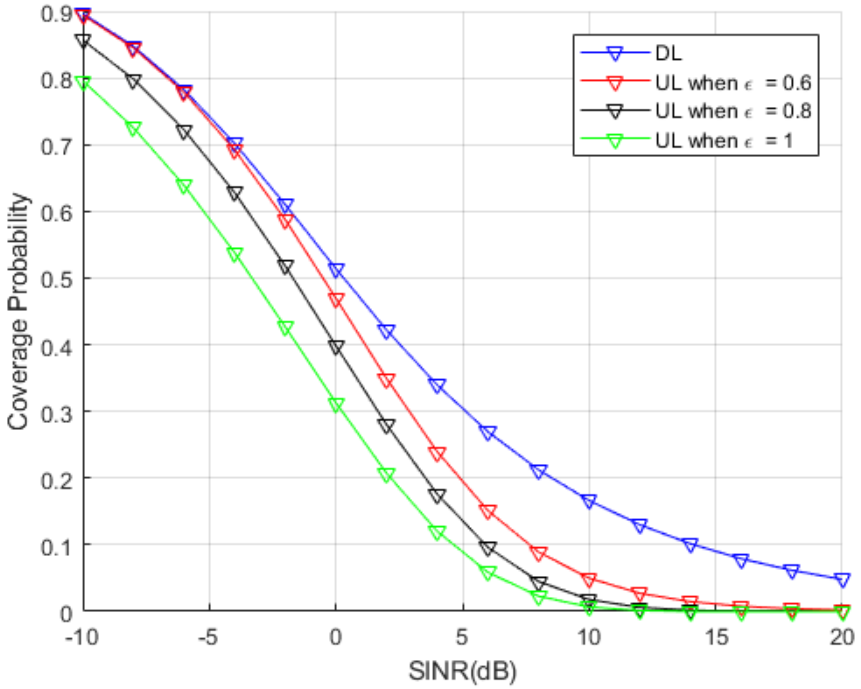

Figure 7.2: Comparison of the coverage probability of the downlink and the uplink in a single tier system (compared with the reference literature)

- Comparison between downlink and uplink

  Figure 7.3 gives the comparison between downlink and uplink. The simulation results are collected from Figure 5.4 and Figure 6.6. The coverage probability of the uplink is better than that of the downlink. This conclusion is inconsistent with the comparison with the reference literature of single tier in the above subsection. It shows that the relationship between the downlink and the uplink performance is not fixed (e.g., the downlink is always better or the uplink is always better). It is because the downlink coverage is calculated by the receiving signal from the associated BS and the receiving interference from all other BSs on the view of a typical user in the downlink and the uplink coverage is calculated by the receiving signal from the associated active user

and the receiving interference from all other active users on the view of a BS in the uplink.

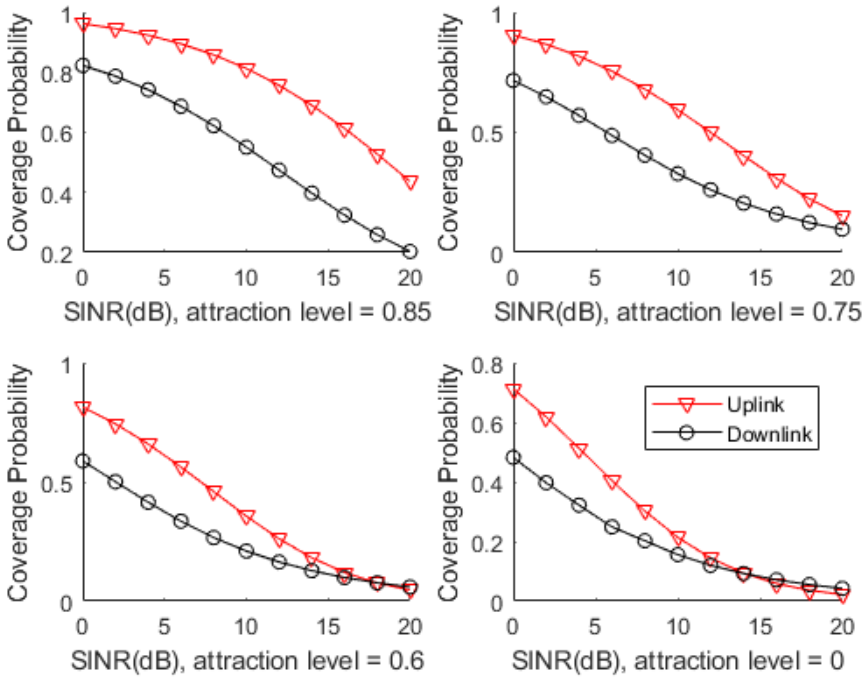

Figure 7.3: Comparison of the coverage probability of the downlink and the uplink in a 2-tier system

7.4 Effect of System Parameters

For the downlink and the uplink analysis, the effect of system parameters is based on the same simulation parameters.

7.4.1 Effect of BS Density Ratio between Small Cells and Macro Cells

The summary of the effect of the BS ratio between small cells and macro cells in small cells is in the following table.

Summary	**Effect of $\frac{\lambda_2}{\lambda_1}$**	**Effect of Path Loss Exponent**
Downlink		
Low attraction	High path loss: ↑ Same path loss: ↑ Low path loss: ↑	High path loss exponent has high performance.
Medium attraction	High path loss: ↑ Same path loss: ↑→↓ Low path loss: ↑→↓	Low path loss exponent has high performance at low BS density ratio and high path loss exponent has high performance at high BS density ratio.
High attraction	High path loss: ↑→↓ Same path loss: ↑→↓ Low path loss: ↑→↓	Same as medium attraction case.
Uplink		
Low attraction	High path loss: ↓ Same path loss: ↓ Low path loss: ↓	High path loss exponent has high performance.
Medium attraction	High path loss: ↓ Same path loss: ↓ Low path loss: ↓	High path loss exponent has high performance.
High attraction	High path loss: ↓ Same path loss: ↓ Low path loss: ↓	High path loss exponent has high performance.

Note:
↑ means that the coverage probability increases with the increase of BS density ratio $\frac{\lambda_2}{\lambda_1}$.
↓ means that the coverage probability decreases with the increase of the BS density ratio $\frac{\lambda_2}{\lambda_1}$.
↑→↓ means that the coverage probability increases, and then decreases with the increase of BS density ratio $\frac{\lambda_2}{\lambda_1}$ after a turning point.

7.4.2 Effect of Cell Extension of Small Cells

The summary of the effect of BS cell extension bias factor C_2 in small cells is in the following table.

Summary	**Effect of C_2**	**Effect of Path Loss Exponent**
Downlink		
Low attraction	High path loss: $\downarrow$ Same path loss: $\downarrow$ Low path loss: $\downarrow$	High path loss exponent has high performance.
Medium attraction	High path loss: $\downarrow$ Same path loss: $\downarrow$ Low path loss: $\downarrow$	Low path loss exponent has high performance.
High attraction	High path loss: $\sim$ Same path loss: $\sim$ Low path loss: $\sim$	Low path loss exponent has high performance.
Uplink		
Low attraction	High path loss: $\downarrow$ Same path loss: $\downarrow$ Low path loss: $\sim$	High path loss exponent has high performance.
Medium attraction	High path loss: $\sim$ Same path loss: $\sim$ Low path loss: $\sim$	High path loss exponent has high performance.
High attraction	High path loss: $\sim$ Same path loss: $\sim$ Low path loss: $\sim$	High path loss exponent has high performance.

Note:
$\downarrow$ means that the coverage probability decreases with the increase of BS cell extension bias factor C_2.
$\sim$ means that the coverage probability does not vary with the increase of BS cell extension bias factor C_2.

7.4.3 Effect of Transmit Power of Small Cells

The summary of the effect of BS transmit power P_2 in small cells is in the following table.

Summary	**Effect of P_2**	**Effect of Path Loss Exponent**
Downlink		
Low attraction	High path loss: $\uparrow$ Same path loss: $\uparrow$ Low path loss: $\sim$	High path loss exponent has high performance.
Medium attraction	High path loss: $\uparrow$ Same path loss: $\uparrow$ Low path loss: $\uparrow$	Low path loss exponent has high performance.
High attraction	High path loss: $\uparrow$ Same path loss: $\uparrow$ Low path loss: $\uparrow$	Low path loss exponent has high performance.
Uplink		
Low attraction	High path loss: $\downarrow$ Same path loss: $\downarrow$ Low path loss: $\sim$	High path loss exponent has high performance.
Medium attraction	High path loss: $\sim$ Same path loss: $\sim$ Low path loss: $\sim$	High path loss exponent has high performance.
High attraction	High path loss: $\sim$ Same path loss: $\sim$ Low path loss: $\sim$	High path loss exponent has high performance.

Note:
$\uparrow$ means that the coverage probability increases with the increase of P_2.
$\downarrow$ means that the coverage probability decreases with the increase of P_2.
$\sim$ means that the coverage probability does not vary with the increase of P_2.

7.5 Conclusions

This chapter summarized the difference between the downlink and the uplink analysis. The same non-uniform UE model is used in the research of the downlink and the uplink analysis. For the downlink, SINR of each UE in the cluster from its associated BS and all other interfering BSs in the downlink is calculated and the average downlink coverage probability is obtained by the CCDF of all calculated dowlink SINRs. For the uplink, SINR of each BS from the associated active UE and all other interfering active UEs in the

uplink is calculated and the average uplink coverage probability is obtained by the CCDF of all calculated uplink SINRs. So the downlink analysis is dependent on all UEs in the cluster while the uplink analysis is only dependent on the active UEs.

The comparison between the downlink and the uplink is also given, such as the coverage definition, assumptions and coverage probability derivation. The simulation results are shown to confirm the relevant analysis. The downlink analysis is the accurate analysis while the uplink analysis is the approximated analysis due to the simplifying assumptions. Finally, the effect of BS system parameters is listed. The effect in the downlink and the uplink is quite different.

Chapter 8

Conclusions and Future Work

8.1 Conclusions

5G networks demand high data capacity. Small cell deployment is a great solution to this demand. Conventional networks combined with small cells, such as pico cells, femto cells consist of HetNets. Distribution models of BS and UE are significant for system design and evaluation. In the literature, the non-uniform UE distribution model is very limited. This thesis designed a comprehensive framework of the non-uniform UE distribution to have a tractable downlink and uplink analysis in HetNets. It shown that deploying small BSs at the UE cluster centers can improve the coverage probability. Physical constraints let small BSs deployment challenging such that small BSs are placed at the position with a base station offset to the UE cluster center. To address the existing problems, in this thesis: (1) A new non-uniform UE model based on K-tier BS HetNets was proposed. (2) The downlink and uplink coverage probability was analyzed.

We proposed a new non-uniform UE distribution model based on the existing K-tier BS distribution. The UE model is PCP, in which the UEs are symmetrically distributed around SAs that have a base station offset with their BSs. The UE distribution model with the combination of the attraction level and the dependency level covers most of the practical scenarios. The heterogeneity of the non-uniform UE model based on coefficient of variant (CoV) was illustrated. Voronoi cell area was chosen as the CoV statistic measurement confirmed by the simulation results. CoV in this thesis is the standard deviation of Voronoi cell area divided by the mean of Voronoi cell area. Normalized CoV can represent the UE pattern is sub-Poisson, Poisson or super-Poisson. As the path loss exponent is a good indication of the large scale fading, normalized CoV can be regarded as a good indication

of user's spatial heterogeneity. The relationship between the normalized CoV and the UE model's parameters was discussed. The relationship between the coverage probability and the UE model's parameter was also discussed.

This thesis derived the theoretical analysis of the coverage probability for the non-uniform UE distribution model in the downlink and the uplink. The researchers can rely on equations we derived instead of time-consuming simulations to know the performance based on the non-uniform UE distribution.

In the downlink, SINR of all UEs in a cluster is used to calculate or derive the coverage probability. The UE of interest is located inside a UE cluster, which has the base station offset with a BS. This UE is called to belong to this BS. The BS that the UE of interest is associated with can be described into two cases. Case1 is that the UE is associated with the BS that the UE of interest belongs to and case2 is that the UE is associated with other BS. The key part of the performance derivation is the characterization of the distance between the UE of interest and the BS that the UE of interest belongs to and the distance between the UE of interest and the closest BS in different tier. The simulation results were implemented to show the closely matching with our theoretical analysis. The effect of base station offset was also given. Low base station offset will have high coverage probability, vice versa. When the base station offset is approaching a threshold, the performance converges to the uniform case, which means that deploying a large base station offset will not bring any benefit. Hence, all research in this thesis focus on a reasonable base station offset less than the threshold, which still brings benefits compared with the uniform case. Furthermore, the effect of BS system parameters was demonstrated (e.g., the BS density ratio between small cells and macro cells, the BS cell extension bias factor of small cells and the BS transmit power of small BSs). The conclusions from our research of the non-uniform UE distribution were quite different compared with the uniform cases that had introduced in the literature. For example, [20] had the conclusion about the uniform case that "more BSs can be added in any tier without affecting the coverage and hence the net network capacity can be increased linearly with the number of BSs" when SINR threshold is the same in all tiers. But the conclusion was different when the non-uniform user distribution was introduced, which had the conclusion in our thesis that the coverage probability increased, then decreased after a turning point with the increase of the BS density ratio between small cells and macro cells. Hence, this turning point is an optimum deployed density ratio.

In the uplink, SINR of an active UE randomly chosen in one cell was used to calculate or derive the coverage probability since we assume orthogonal multiple access technique.

Unlike the downlink analysis, all interference power comes from BSs with fixed position, such as PPP, all interference power in the uplink comes from UEs with mobile position so that it is challenging to get the characterization of all uplink interference power. Another reason is the uplink power control, which causes the UE transmit power to fluctuate. Therefore, this thesis makes some assumptions in order to get a tractable analysis or closed-form equations. The assumptions made in this thesis were that (1) there is one active UE in each cell, (2) an active UE is assumed in the cluster that has a base station offset with the BS of interest, (3) the base station offset is less than a threshold and (4) the active UEs in each tier form a homogeneous and independent PPP. Because of the above assumptions, the simulation results do not closely match with the analysis results. However, the gap was less than 1 dB, which was acceptable if the system requirement was not tight. The effect of base station offset was also presented. It can be observed that there was no obvious difference when the base station offset D was less than Matern cluster radius R. And the coverage probability converged to the uniform case at the high base station offset. The effect of BS system parameters was simulated, too. For example, the coverage probability always decreased with the increase of the density ratio so that we cannot deploy small cells as much as possible if considering the uplink performance.

Finally, the comparison of the coverage probability definition, the assumptions, the coverage probability derivation and simulation results between the uplink and the downlink was summarized. In addition, the comparison of the effect of BS system parameters was also discussed.

This thesis filled the gap of the non-uniform UE distribution. The combination of the attraction level and the dependency level can cover most of non-uniform UE scenarios. The target customers of this non-uniform UE model are researchers or operators who design and evaluate HetNets. Once the specific non-uniform UE distribution was defined, the downlink or the uplink coverage probability would be obtained by our theoretical analysis equations derived in this thesis. The distribution of BSs is assumed as PPP in this thesis, which has the possibility that the distance between two BSs is zero. We should consider more practical scenarios of BS distribution in future work. However, our research of the non-uniform UE model and its downlink/uplink performance analysis in this thesis still can be regarded as the baseline of the research of the non-uniform UE distribution.

8.2 Future Work

- **Other metrics and mobility**: In this thesis, we derived the downlink and the

uplink coverage probability for the spatial UE model using the tools of stochastic geometry. In future work, other performance metrics rather than the coverage probability should be researched, such as the ergodic rate, the effective rate, the symbol error rate (SER). At the same time, the UEs may be mobile so we should research on spatiotemporal model using stochastic geometry and queuing theory.

- **General channel model:** All theoretical results and simulations in this thesis assumed that the fading type was Rayleigh. In the future, more general fading should be considered, such as Nakagami-m fading as in [104]. Nakagami-m is accurate and flexible to match a real scenario compared with Rayleigh, Rician, etc. Rayleigh fading, one-sided Gaussian and Rician distribution are included in Nakagami-m. When $m = 1$, it is Rayleigh fading. When $m = \frac{1}{2}$, it is one-sided Gaussian fading. When $m > 1$, it is equivalent to Rician fading. Beyond Nakagami-m fading, we should continue to research the UE behavior based on more general fading [44, 105].

- **General BS spatial distribution:** In this thesis, we carried out the research about the UE spatial distribution model and remain the BS assumption as a K-tier distribution. In further research, we should study non-uniform UE over more general BS spatial distribution, such as determinantal process, Matern process, PCP, and PHP. At the same time, three dimensional (3D) BSs should also been considered. Most of research about BS spatial distribution is based on 2D. In practice, BSs can not be placed directly on the ground and they should have height. Moreover, the height of BSs may be variable, which results in more complicated analytical derivation. In the literature, there is some research based on drone or unmanned aerial vehicle (UVA) [106–109], in which BSs have variable height.

- **Multi-input multi-output (MIMO) and millimeter Wave (mmWave):** In 5G, another two key features are MIMO and mmWave. Combining these two features into the UE spatial model is very practical. For MIMO, the channel power gain from associated BSs and interfering BSs is quite different, which has been proven in [110–113] so that we need to pay attention to this new phenomenon when designing and analyzing the UE models. For mmWave, the operating frequency is normally above 30 GHz, which leads the blocking of transmit wave. The popular modeling of link is to separate modeling into Line-of-Sight (LOS) and non-LOS (NLOS). The wireless link is a combination of LOS and NLOS with their own probability. How to shape LOS and NLOS link [114, 115] is what we should focus on research of the UE spatial behavior under mmWave.

Appendix

Appendix A

Downlink Coverage Performance Analysis

A.1 Proof of Corollary 5-1

When $D_m \geq R_m$,

- $l \leq D_m - R_m$

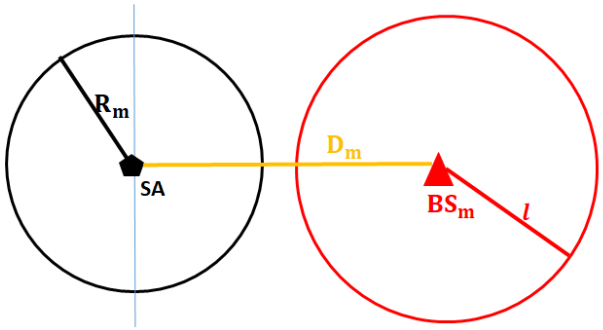

Figure A.1: PDF and CCDF when $D_m \geq R_m$ and $l \leq D_m - R_m$

From Figure A.1, the random distance L of all users in black disc to BS_m is more than l. So CCDF $\bar{F}_L^{(m)}(l) = \mathbb{P}^{(m)}(L > l) = 1$. PDF $f_L^{(m)}(l) = 0$.

- $D_m - R_m < l \leq \sqrt{{D_m}^2 + R_m^2}$

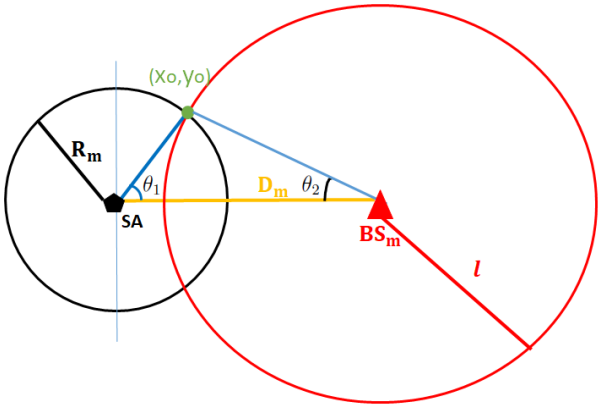

Figure A.2: PDF and CCDF when $D_m \geq R_m$ and $D_m - R_m < l \leq \sqrt{{D_m}^2 + R_m^2}$

Then, $\theta_1 = \arctan\frac{y_0}{x_0}$, $\theta_2 = \arctan\frac{y_0}{D_m - x_0}$.
So CCDF $\bar{F}_L^{(m)}(l) = \mathbb{P}^{(m)}(L > l) = 1 - \frac{\theta_1 R_m^2 + \theta_2 l^2 - D_m y_0}{\pi R_m^2}$ in which $\theta_1 R_m^2 + \theta_2 l^2 - D_m y_0$ is the joint area between the black circle and the red circle. PDF $f_L^{(m)}(l) = \frac{2\theta_2 l}{\pi R_m^2}$.

- $\sqrt{{D_m}^2 + R_m^2} < l < D_m + R_m$

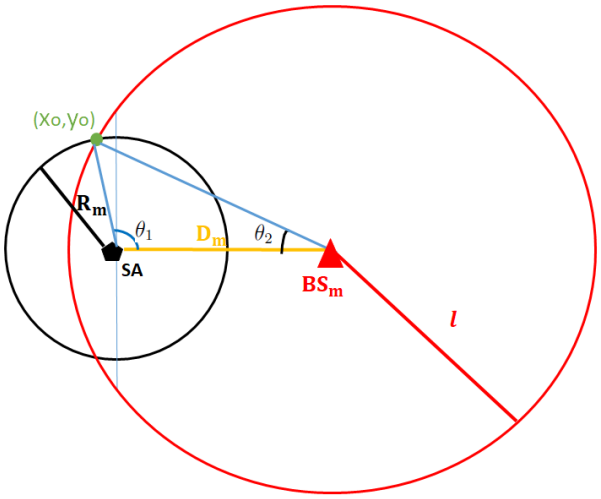

Figure A.3: PDF and CCDF when $D_m \geq R_m$ and $\sqrt{{D_m}^2 + R_m^2} < l < D_m + R_m$

Then, $\theta_1 = \arctan\frac{y_0}{x_0} + \pi$, $\theta_2 = \arctan\frac{y_0}{D_m - x_0}$.
So CCDF $\bar{F}_L^{(m)}(l) = \mathbb{P}^{(m)}(L > l) = 1 - \frac{\theta_1 R_m^2 + \theta_2 l^2 - D_m y_0}{\pi R_m^2}$. PDF $f_L^{(m)}(l) = \frac{2\theta_2 l}{\pi R_m^2}$.

- $D_m + R_m \leq l$

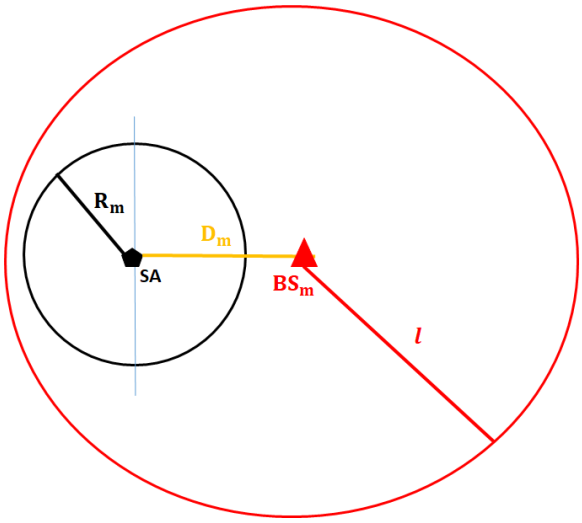

Figure A.4: PDF and CCDF when $D_m \geq R_m$ and $D_m + R_m \leq l$

So CCDF $\bar{F}_L^{(m)}(l) = \mathbb{P}^{(m)}(L > l) = 0$. PDF $f_L^{(m)}(l) = 0$.

When $D_m < R_m$,

- $l \leq R_m - D_m$

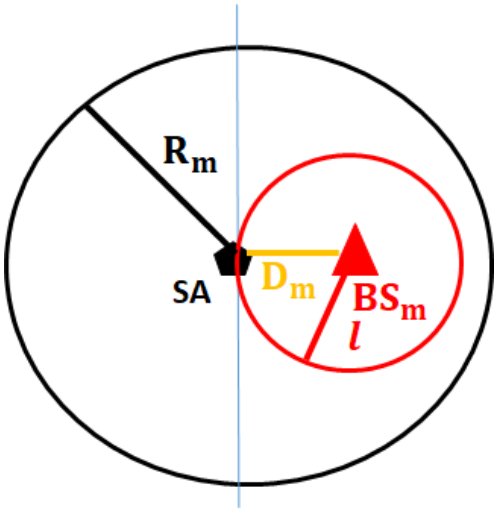

Figure A.5: PDF and CCDF when $D_m < R_m$ and $l \leq R_m - D_m$

So CCDF $\bar{F}_L^{(m)}(l) = \mathbb{P}^{(m)}(L > l) = 1 - \frac{l^2}{R_m^2}$. PDF $f_L^{(m)}(l) = \frac{2l}{R_m^2}$.

- $R_m - D_m < l \leq \sqrt{R^2 - {D_m}^2}$

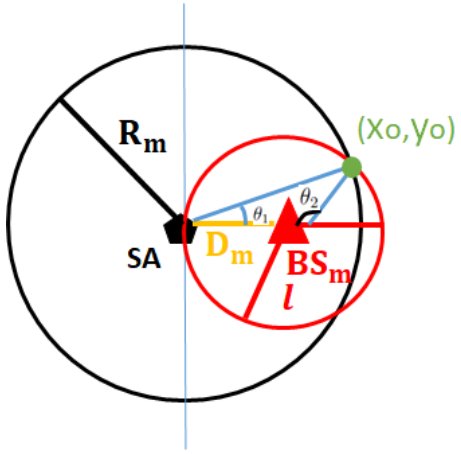

Figure A.6: PDF and CCDF when $D_m < R_m$ and $R_m - D_m < l \leq \sqrt{R_m^2 - {D_m}^2}$

Then, $\theta_1 = \arctan\frac{y_0}{x_0}$, $\theta_2 = \arctan\frac{y_0}{D_m - x_0} + \pi$.
So CCDF $\bar{F}_L^{(m)}(l) = \mathbb{P}(L > l) = 1 - \frac{\theta_1 R_m^2 + \theta_2 l^2 - D_m y_0}{\pi R_m^2}$. PDF $f_L^{(m)}(l) = \frac{2\theta_2 l}{\pi R_m^2}$.

- $\sqrt{R_m^2 - {D_m}^2} < l \leq \sqrt{R_m^2 + {D_m}^2}$

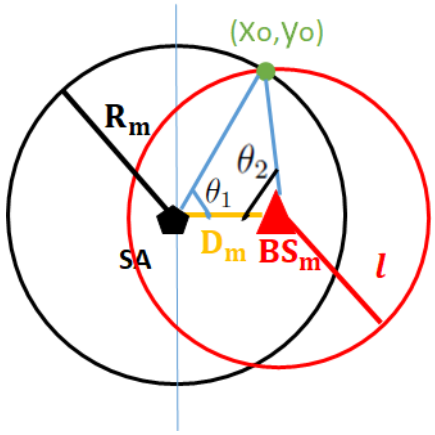

Figure A.7: PDF and CCDF when $D_m < R_m$ and $\sqrt{R_m^2 - {D_m}^2} < l \leq \sqrt{R_m^2 + {D_m}^2}$

Then, $\theta_1 = \arctan\frac{y_0}{x_0}$, $\theta_2 = \arctan\frac{y_0}{D_m - x_0}$.
So CCDF $\bar{F}_L^{(m)}(l) = \mathbb{P}^{(m)}(L > l) = 1 - \frac{\theta_1 R_m^2 + \theta_2 l^2 - D_m y_0}{\pi R^2}$. PDF $f_L^{(m)}(l) = \frac{2\theta_2 l}{\pi R_m^2}$.

- $\sqrt{R^2 + {D_m}^2} < l < R_m + D_m$

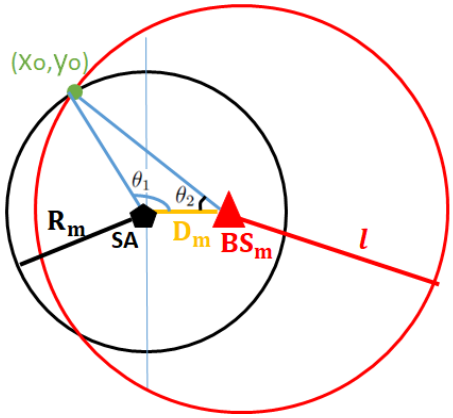

Figure A.8: PDF and CCDF when $D_m < R_m$ and $\sqrt{R_m^2 + {D_m}^2} < l < R_m + D_m$

Then, $\theta_1 = \arctan\frac{y_0}{x_0} + \pi$, $\theta_2 = \arctan\frac{y_0}{D_m - x_0}$.

So CCDF $\bar{F}_L^{(m)}(l) = \mathbb{P}(L > l) = 1 - \frac{\theta_1 R^2 + \theta_2 l^2 - D_m y_0}{\pi R_m^2}$. PDF $f_L^{(m)}(l) = \frac{2\theta_2 l}{\pi R_m^2}$.

- $R_m + D_m \leq l$

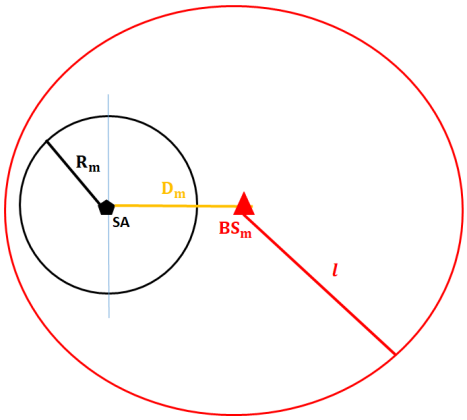

Figure A.9: PDF and CCDF when $D_m < R_m$ and $R_m + D_m \leq l$

So CCDF $\bar{F}_L^{(m)}(l) = \mathbb{P}^{(m)}(L > l) = 0$. PDF $f_L^{(m)}(l) = 0$.

When $D_m = 0$,

- $l \geq R_m$

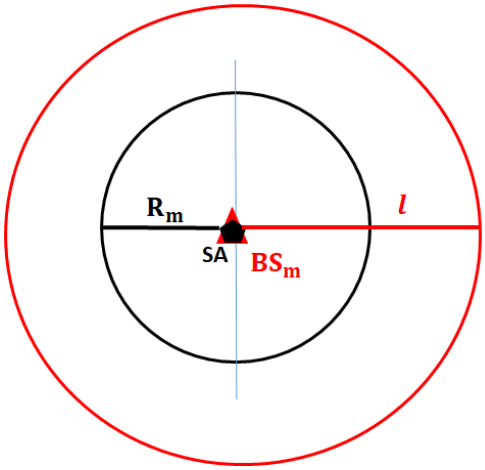

Figure A.10: PDF and CCDF when $D_m = 0$ and $l \geq R_m$

So CCDF $\bar{F}_L^{(m)}(l) = \mathbb{P}^{(m)}(L > l) = 0$. PDF $f_L^{(m)}(l) = 0$.

- $l < R_m$

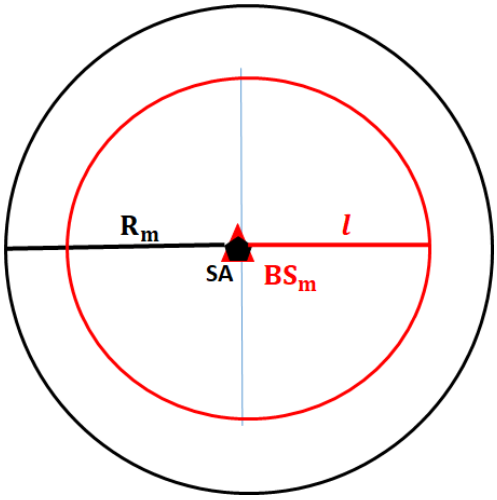

Figure A.11: PDF and CCDF when $D_m = 0$ and $l < R_m$

So CCDF $\bar{F}_L^{(m)}(l) = \mathbb{P}^{(m)}(L > l) = 1 - \frac{l^2}{R_m^2}$. PDF $f_L^{(m)}(l) = \frac{2l}{R_m^2}$.

A.2 Proof of Lemma 5-2

The probability that a UE of interest in the mth tier is associated with the BS that the UE belongs to is (conditioned on the distance l between the UE of interest and the BS that the UE belongs to)

$$
\begin{aligned}
&\mathbb{P}_{|l}^{(m)}(A_{case1}) \\
&= \mathbb{P}_{|l}[P_{RP_m} > \text{any} \underbrace{P_{RP_i}}_{i=1:K}], \\
&= \prod_{i=1}^{K} \mathbb{P}_{|l}[P_{RP_m} > P_{RP_i}], \\
&= \prod_{i=1}^{K} \mathbb{P}_{|l}[P_m C_m l^{-\alpha_m} > P_i C_i V_i^{-\alpha_i}], \\
&= \prod_{i=1}^{K} \mathbb{P}_{|l}[V_i > (\frac{P_i C_i}{P_m C_m})^{\frac{1}{\alpha_i}} \cdot l^{\frac{\alpha_m}{\alpha_i}}], \\
&\overset{(a)}{=} \prod_{i=1}^{K} \exp(-\lambda_i \pi (\frac{P_i C_i}{P_m C_m})^{\frac{2}{\alpha_i}} \cdot l^{\frac{2\alpha_m}{\alpha_i}}),
\end{aligned}
$$

where for step (a), the BS spatial distribution is PPP in the ith tier and it is from Equation 5.5 (CCDF of V in the ith tier).

A.3 Proof of Lemma 5-3

The coverage probability associated with the BS that a UE of interest belongs to is (conditioned on the distance l between the UE of interest and the BS that the UE belongs to)

$$
\begin{aligned}
&\mathbb{P}_{|l}^{(m)}[SINR_m(l) > T_m | A_{case1}] \\
&= \mathbb{P}_{|l}^{(m)}[\frac{P_m G_m l^{-\alpha_m}}{I_r + \frac{\sigma^2}{L_0}} > T_m], \\
&= \mathbb{P}_{|l}^{(m)}[G_m > (I_r + \frac{\sigma^2}{L_0}) T_m {P_m}^{-1} \cdot l^{\alpha_m}], \\
&\overset{(a)}{=} \mathbb{E}_{I_r}[\exp(-(I_r + \frac{\sigma^2}{L_0}) T_m {P_m}^{-1} \cdot l^{\alpha_m})], \\
&= \exp(-\frac{\sigma^2}{L_0} T_m {P_m}^{-1} l^{\alpha_m}) \cdot \ \mathbb{E}_{I_r}[\exp(-I_r T_m {P_m}^{-1} l^{\alpha_m})], \\
&\overset{(b)}{=} \exp(-\frac{\sigma^2}{L_0} T_m {P_m}^{-1} l^{\alpha_m}) \cdot \prod_{i=1}^{K} \mathscr{L}_{I_{ri}}(T_m {P_m}^{-1} l^{\alpha_m}),
\end{aligned}
$$

where (a) is from the assumption that the channel fading envelope $\sqrt{G_m}$ is Rayleigh distribution and the channel fading power G_m is exponential distribution. (b) gives the Laplace transform $\mathscr{L}_x(s)$ of the total interference.

A.4 Proof of Lemma 5-4

The probability that a UE of interest is associated with a BS in the kth tier rather than the BS to which the UE belongs is (conditioned on the distance v between the UE of interest and the closest BS in kth tier)

$$
\begin{aligned}
&\mathbb{P}^{(m)}_{|v}(A_{k,case2}) \\
&= \mathbb{P}^{(m)}_{|v}[P_{RP_k} > \text{any } P_{RP_i}], \\
&= \mathbb{P}_{|v}[P_{RP_k} > P_{RP_m}] \cdot \prod_{i=1, i\neq k}^{K} \mathbb{P}_{|v}[P_{RP_k} > P_{RP_i}], \\
&\overset{(a)}{=} \mathbb{P}_{|v}[P_k C_k v^{-\alpha_k} > P_m C_m L^{-\alpha_m}] \cdot \prod_{i=1, i\neq k}^{K} \mathbb{P}_{|v}[P_k C_k v^{-\alpha_k} > P_i C_i V_i^{-\alpha_i}], \\
&= \mathbb{P}_{|v}[L > (\frac{P_m C_m}{P_k C_k})^{\frac{1}{\alpha_m}} \cdot v^{\frac{\alpha_k}{\alpha_m}}] \cdot \prod_{i=1, i\neq k}^{K} \mathbb{P}_{|v}[V_i > (\frac{P_i C_i}{P_k C_k})^{\frac{1}{\alpha_i}} \cdot v^{\frac{\alpha_k}{\alpha_i}}], \\
&\overset{(b)}{=} \bar{F}^{(m)}_L((\frac{P_m C_m}{P_k C_k})^{\frac{1}{\alpha_m}} \cdot v^{\frac{\alpha_k}{\alpha_m}}) \cdot \prod_{i=1, i\neq k}^{K} \bar{F}^{(i)}_V((\frac{P_i C_i}{P_k C_k})^{\frac{1}{\alpha_i}} \cdot v^{\frac{\alpha_k}{\alpha_i}}), \\
&= \bar{F}^{(m)}_L((\frac{P_m C_m}{P_k C_k})^{\frac{1}{\alpha_m}} \cdot v^{\frac{\alpha_k}{\alpha_m}}) \cdot \prod_{i=1, i\neq k}^{K} \exp(^{-\lambda_i \pi (\frac{P_i C_i}{P_k C_k})^{\frac{2}{\alpha_i}} \cdot v^{\frac{2\alpha_k}{\alpha_i}}}),
\end{aligned}
$$

where step (a) is from the distance between the UE of interest and the closest BS in the ith tier being V_i and the distance between the UE of interest and the BS to which the UE of interest belongs being L in the mth tier. For step (b), $\bar{F}^{(m)}_L(l) = \mathbb{P}[L > l]$ is complementary cumulative distribution function (CCDF) of random variable L in the mth tier from 5.2.1.2. $\bar{F}^{(i)}_V(v) = \mathbb{P}[V_i > v]$ is CCDF of of random variable V_i in the ith tier from 5.2.1.1.

Appendix B

Uplink Coverage Performance Analysis

B.1 Proof of Lemma 6-4

The coverage probability of the BS of interest conditioned on the distance between the active UE and the BS of interest as l is

$$
\begin{aligned}
&\mathbb{P}_{|l}^{(m)}[SINR_m(l) > T_m | A_{case1}] \\
&= \mathbb{P}_{|l}^{(m)}[\frac{l^{\alpha_m(\epsilon-1)} G_m}{I_r + \frac{\sigma^2}{L_0}} > T_m], \\
&= \mathbb{P}_{|l}^{(m)}[G_m > (I_r + \frac{\sigma^2}{L_0}) T_m l^{\alpha_m(1-\epsilon)}], \\
&\overset{(a)}{=} \mathbb{E}_{I_r}[\exp(-(I_r + \frac{\sigma^2}{L_0}) T_m l^{\alpha_m(1-\epsilon)})], \\
&= \exp(-\frac{\sigma^2}{L_0} T_m l^{\alpha_m(1-\epsilon)}) \cdot \ \mathbb{E}_{I_r}[\exp(-I_r T_m l^{\alpha_m(1-\epsilon)})], \\
&\overset{(b)}{=} \exp(-\frac{\sigma^2}{L_0} T_m l^{\alpha_m(1-\epsilon)}) \cdot \prod_{i=1}^{S} \mathscr{L}_{I_{ri}}(T_m l^{\alpha_m(1-\epsilon)}),
\end{aligned}
$$

where (a) is from the assumption that the channel fading envelope $\sqrt{G_m}$ is Rayleigh fading. (b) gives the Laplace transform $\mathscr{L}_x(s)$. L_0 is the path loss at a reference distance of 1 m. S is the total number of tiers distributed with our designed non-uniform UEs.

Appendix C

Simulation Setting

This chapter gives the simulation setting when evaluating the non-uniform distribution.

C.1 Downlink Coverage Probability

In this section, the simulation setting of the downlink coverage probability is given.

- Step1: Generate a BS pattern
  In a given square (such as a square of 1 km by 1 km or a square of 2 km by 2 km), generate a BS pattern or a BS realization of K-tier. BSs in each tier have their own density (in the ith tier, the BS density is λ_i). The distribution of BSs in each tier is an independent homogeneous PPP. An example of BS pattern is shown in Figure C.1. The procedure to generate a BS pattern in the ith tier is:
  - The area of the given square is A_{si}. The mean number of distributed BSs in the given square of the ith tier is $A_{si} * \lambda_i$.
  - Generate a random number of Poisson distribution with the mean of $A_{si} * \lambda_i$. Matlab code is *poissrnd($A_{si} * \lambda_i$)*. The generated random number is the real number of BSs of the given square of the ith tier in this BS pattern.
  - Generate the distributed BSs in the given square based on the above real number of BSs. The distribution of BSs in the given square is uniform. Matlab code to generate a horizontal or vertical coordinates is *random('unif',0,Side length of the square,1,real number of BS)*.

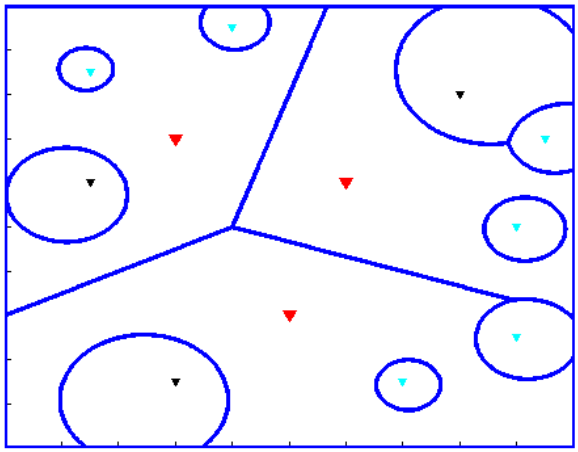

Figure C.1: An Example of BS Pattern (Red triangles are BSs in the first tier with $\lambda_1 = 3 * 10^{-6}$. Black triangles are BSs in the second tier with $\lambda_2 = 3 * 10^{-6}$. Cyan triangles are BSs in the third tier with $\lambda_3 = 6 * 10^{-6}$. The area is a square of 1 km by 1 km. Blue curves are cell boundaries.)

- Step2: Generate a UE pattern

  The UE model is that the UE concentrates around the social attractor (SA) and SA has a base station offset to its BS. The procedure to generate UE pattern of the ith tier is:

  - For each BS in the ith tier, generate a SA which is uniformly distributed around a BS of the radius D_i.
  - Generate clustered UEs with the center being the above generated SA.
  - The cluster UEs are uniformly distributed within a circular disc with radius R_i which is called as Matern cluster.

- Step3: Calculation of SINR
  Based on BS pattern and UE pattern generated above, calculate instantaneous SINR for each UE. We assume the distance between the UE and its associated BS as d and the distance between the UE and the jth interfering BS_{ij} in the ith tier as d_{ij}. The path loss exponent in the ith tier is α_i. The transmit power of the ith tier BS is P_i. The random amplitude fading type is Rayleigh fading with unity mean power gain which means the power is exponential distribution with unity.

  - Generate random exponential power gain G for each UE with Matlab code: *random('exp',1)*.

  - Received signal power from associated BS B_0 is $Pd^{-\alpha}G$. The received signal power considers the large scale fading which is dependent on distance $d^{-\alpha}$ and small scale fading which is the random variable G. Shadowing is not considered in this thesis.
  - Interference power from other interfering BS_{ij} is $P_i {d_{ij}}^{-\alpha_i} G_{ij}$.
  - The instantaneous SINR is $\frac{Pd^{-\alpha}G}{\sum_{i=1}^{K}\sum_{B_{ij}\in\phi_i\setminus B_0} P_i {d_{ij}}^{-\alpha_i} G_{ij}+Noise}$.

- Step4: Calculation of downlink coverage probability
  Repeat Step1 to Step3 for 1,000 times and record the calculated SINR for every UE. The downlink coverage probability is the CCDF of the recorded SINRs.

C.2 Uplink Coverage Probability

In this section, the simulation setting of the uplink coverage probability is given.

- Step1: Generate a BS pattern
  It is the same to Step1 in the simulation setting of the downlink coverage probability.

- Step2: Generate a UE pattern
  The UE model is that the UEs concentrate around the social attractor (SA) and SA has a base station offset to its BS. The procedure to generate the active UE pattern of the ith tier is:

  - For each BS in ith tier, generate a SA which is uniformly distributed around the BS with radius D_i.
  - Generate the clustered UEs with the cluster center being the above generated SA.
  - The clustered UEs are uniformly distributed within a circular disc of the radius R_i which is called Matern cluster process.
  - In the coverage area of each cell, choose an active UE randomly.

- Step3: Calculation of SINR
  Based on BS pattern and active UE pattern generated above, calculate the instantaneous SINR for the BS of interest. We assume L is the distance between the BS of interest and the associated active UE. L_{ji} is the distance between the ith active UE

and their associated BSs in the jth tier. V_{ji} is the distance between the ith active UE in the jth tier and the BS of interest. G_i denotes the channel random power gain in the ith tier. The path loss exponent in the ith tier is α_i. The transmit power of the active UE associated with the BS of interest is $L^{\alpha_k \epsilon}$ and the transmit power of the ith active UE in the jth tier is $L_{ji}^{\alpha_j \epsilon}$ which considers the uplink fractional power control policy with factional factor ϵ. The random amplitude fading type is Rayleigh fading with unity mean power gain which means the power is exponential distribution with unity.

  - Generate random exponential power gain G_k with Matlab code: *random('exp',1)*.
  - Received signal power from the active UE associated with the BS of interest is $L^{\alpha_k(\epsilon-1)} G_k$.
  - Interference power from all other interfering active UEs is $L_{ji}^{\alpha_j \epsilon} G_j {V_{ji}}^{-\alpha_j}$
  - The instantaneous uplink SINR is $\frac{L^{\alpha_k(\epsilon-1)} G_k}{\sum_{j=1}^{S} \sum_{\in \phi_j} L_{ji}^{\alpha_j \epsilon} G_j {V_{ji}}^{-\alpha_j} + Noise}$.

- Step4: Calculation of uplink coverage probability
  Repeat Step1 to Step3 for 1,000 times and record the calculated SINR. The uplink coverage probability is the CCDF of the accumulated SINR.

C.3 Heterogeneity Analysis based on CoV

In this section, the simulation setting of the heterogeneity analysis based on CoV is given.

- Step1: Generate a BS pattern
  It is the same to Step1 in the simulation setting of the downlink coverage probability.

- Step2: Generate a UE pattern
  It is the same to Step2 in the simulation setting of the downlink coverage probability.

- Step3: Calculate the CoV of Voronoi cell area
  For the UE pattern, we generate the Voronoi and Delaunay tessellations and find the relative Voronoi cell area. For each UE pattern, we obtain one measured CoV of Voronoi cell area. CoV is the standard deviation divided by the mean of measured Voronoi cell area.

- Step4: Generate the final mean CoV
  Repeat Step1 to Step3 for 1,000 times and calculate the mean CoV among 1,000 measured CoV.

The procedure generating CoV of Delaunay cell edge length and Delaunay cell area is the same as that of Voronoi cell area.

References

[1] Phillip Tracy. Small cells: Backhaul difficulties and a 5G future. Technical report, http://www.rcrwireless.com/20160711/network-infrastructure/small-cells-tag31-tag99.

[2] Jianping An, Kai Yang, Jinsong Wu, Neng Ye, Song Guo, and Zhifang Liao. Achieving Sustainable Ultra-Dense Heterogeneous Networks for 5G. *IEEE Communications Magazine*, 55(12):84–90, 2017.

[3] Aleksandar Damnjanovic, Juan Montojo, Yongbin Wei, Tingfang Ji, Tao Luo, Madhavan Vajapeyam, Taesang Yoo, Osok Song, and Durga Malladi. A survey on 3GPP heterogeneous networks. *Wireless Communications, IEEE*, 18(3):10–21, 2011.

[4] Sara Landström, Anders Furuskär, Klas Johansson, Laetitia Falconetti, and Frederic Kronestedt. Heterogeneous networks–increasing cellular capacity. *The data boom: opportunities and challenges*, 4, 2011.

[5] Takehiro Nakamura, Satoshi Nagata, Anass Benjebbour, Yoshihisa Kishiyama, Tang Hai, Shen Xiaodong, Yang Ning, and Li Nan. Trends in small cell enhancements in LTE advanced. *IEEE Communications Magazine*, 51(2):98–105, 2013.

[6] Naga Bhushan, Junyi Li, Durga Malladi, Rob Gilmore, Dean Brenner, Aleksandar Damnjanovic, Ravi Teja Sukhavasi, Chirag Patel, and Stefan Geirhofer. Network densification: the dominant theme for wireless evolution into 5G. *IEEE Communications Magazine*, 52(2):82–89, 2014.

[7] Jeffrey G Andrews, Holger Claussen, Mischa Dohler, Sundeep Rangan, and Mark C Reed. Femtocells: Past, Present, and Future. *Selected Areas in Communications, IEEE Journal on*, 30(3):497–508, 2012.

[8] Vikram Chandrasekhar, Jeffrey G Andrews, and Alan Gatherer. Femtocell networks: a survey. *Communications Magazine, IEEE*, 46(9):59–67, 2008.

[9] Jeffrey G Andrews, Stefano Buzzi, Wan Choi, Stephen V Hanly, Angel Lozano, Anthony CK Soong, and Jianzhong Charlie Zhang. What will 5G be? *IEEE Journal on Selected Areas in Communications*, 32(6):1065–1082, 2014.

[10] Evolved Universal Terrestrial Radio Access. Mobility enhancements in heterogeneous networks, 3GPP TS 36.839. *V11*, 1, 2013.

[11] Aleksandar Damnjanovic, Juan Montojo, Yongbin Wei, Tingfang Ji, Tao Luo, Madhavan Vajapeyam, Taesang Yoo, Osok Song, and Durga Malladi. A survey on 3GPP heterogeneous networks. *IEEE Wireless Communications*, 18(3):10–21, 2011.

[12] Ralf Bendlin, Vikram Chandrasekhar, Runhua Chen, Anthony Ekpenyong, and Eko Onggosanusi. From homogeneous to heterogeneous networks: A 3GPP Long Term Evolution rel. 8/9 case study. In *Information Sciences and Systems (CISS), 2011 45th Annual Conference on*, pages 1–5. IEEE, 2011.

[13] Sayandev Mukherjee. *Analytical Modeling of Heterogeneous Cellular Networks*. Cambridge University Press, 2014.

[14] Xavier Lagrange. Multitier cell design. *IEEE Communications Magazine*, 35(8):60–64, 1997.

[15] Jerry Sydir and Rakesh Taori. An evolved cellular system architecture incorporating relay stations. *IEEE Communications Magazine*, 47(6), 2009.

[16] Konstantinos Samdanis, Tarik Taleb, and Stefan Schmid. Traffic Offload Enhancements for eUTRAN. *IEEE Communications Surveys & Tutorials*, 14(3):884–896, 2012.

[17] Sumit Katiyar, Prof Jain, Prof Agrawal, et al. An Intelligent Approach for Dense Urban Area in existing 2G/2.5 G. *arXiv preprint arXiv:1204.2097*, 2012.

[18] Klein S Gilhousen, Irwin M Jacobs, Roberto Padovani, Andrew J Viterbi, Lindsay A Weaver, and Charles E Wheatley. On the capacity of a cellular CDMA system. *IEEE transactions on vehicular technology*, 40(2):303–312, 1991.

[19] Jiaming Xu, Jun Zhang, and Jeffrey G Andrews. On the accuracy of the Wyner model in cellular networks. *IEEE Transactions on Wireless Communications*, 10(9):3098–3109, 2011.

[20] Harpreet S Dhillon, Radha Krishna Ganti, Francois Baccelli, and Jeffrey G Andrews. Modeling and Analysis of K-Tier Downlink Heterogeneous Cellular Networks. *Selected Areas in Communications, IEEE Journal on*, 30(3):550–560, 2012.

[21] Harpreet S Dhillon, Radha Krishna Ganti, and Jeffrey G Andrews. A tractable framework for coverage and outage in heterogeneous cellular networks. In *Information Theory and Applications Workshop (ITA), 2011*, pages 1–6. IEEE, 2011.

[22] Sayandev Mukherjee. Distribution of Downlink SINR in Heterogeneous Cellular Networks. *Selected Areas in Communications, IEEE Journal on*, 30(3):575–585, 2012.

[23] Chiranjib Saha and Harpreet S Dhillon. Downlink coverage probability of K-Tier HetNets with general non-uniform user distributions. In *Communications (ICC), 2016 IEEE International Conference on*, pages 1–6. IEEE, 2016.

[24] Chiranjib Saha, Mehrnaz Afshang, and Harpreet S Dhillon. Enriched K -Tier HetNet Model to Enable the Analysis of User-Centric Small Cell Deployments. *arXiv preprint arXiv:1606.06223*, 2016.

[25] Sung Nok Chiu, Dietrich Stoyan, Wilfrid S Kendall, and Joseph Mecke. *Stochastic Geometry and its Applications*. John Wiley & Sons, 2013.

[26] Hesham ElSawy, Ekram Hossain, and Martin Haenggi. Stochastic Geometry for Modeling, Analysis, and Design of Multi-Tier and Cognitive Cellular Wireless Networks: A Survey. *Communications Surveys & Tutorials, IEEE*, 15(3):996–1019, 2013.

[27] Aaron D Wyner. Shannon-theoretic approach to a Gaussian cellular multiple-access channel. *IEEE Transactions on Information Theory*, 40(6):1713–1727, 1994.

[28] M-S Alouini and Andrea J Goldsmith. Area spectral efficiency of cellular mobile radio systems. *IEEE Transactions on vehicular technology*, 48(4):1047–1066, 1999.

[29] Che-Sheng Chiu and Chen-Chiu Lin. Comparative downlink shared channel evaluation of WCDMA release 99 and HSDPA. In *Networking, Sensing and Control, 2004 IEEE International Conference on*, volume 2, pages 1165–1170. IEEE, 2004.

[30] Raj Jain, Chakchai So-In, et al. System-level modeling of IEEE 802.16 E mobile WiMAX networks: key issues. *IEEE Wireless Communications*, 15(5), 2008.

[31] Josep Colom Ikuno, Martin Wrulich, and Markus Rupp. System level simulation of LTE networks. In *Vehicular Technology Conference (VTC 2010-Spring), 2010 IEEE 71st*, pages 1–5. IEEE, 2010.

[32] Martin Haenggi, Jeffrey G Andrews, François Baccelli, Olivier Dousse, and Massimo Franceschetti. Stochastic geometry and random graphs for the analysis and design of wireless networks. *Selected Areas in Communications, IEEE Journal on*, 27(7):1029–1046, 2009.

[33] François Baccelli and Bartlomiej Blaszczyszyn. Stochastic Geometry and Wireless Networks, Volume I-Applications. 2009.

[34] François Baccelli and Bartlomiej Blaszczyszyn. Stochastic Geometry and Wireless Networks, Volume II-Applications. 2009.

[35] Martin Haenggi. *Stochastic Geometry for Wireless Networks*. Cambridge University Press, 2012.

[36] Paulo Cardieri. Modeling interference in wireless ad hoc networks. *IEEE Communications Surveys Tutorials*, 12(4):551–572, 2010.

[37] Martin Haenggi, Radha Krishna Ganti, et al. Interference in large wireless networks. *Foundations and Trends in Networking*, 3(2):127–248, 2009.

[38] Steven Weber, Jeffrey G Andrews, et al. Transmission capacity of wireless networks. *Foundations and Trends in Networking*, 5(2–3):109–281, 2012.

[39] Hesham ElSawy, Ahmed Sultan-Salem, Mohamed-Slim Alouini, and Moe Z Win. Modeling and analysis of cellular networks using stochastic geometry: A tutorial. *IEEE Communications Surveys & Tutorials*, 19(1):167–203, 2017.

[40] François Baccelli, Maurice Klein, Marc Lebourges, and Sergei Zuyev. Stochastic geometry and architecture of communication networks. *Telecommunication Systems*, 7(1):209–227, 1997.

[41] Daryl J Daley and David Vere-Jones. *An introduction to the theory of point processes: volume II: general theory and structure*. Springer Science & Business Media, 2007.

[42] David R Brillinger, Peter M Guttorp, and Frederic Paik Schoenberg. Point processes, temporal. *Wiley StatsRef: Statistics Reference Online*, 2002.

[43] Jeffrey G Andrews, François Baccelli, and Radha Krishna Ganti. A Tractable Approach to Coverage and Rate in Cellular Networks. *Communications, IEEE Transactions on*, 59(11):3122–3134, 2011.

[44] Holger Paul Keeler, Bartlomiej Blaszczyszyn, and Mohamed Kadhem Karray. SINR-based k-coverage probability in cellular networks with arbitrary shadowing. In *Information Theory Proceedings (ISIT), 2013 IEEE International Symposium on*, pages 1167–1171. IEEE, 2013.

[45] Jeffrey G Andrews, Abhishek K Gupta, and Harpreet S Dhillon. A Primer on Cellular Network Analysis Using Stochastic Geometry. *arXiv preprint arXiv:1604.03183*, 2016.

[46] Adrian Baddeley, Imre Bárány, and Rolf Schneider. Spatial point processes and their applications. *LECTURE NOTES IN MATHEMATICS-SPRINGER-VERLAG-*, 1892:1, 2007.

[47] Harpreet S Dhillon, Radha Krishna Ganti, and Jeffrey G Andrews. Modeling Non-Uniform UE Distributions in Downlink Cellular Networks. *Wireless Communications Letters, IEEE*, 2(3):339–342, 2013.

[48] Young Jin Chun, Mazen O Hasna, and Ali Ghrayeb. Modeling heterogeneous cellular networks interference using Poisson cluster processes. *IEEE Journal on Selected Areas in Communications*, 33(10):2182–2195, 2015.

[49] Aymen Jaziri, Ridha Nasri, and Tijani Chahed. System-Level Analysis of Heterogeneous Networks Under Imperfect Traffic Hotspot Localization. *IEEE Transactions on Vehicular Technology*, 65(12):9862–9872, 2016.

[50] Jeffrey G Andrews, Radha Krishna Ganti, Martin Haenggi, Nihar Jindal, and Steven Weber. A primer on spatial modeling and analysis in wireless networks. *Communications Magazine, IEEE*, 48(11):156–163, 2010.

[51] Ziyang Wang, Rainer Schoenen, Halim Yanikomeroglu, and Marc St-Hilaire. The impact of user spatial heterogeneity in heterogeneous cellular networks. In *Globecom Workshops (GC Wkshps), 2014*, pages 1278–1283. IEEE, 2014.

[52] Mohamed Elalem and Lian Zhao. Realistic user distribution and its impact on capacity and coverage for a WCDMA mobile network. In *Sarnoff Symposium, 2009. SARNOFF'09. IEEE*, pages 1–5. IEEE, 2009.

[53] Premvir K Jain and Harald Haas. Effects of user distributions on CDMA system performance. In *Personal, Indoor and Mobile Radio Communications, 2005. PIMRC 2005. IEEE 16th International Symposium on*, volume 3, pages 1652–1656. IEEE, 2005.

[54] Evolved Universal Terrestrial Radio Access. Further advancements for E-UTRA physical layer aspects. *3GPP Technical Specification TR*, 36:V2, 2010.

[55] Dongheon Lee, Sheng Zhou, Xiaofeng Zhong, Zhisheng Niu, Xuan Zhou, and Honggang Zhang. Spatial modeling of the traffic density in cellular networks. *IEEE Wireless Communications*, 21(1):80–88, 2014.

[56] Uwe Gotzner and R Rathgeber. Spatial traffic distribution in cellular networks. In *Vehicular Technology Conference, 1998. VTC 98. 48th IEEE*, volume 3, pages 1994–1998. IEEE, 1998.

[57] Rajamani Ganesh and Kuriacose Joseph. Effect of non-uniform traffic distributions on performance of a cellular CDMA system. In *Universal Personal Communications Record, 1997. Conference Record., 1997 IEEE 6th International Conference on*, volume 2, pages 598–602. IEEE, 1997.

[58] Meisam Mirahsan, Rainer Schoenen, and Halim Yanikomeroglu. HetHetNets: Heterogeneous Traffic Distribution in Heterogeneous Wireless Cellular Networks. *IEEE Journal on Selected Areas in Communications*, 33(10):2252–2265, 2015.

[59] Chao Li, Abbas Yongacoglu, and Claude D'Amours. Coverage probability of the downlink in heterogeneous cellular networks considering the effect of user clustering around spatially depended social attractors. In *Computer Aided Modelling and Design of Communication Links and Networks (CAMAD), 2016 IEEE 21st International Workshop on*, pages 48–52. IEEE, 2016.

[60] Chao Li, Abbas Yongacoglu, and Claude D'Amours. Heterogeneous cellular network user distribution model. In *Communications (LATINCOM), 2016 8th IEEE Latin-American Conference on*, pages 1–6. IEEE, 2016.

[61] Christian Bettstetter, Michael Gyarmati, and Udo Schilcher. An inhomogeneous spatial node distribution and its stochastic properties. In *Proceedings of the 10th ACM Symposium on Modeling, analysis, and simulation of wireless and mobile systems*, pages 400–404. ACM, 2007.

[62] Chao Li, Abbas Yongacoglu, and Claude D'Amours. Mixed Spatial Traffic Modeling of Heterogeneous Cellular Networks. In *Ubiquitous Wireless Broadband (ICUWB), 2015 IEEE International Conference on*, pages 1–5. IEEE, 2015.

[63] Martin Taranetz, Tianyang Bai, Robert W Heath, and Markus Rupp. Analysis of small cell partitioning in urban two-tier heterogeneous cellular networks. In *Wireless Communications Systems (ISWCS), 2014 11th International Symposium on*, pages 739–743. IEEE, 2014.

[64] Mehrnaz Afshang, Harpreet S Dhillon, and Peter Han Joo Chong. Modeling and performance analysis of clustered device-to-device networks. *IEEE Transactions on Wireless Communications*, 15(7):4957–4972, 2016.

[65] Mehrnaz Afshang, Harpreet S Dhillon, and Peter Han Joo Chong. Fundamentals of cluster-centric content placement in cache-enabled device-to-device networks. *IEEE Transactions on Communications*, 64(6):2511–2526, 2016.

[66] Mehrnaz Afshang and Harpreet S Dhillon. Spatial modeling of device-to-device networks: Poisson cluster process meets Poisson hole process. In *Signals, Systems and Computers, 2015 49th Asilomar Conference on*, pages 317–321. IEEE, 2015.

[67] Mehrnaz Afshang, Harpreet S Dhillon, and Peter Han Joo Chong. Coverage and area spectral efficiency of clustered device-to-device networks. In *Global Communications Conference (GLOBECOM), 2015 IEEE*, pages 1–6. IEEE, 2015.

[68] Sergey Andreev, Alexander Pyattaev, Kerstin Johnsson, Olga Galinina, and Yevgeni Koucheryavy. Cellular traffic offloading onto network-assisted device-to-device connections. *IEEE Communications Magazine*, 52(4):20–31, 2014.

[69] Thomas D Novlan, Harpreet S Dhillon, and Jeffrey G Andrews. Analytical modeling of uplink cellular networks. *IEEE Transactions on Wireless Communications*, 12(6):2669–2679, 2013.

[70] Zolfa Zeinalpour-Yazdi and Shirin Jalali. Outage analysis of uplink two-tier networks. *IEEE Transactions on Communications*, 62(9):3351–3362, 2014.

[71] Sarabjot Singh, Xinchen Zhang, and Jeffrey G Andrews. Joint rate and SINR coverage analysis for decoupled uplink-downlink biased cell associations in HetNets. *IEEE Transactions on Wireless Communications*, 14(10):5360–5373, 2015.

[72] Prasanna Herath, Chintha Tellambura, and Witold A Krzymien. Stochastic geometry modeling of cellular uplink power control under composite Rayleigh-lognormal fading. In *Vehicular Technology Conference (VTC Fall), 2015 IEEE 82nd*, pages 1–5. IEEE, 2015.

[73] Hesham ElSawy and Ekram Hossain. On stochastic geometry modeling of cellular uplink transmission with truncated channel inversion power control. *IEEE Transactions on Wireless Communications*, 13(8):4454–4469, 2014.

[74] Hyung Yeol Lee, Young Jin Sang, and Kwang Soon Kim. On the uplink SIR distributions in heterogeneous cellular networks. *IEEE Communications Letters*, 18(12):2145–2148, 2014.

[75] Han-Shin Jo, Young Jin Sang, Ping Xia, and Jeffrey G Andrews. Heterogeneous Cellular Networks with Flexible Cell Association: A Comprehensive Downlink SINR Analysis. *Wireless Communications, IEEE Transactions on*, 11(10):3484–3495, 2012.

[76] Prasanna Madhusudhanan, Juan G Restrepo, Youjian Liu, and Timothy X Brown. Analysis of downlink connectivity models in a heterogeneous cellular network via stochastic geometry. *IEEE Transactions on Wireless Communications*, 15(6):3895–3907, 2016.

[77] Harpreet S Dhillon, Radha Krishna Ganti, and Jeffrey G Andrews. Load-aware modeling and analysis of heterogeneous cellular networks. *IEEE Transactions on Wireless Communications*, 12(4):1666–1677, 2013.

[78] Sarabjot Singh, Harpreet S Dhillon, and Jeffrey G Andrews. Offloading in heterogeneous networks: Modeling, analysis, and design insights. *IEEE Transactions on Wireless Communications*, 12(5):2484–2497, 2013.

[79] Wang Chi Cheung, Tony QS Quek, and Marios Kountouris. Throughput optimization, spectrum allocation, and access control in two-tier femtocell networks. *IEEE Journal on Selected Areas in Communications*, 30(3):561–574, 2012.

[80] Yingzhe Li, François Baccelli, Harpreet S Dhillon, and Jeffrey G Andrews. Statistical modeling and probabilistic analysis of cellular networks with determinantal point processes. *IEEE Transactions on Communications*, 63(9):3405–3422, 2015.

[81] Hesham ElSawy and Ekram Hossain. Two-tier HetNets with cognitive femtocells: Downlink performance modeling and analysis in a multichannel environment. *IEEE Transactions on Mobile Computing*, 13(3):649–663, 2014.

[82] Na Deng, Wuyang Zhou, and Martin Haenggi. Heterogeneous cellular network models with dependence. *IEEE Journal on Selected Areas in Communications*, 33(10):2167–2181, 2015.

[83] Zeinab Yazdanshenasan, Harpreet S Dhillon, Mehrnaz Afshang, and Peter HJ Chong. Poisson hole process: Theory and applications to wireless networks. *IEEE Transactions on Wireless Communications*, 15(11):7531–7546, 2016.

[84] Chia-han Lee and Martin Haenggi. Interference and outage in Poisson cognitive networks. *IEEE Transactions on Wireless Communications*, 11(4):1392–1401, 2012.

[85] Young Jin Chun, Mazen O Hasna, and Ali Ghrayeb. Modeling heterogeneous cellular networks interference using Poisson cluster processes. *IEEE Journal on Selected Areas in Communications*, 33(10):2182–2195, 2015.

[86] Chunlin Chen, Robert C Elliott, and Witold A Krzymien. Downlink coverage analysis of N-tier heterogeneous cellular networks based on clustered stochastic geometry. In *Signals, Systems and Computers, 2013 Asilomar Conference on*, pages 1577–1581. IEEE, 2013.

[87] Martin Taranetz and Markus Rupp. Performance of femtocell access point deployments in user hot-spot scenarios. In *Telecommunication Networks and Applications Conference (ATNAC), 2012 Australasian*, pages 1–5. IEEE, 2012.

[88] Qianlan Ying, Zhifeng Zhao, Yifan Zhou, Rongpeng Li, Xuan Zhou, and Honggang Zhang. Characterizing spatial patterns of base stations in cellular networks. In *Communications in China (ICCC), 2014 IEEE/CIC International Conference on*, pages 490–495. IEEE, 2014.

[89] Yi Zhong and Wenyi Zhang. Multi-channel hybrid access femtocells: A stochastic geometric analysis. *IEEE Transactions on Communications*, 61(7):3016–3026, 2013.

[90] Anjin Guo and Martin Haenggi. Asymptotic deployment gain: A simple approach to characterize the SINR distribution in general cellular networks. *IEEE Transactions on Communications*, 63(3):962–976, 2015.

[91] Martin Haenggi. The mean interference-to-signal ratio and its key role in cellular and amorphous networks. *IEEE Wireless Communications Letters*, 3(6):597–600, 2014.

[92] Qiaoyang Ye, Beiyu Rong, Yudong Chen, Mazin Al-Shalash, Constantine Caramanis, and Jeffrey G Andrews. User association for load balancing in heterogeneous cellular networks. *IEEE Transactions on Wireless Communications*, 12(6):2706–2716, 2013.

[93] Jeffrey G Andrews, Sarabjot Singh, Qiaoyang Ye, Xingqin Lin, and Harpreet S Dhillon. An overview of load balancing in HetNets: Old myths and open problems. *IEEE Wireless Communications*, 21(2):18–25, 2014.

[94] Meisam Mirahsan, Ziyang Wang, Rainer Schoenen, Halim Yanikomeroglu, and Marc St-Hilaire. Unified and non-parameterized statistical modeling of temporal and spatial traffic heterogeneity in wireless cellular networks. In *Communications Workshops (ICC), 2014 IEEE International Conference on*, pages 55–60. IEEE, 2014.

[95] Meisam Mirahsan, Rainer Schoenen, and Halim Yanikomeroglu. Statistical Modeling of Spatial Traffic Distribution with Adjustable Heterogeneity and BS-Correlation in Wireless Cellular Networks. In *Global Communications Conference (GLOBECOM), 2014 IEEE*, pages 3647–3652. IEEE, 2014.

[96] Jeffrey G Andrews, François Baccelli, and Radha Krishna Ganti. A Tractable Approach to Coverage and Rate in Cellular Networks. *Communications, IEEE Transactions on*, 59(11):3122–3134, 2011.

[97] JF Whitehead. Signal-level-based dynamic power control for co-channel interference management. In *Vehicular Technology Conference, 1993., 43rd IEEE*, pages 499–502. IEEE, 1993.

[98] Roy D. Yates. A framework for uplink power control in cellular radio systems. *IEEE Journal on selected areas in communications*, 13(7):1341–1347, 1995.

[99] Harri Holma and Antti Toskala. *WCDMA for UMTS: HSPA Evolution and LTE*. john Wiley & sons, 2007.

[100] Jeffrey D Herdtner and Edwin KP Chong. Analysis of a class of distributed asynchronous power control algorithms for cellular wireless systems. *IEEE Journal on Selected Areas in Communications*, 18(3):436–446, 2000.

[101] Arne Simonsson and Anders Furuskar. Uplink power control in LTE-overview and performance, subtitle: principles and benefits of utilizing rather than compensating for SINR variations. In *Vehicular Technology Conference, 2008. VTC 2008-Fall. IEEE 68th*, pages 1–5. IEEE, 2008.

[102] Carlos Ubeda Castellanos, Dimas López Villa, Claudio Rosa, Klaus I Pedersen, Francesco Davide Calabrese, Per-Henrik Michaelsen, and Jurgen Michel. Performance of uplink fractional power control in UTRAN LTE. In *Vehicular Technology Conference, 2008. VTC Spring 2008. IEEE*, pages 2517–2521. IEEE, 2008.

[103] Marceau Coupechoux and Jean-Marc Kelif. How to set the fractional power control compensation factor in LTE? In *Sarnoff Symposium, 2011 34th IEEE*, pages 1–5. IEEE, 2011.

[104] Chao Li, Abbas Yongacoglu, and Claude D'Amours. Coverage probability of the downlink in heterogeneous cellular networks on Nakagami-m fading channel. In *Communication Systems (ICCS), 2016 IEEE International Conference on*, pages 1–6. IEEE, 2016.

[105] Harpreet S Dhillon and Jeffrey G Andrews. Downlink rate distribution in heterogeneous cellular networks under generalized cell selection. *IEEE Wireless Communications Letters*, 3(1):42–45, 2014.

[106] Elham Kalantari, Halim Yanikomeroglu, and Abbas Yongacoglu. On the number and 3D placement of drone base stations in wireless cellular networks. In *Vehicular Technology Conference (VTC-Fall), 2016 IEEE 84th*, pages 1–6. IEEE, 2016.

[107] Akram Al-Hourani, Sithamparanathan Kandeepan, and Abbas Jamalipour. Modeling air-to-ground path loss for low altitude platforms in urban environments. In *Global Communications Conference (GLOBECOM), 2014 IEEE*, pages 2898–2904. IEEE, 2014.

[108] R Irem Bor-Yaliniz, Amr El-Keyi, and Halim Yanikomeroglu. Efficient 3-D placement of an aerial base station in next generation cellular networks. In *Communications (ICC), 2016 IEEE International Conference on*, pages 1–5. IEEE, 2016.

[109] Akram Al-Hourani, Sithamparanathan Kandeepan, and Simon Lardner. Optimal LAP altitude for maximum coverage. *IEEE Wireless Communications Letters*, 3(6):569–572, 2014.

[110] Harpreet S Dhillon, Marios Kountouris, and Jeffrey G Andrews. Downlink MIMO HetNets: Modeling, ordering results and performance analysis. *IEEE Transactions on Wireless Communications*, 12(10):5208–5222, 2013.

[111] Abhishek K Gupta, Harpreet S Dhillon, Sriram Vishwanath, and Jeffrey G Andrews. Downlink multi-antenna heterogeneous cellular network with load balancing. *IEEE Transactions on Communications*, 62(11):4052–4067, 2014.

[112] Chang Li, Jun Zhang, and Khaled B Letaief. Throughput and energy efficiency analysis of small cell networks with multi-antenna base stations. *IEEE Transactions on Wireless Communications*, 13(5):2505–2517, 2014.

[113] Chang Li, Jun Zhang, Jeffrey G Andrews, and Khaled B Letaief. Success probability and area spectral efficiency in multiuser MIMO HetNets. *IEEE Transactions on Communications*, 64(4):1544–1556, 2016.

[114] Tianyang Bai and Robert W Heath. Coverage and rate analysis for millimeter-wave cellular networks. *IEEE Transactions on Wireless Communications*, 14(2):1100–1114, 2015.

[115] Tianyang Bai, Rahul Vaze, and Robert W Heath. Analysis of blockage effects on urban cellular networks. *IEEE Transactions on Wireless Communications*, 13(9):5070–5083, 2014.